



UNIVERSITÀ DEGLI STUDI DI MILANO  
Scuola di Dottorato in Scienze Farmacologiche  
Dipartimento di Biotecnologie Mediche e Medicina Traslazionale

*CORSO DI DOTTORATO IN SCIENZE FARMACOLOGICHE*  
*Ciclo XXVIII*

**“ Effects of Microvesicles derived from Bone Marrow  
Mesenchymal Stem Cells in Experimental Models of  
Alzheimer's Disease”**

BIO/14

Chiara Adriana ELIA  
Matricola: R10125

TUTOR: Prof.re Fabrizio GARDONI  
CO-TUTOR: Dott.ssa Elisabetta MENNA  
COORDINATORE: Prof.re Alberto CORSINI

A.A. 2014-2015

## Table of contents

<b>ABSTRACT</b>	<b>4</b>
<b>INTRODUCTION</b>	<b>6</b>
1. <i>Mesenchymal Stem Cells (MSCs)</i>	6
1.1 In vitro MSC characterization	8
1.2 Bone Marrow-derived MSCs	9
1.3 Therapeutic properties of MSCs	10
1.4 Immunomodulatory properties of MSCs	12
2. <i>Microvesicles (MVs)</i>	15
2.1 Isolation of EVs	18
2.2 Exosomes (Exo)	18
2.2.1 Origin and molecular composition of Exo	18
2.3 The shedding vesicles (SV)	19
2.3.1 Biogenesis and molecular composition of shedding vesicles	20
2.4 Interaction with target cells	20
2.5 EV content and biological role	21
2.6 BM MSC-derived microvesicles	22
2.7 Therapeutic applications of BM-MSC derived MVs	24
3. <i>Microglia</i>	26
3.1 Microglia development	27
3.2 Microglia phenotypes	28
3.3 Microglia functions and disease	31
4. <i>Alzheimer's Disease</i>	33
4.1 Pathological hallmarks of AD	34
4.1.1 $\beta$ -Amyloid protein	35
4.2 Hypothesis for explaining AD pathogenesis	36
4.3 The role of microglial cells in the pathogenesis of AD	37
5. <i>Genetics of AD</i>	41
5.1. Animal Models of Alzheimer's disease	41
5.1.1 Single APP transgenic models	42
5.1.2 APP/PS double transgenic models	43
5.1.3 Tau-based transgenic models	44
5.1.4 Triple transgenic models	44
6. <i>Drug treatment for Alzheimer's disease</i>	45
6.1 New therapeutic targets for AD	45
6.2 Therapeutic potential of Bone Marrow-derived Mesenchymal Stem Cells in the treatment of Alzheimer's disease	46
<b>MATERIALS and METHODS</b>	<b>48</b>
1. <i>IN VITRO EXPERIMENTS</i>	48
1.1 Isolation and culture of murine Bone Marrow-derived Mesenchymal Stem Cells (BM-MSCs)	48
1.2 Osteogenic and Adipogenic differentiation assay	49
1.3 Determination of BM-derived MSC surface antigen profile	50
1.4 Isolation of BM-MSC derived MVs	51

1.5 Characterization of BM MSC-derived MVs	52
1.6 Microglial dissection and culture	52
1.7 Microglial treatment with the $\beta$ -amyloid peptide and MVs	53
1.8 Cytokine profiles	54
1.9 Immunofluorescence staining of cultured N9 and microglial cells	54
<b>2. IN VIVO EXPERIMENTS</b>	<b>56</b>
2.1 Animals	56
2.2 Injection of BM-MSC derived MVs in APP/PS1 Double Mutant Mice	56
2.3 Preparation of tissue for immunohistochemical staining	57
2.4 Immunohistochemical staining	57
2.5 Tissue homogenation for biochemical assay	58
2.6 Biochemical assay	59
<b>3. ACQUISITIONS and DATA ANALYSIS</b>	<b>59</b>
3.1 Analysis of the immunohistochemistry stain	59
3.2 Analysis of the immunofluorescence	60
3.2 Analysis of results obtained by FACS	60
3.3 Analysis of ELISA results	60
<b>RESULTS and DISCUSSION</b>	<b>62</b>
<i>1. Immunophenotypical characterization of Bone Marrow isolated Mesenchymal Stem Cells and own released Microvesicles</i>	62
a. Characterization of immune- phenotypical markers of Mesenchymal Stem Cells	62
b. Characterization of MSC-released Microvesicles (MVs)	66
<i>2. In vitro evaluation of cytokine release by cells treated with human-A<math>\beta</math><sub>1-42</sub> and BM MSC-derived MVs</i>	69
a. Experimental Design.	69
b. Analysis of cytokine release in N9 cells exposed to h-A $\beta$ <sub>1-42</sub> and MVs- e	70
c. Analysis of cytokine release by treated primary microglia cells	72
<i>3. Phenotype assessment of microglia cells upon- A<math>\beta</math><sub>1-42</sub> and BM- MSC derived MVs treatment</i>	74
a. Evaluation of the expression of MHC II, M1 marker, in MV-treated microglia	74
b. Evaluation of the expression of M2 marker CD206 by MV treated microglia	77
c. Evaluation of the internalization of $\beta$ -amyloid in MV treated microglia	79
a. Experimental Design.	83
b. MV injection reduces A $\beta$ <sub>42</sub> deposition in APP/PS1 mice.	84
c. Detection of soluble A $\beta$ <sub>42</sub> in brain and in blood	90
d. MV treatment reduces TNF $\alpha$ levels without affecting IL10 in APP/PS1 mice	91
<b>CONCLUSIONS</b>	<b>95</b>
<b>REFERENCES</b>	<b>97</b>

## **“ Effects of Microvesicles derived from Bone Marrow Mesenchymal Stem Cells in experimental models of Alzheimer's disease”**

### ABSTRACT

Alzheimer's disease (AD) is the most common form of neurodegenerative illness leading to dementia characterized by the accumulation of abnormally folded  $\beta$ -Amyloid ( $A\beta$ ) and tau proteins, forming amyloid plaques and neurofibrillary tangles, respectively.

Recent evidences have highlighted that inflammation plays a critical role in AD, even though it remains unclear whether it represents a cause or a consequence of the pathology. Deposition of  $A\beta$  peptides and tangles are able to stimulate a chronic inflammatory reaction, involving microglial activation and production of inflammatory cytokines likely contributing to neuronal dysfunction and cell death *per se*.

Regarding immunomodulatory strategy development, during the last years, it has been shown that Mesenchymal Stem Cells (MSCs) play a strongly immunomodulatory role, protecting the injured tissue and guiding anti-inflammatory processes by the secretion of cytokines and microvesicles (MVs), involved in their paracrine effects.

Furthermore many clinical studies are now performing therapies with MSCs and some phase I and phase II clinical trials in the oncology field are also studying MSC derived MVs (Dai et al, 2008 and Chaput and Théry, 2011).

Since the possibility that inflammation is not a mere consequence but a primary contributing factor in AD is becoming concrete, and given upregulation of inflammatory molecules (pro-inflammatory cytokines and chemokines) and activated glial cells surrounding the senile plaques in AD patients brains and AD transgenic animal models are now recognized as typical features of AD, the aim of this project is to assess the anti-inflammatory effects of MVs released by Bone Marrow Mesenchymal Stem Cells (BM-MSCs) in an AD context.

Both *in vitro* and *in vivo* experimental approaches are used to investigate the MV immunomodulatory effect and their ability to affect  $A\beta$  deposition and degradation.

Pro- inflammatory (TNF $\alpha$  and IL6) and anti-inflammatory cytokines (IL10) release was investigated by *in vitro* experiments performed on both microglial N9 cell line and on primary cortical cells exposed to human- $A\beta_{1-42}$  (h-  $A\beta_{1-42}$  ) and MSC derived MVs. For a more complete analysis of the cell inflammatory state, the microglia phenotype was assessed in order to determine whether a change from M1 to M2 cell phenotype was detectable.

The *in vivo* approach consisted of MV intracranial injections in a well-established transgenic AD chimeric murine model (APP<sup>swe</sup>/PS1<sup>dE9</sup>) that recapitulates many of the aspects of the human disease; to investigate whether MVs effects could be effective on the clearance and production of A $\beta$ , possibly ameliorating the neurodegenerative context, we analyzed A $\beta$  load, plaque area and density in three different brain areas: cerebral cortex, hippocampus and cerebellum.

The results obtained *in vitro* indicate that i) the administration of MVs promotes *in vitro* the secretion of anti-inflammatory cytokines, such as IL10; ii) MVs promote the switch of microglial cell to M2 phenotype, characterized by the typical amoeboid morphology, and increase the expression of CD206, a marker associated to the anti-inflammatory abilities; iii) MV administration significantly inhibits the release of the pro-inflammatory cytokines TNF $\alpha$  and IL 6 *in vitro* and accordingly, MHC II expression, which is associated with a pro-inflammatory phenotype, is down regulated in the presence of MSC-MVs.

On the other hand, *in vivo* results show that a single MV administration causes a significant reduction of A $\beta$  load into amyloid plaques and a decreased plaque area, into all three brain regions analyzed in 6 month old mice. In 3 month old treated mice, MV administration only affected A $\beta$  plaque density, that resulted smaller respect to untreated mice.

In conclusion, MVs released from BM-derived MSCs can exert, *in vivo*, a protective effect reducing the accumulation in plaques of A $\beta$ , possibly promoting the degradation and elimination of A $\beta$ <sub>42</sub> and participating in the regulation of neuroinflammation.

Future experiments will be directed to assess the safety of MV administration and to define whether a significant improvement of cognitive impairment is detectable in AD mice treated with BM-derived MSCs .

## INTRODUCTION

### **1. Mesenchymal Stem Cells (MSCs)**

Mesenchymal Stem Cell (MSCs), are classified as *Adult Stem Cells* (ASC), according to a classification based on their origin: in particular ASCs are present in most of the organs where they contribute to the structural and functional maintenance of the tissues.

Other types of stem cells are:

- *Embryonic stem cells* (ESCs), derived from embryos;
- *Stem cells* from extra-embryonic tissues (umbilical cord, placenta, amnios);
- *Induced Pluripotent Stem cells* (iPSCs), that originate from adult, somatic cells which have been reprogrammed to a stem cell-like state through the induction of some specific “pluripotency” factors.

Stem cells can be further classified on the basis of their differentiation ability. Accordingly, MSCs are Multipotent cells. Hematopoietic Stem Cells (HSCs) also belong to this category.

Two further categories are:

- *Totipotent cells*: they can originate all the lineages of the organism; a totipotent cell can give rise to Embryonic as well as extra-embryonic tissues in mammals, only the zygote and the first division-derived blastomeres up to the morula stage are totipotent.
- *Pluripotent cells*: they can differentiate into all the cell types derived from the three germ layers and into germ line cells, both in vitro and in vivo. This cell do not possess the ability to form extra-embryonic tissues. Embryonic stem cells (ESCs) are pluripotent cells.
- *Unipotent cells*: they can differentiate into a single cell type, These cells, which are only capable of self-renewal, are responsible for maintaining the structure and the homeostasis of adult tissues (Lodi D. et al., 2011).

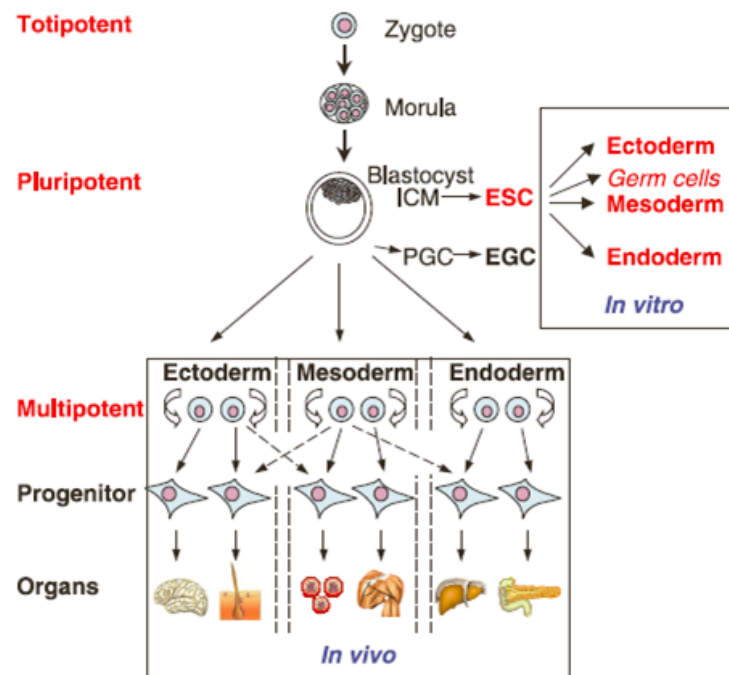


**Figure 1. Differentiation ability of stem cells.** **Totipotent stem cells** such as the zygote and the blastomeres up to the morula stage are able to form all the lineages of the organism. **Pluripotent stem cells**, such as embryonic stem cells, Originate from the inner cell mass and are capable of differentiating into all the cell types deriving from all the three embryonic germ layers: the ectoderm, the mesoderm and the endoderm. Conversely, **multipotent stem cells** can only differentiate into cell types deriving from a single embryonic layer. Finally, **unipotent cells**, give rise to one cell type only (adapted from Wobus et al., 2005).

In general, *Stem Cells* are undifferentiated cells that are responsible for the maintenance of tissue homeostasis and are able to functionally reconstitute a tissue *in vivo*.

A stem cell can undergo unlimited divisions in culture, to renew itself and differentiate into a specialized cell. Each division gives rise, at the same time, to a cell identical to itself and to a cell capable to become specialized. Thus, stem cells are able to differentiate into various types of specialized cells while preserving their functionality (figure 1).

Mesenchymal Stem Cells (MSCs), also called Mesenchymal Stromal Cells, can be isolated from different types of adult tissues and organs.

They represent a promising therapeutic strategy for many diseases, including cardiovascular, autoimmune and neurodegenerative diseases (Pittenger et al., 1999; Jiang et al., 2002).

The main features associated with the therapeutic effect of these cells are *tissue repair, immunomodulatory and anti-inflammatory activity and paracrine effects* (for a review see Lavoie and Rosu-Myles, 2013).

MSCs were identified and isolated for the first time around 1970, from the Bone Marrow and the Stroma of Spleen and Thymus by Friedenstein and Owen (1974), who described a population of adherent and fibroblast-like cells able to support hematopoiesis and to differentiate into adipogenic, chondrogenic and osteogenic cells.

Subsequent studies showed that MSCs can be also isolated from other tissues, such as adipose tissue, umbilical cord, skin, tendons (Bernardo and Fibbe, 2013), hair follicles, skeletal muscle, dental pulp, exfoliated deciduous teeth (Miura et al, 2003), lung, liver, spleen, thymus, brain (Krampera et al., 2006; Lavoie and Rosu-Myles, 2013), cartilage, periosteum, synovium, synovial fluid, fetal tissue, placenta (Pountos and Giannoudis, 2005) and amniotic fluid (Tsai et al., 2004).

### 1.1 In vitro MSC characterization

MSCs derived from different sources change in morphology, proliferation and differentiation potential capacity in response to diverse stimuli, and in the expression of surface markers (Phinney and Sensebè, 2013; Lofty et al., 2014).

In 2006 the Mesenchymal and Tissue Stem Cell Committee of the International Society for Cellular Therapy (ISCT) has established three minimal requirements that permit to uniformly characterize human MSCs, even when they are isolated from tissues of different origin (Dominici et al., 2006):

- *adherence to plastic*: the cells should grow adherent to plastic when maintained in culture;
- *specific surface antigen (Ag) expression*: more than 95% of the cell population should express CD90 (Thy-1 antigen), CD105 (known as endoglin) and CD73 (known as ecto 5' nucleotidase) (Barry et al., 1999). At the same time, they should be negative ( $\leq 2\%$  positive) for the expression of CD45 (a pan leukocyte marker), CD34 (that labels primitive hematopoietic progenitors and endothelial cells), CD11b or CD14 (markers for monocytes and macrophages), CD19 or CD79 $\alpha$  (markers for B lymphocytes) and HLA-DR (which is only expressed by MSCs upon IFN stimulation). The absence of these markers excludes the presence of hematopoietic cells that may contaminate MSC cultures, especially if BM- isolated.
- *multipotent differentiation potential*: in appropriate culture conditions MSCs should be capable to differentiate into adipocytes (by staining with Oil Red), chondrocytes (by staining with Alcian Blue) and osteoblasts (by staining with Alizarin Red) in vitro.



Over the years several efforts have been made to find single antigens specifically expressed by MSCs. Unfortunately, such a molecule does not seem to exist, as MSCs share common characteristics with many other cells, including endothelial, epithelial and muscle cells (Pountos et al., 2007).

Definitive markers of MSCs were proposed by Pittenger and colleagues (1999) who defined the different surface epitopes that allow MSC recognition:

- integrin receptors, including CD29, CD49a, CD49f, CD51;
- adhesion molecules, such as CD44, CD105, CD106, CD146 and CD166;
- enzymes, such as CD39 and CD73;
- growth factor receptors: CD140b, CD271, CD340 and CD349;
- intermediate filaments, including vimentin, nestin, desmin, neurofilament;
- embryonic antigens, as SSEA1, SSEA4 (Phinney and Sensebè, 2013).

The expansion of MSC in vitro can be affected by several factors, such as age, sex and state of health of the donor, culture methods (including the culture medium) and the in vitro number of passages (Pountos et al., 2007). After a large number of passages, indeed, MSCs lose their proliferative and differentiative capacity progressively losing their multipotency (Muraglia et al, 2000; Wang et al., 2013): this phenomenon is related to the gradual shortening of telomeres, called senescence (Wang et al., 2013).

## 1.2 Bone Marrow-derived MSCs

Two types of stem cells are present in the bone marrow (BM): *Hematopoietic Stem Cell* (HSCs) and *Mesenchymal Stem Cells* (MSCs) (Colter et al., 2001; Boxall and Jones, 2012).

MSCs, whose name was coined by Caplan in 1991, constitute only 0.01% of the BM total cell population (Pountos et al., 2007). Within the vascular system, MSCs are localized in anatomical niches distinct from HSCs areas. The latter in fact, reside in the endosteum, while MSCs are localized in the stroma, the supporting tissue of BM hematopoietic activity (Gebler et al., 2012).

MSCs' support hematopoiesis by producing and secreting factors such as factors, as cytokines, chemokines and adhesion molecules that stimulate hematopoietic stem cell proliferation and differentiation (Zhao et al., 2014). Moreover, they constitute a reservoir of stem cells for tissues of mesengenic origin: they reside within the hematopoietic niches in a state of quiescence, ready to migrate (this ability is called homing) to the various injured districts of the organism for

regeneration (Pountos et al., 2007). Cell migration can be induced by tissue damage, including trauma, fracture, inflammation, necrosis and tumors, or chemotactic signals (Pountos and Giannoudis, 2005).

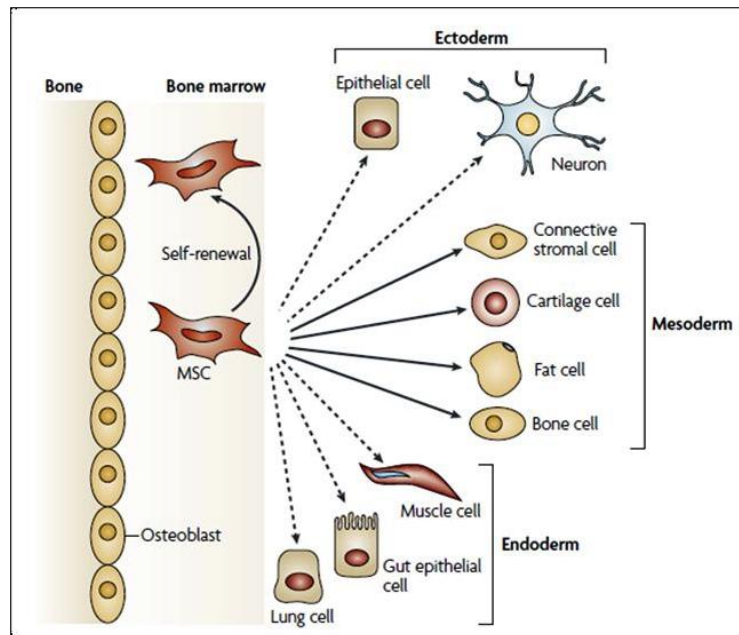


**Figure 2. Differentiating ability of Mesenchymal Stem Cells.** BM-derived MSC ability to proliferate and differentiate mainly into cells of mesodermal origin, and to endodermal and ectodermal origin (from Uccelli et al., 2008).

Despite their common germinal origin, HSCs and MSCs generate different kinds of cells: HSCs might differentiate into blood and immune system cells, while MSCs might differentiate into cells of mesenchymal origin, such as osteoblasts, adipocytes, chondrocytes (Gebler et al., 2012).

MSCs are also able to differentiate into other cell types such as cardiac myocytes (Orlic et al., 2001), fibroblasts, myofibroblast (Dicker et al., 2005), pericytes (Direkze et al., 2003), skeletal myocytes (De Bari et al., 2001), tenocytes (Pittenger et al., 2002), and may trans-differentiate into cells of endodermal and ectodermal origin, as hepatocytes, neurons, astrocytes, microglia and oligodendrocytes (Sanchez-Ramos et al., 2000; Colter et al., 2001; Bossolasco et al., 2005; Lavoie and Rosu-Myles, 2013) (figure 2).

### 1.3 Therapeutic properties of MSCs

In recent years, the therapeutic potential of MSCs has been assessed in different pathologies. indeed these cells are able to produce a large number of factors that influence

immunomodulatory, anti-inflammatory, neuroregulatory and trophic activities and that promote angiogenesis (Phinney and Sensebè, 2013).

Thanks to their *ability to interact with immune system cells and to regenerate a tissue*, MSCs have also been proposed as treatment for some autoimmune diseases, such as type I Diabetes, Rheumatoid Arthritis (RA), Systemic Lupus Erythematosus (SLE) and Multiple Sclerosis (MS) (Bernardo and Fibbe, 2012; Uccelli et al., 2008).

MSCs exert their regenerative action in a paracrine fashion: these cells respond to specific signals by migrating to injured tissues and contributing in loco to their repair. For example, MSCs can cross the blood brain barrier (BBB) and migrate to the injured brain in response to chemotactic factors such as cytokines and chemokines such as like transforming growth factor-beta (TGF- $\beta$ ), prostaglandin-E2 (PGE2), heme oxygenase-1 (HO- 1), indoleamine 2,3-dioxygenase (IDO) and extracellular matrix proteins (MMPs) (Bernardo and Fibbe, 2012; Uccelli et al., 2008).

Furthermore, several studies showed that MSCs are able to induce regeneration and trigger neuroprotective mechanisms both in vivo and in vitro models of neuronal injury (Karussis et al., 2008). In two studies (Zappia et al., 2005; Zhang et al., 2005) using a model of experimental autoimmune encephalomyelitis (EAE) that recapitulates Multiple Sclerosis, the authors observed that systemic MSC injection down-regulates the clinical symptoms of the disease, reducing inflammation and demyelination. These papers demonstrated that MSCs are able to migrate into the Central Nervous System (CNS) where they promote the secretion of various trophic factors, including brain-derived neurotrophic factor (BDNF), that may promote neurogenesis.

MSC administration has been tested in several clinical studies and seems to be safe and efficient. Cells, have been injected to regenerate bone and cartilage, replace pancreatic or liver tissue or to improve cardiac function after myocardial infarction with encouraging results (Caplan and Correa, 2011; Karussis et al., 2008).

Other studies have also demonstrated that MSCs are able to migrate to tumor sites. However, MSC influence on tumor growth have conflicting results in vivo: some studies, including those of Djouad (2003) and Ramasamy (2007) and colleagues, found MSCs to have pro carcinogenic activity. This is mediated by constitutive secretion of angiogenic factors such as VEGF, Interleukin 6 (IL-6) and MMPs, that stimulate neovascularization and promote tumor growth (Khakoo et al., 2006), argue the opposite: Khakoo and colleagues in fact, demonstrated that injection of MSCs inhibit tumor growth through E-cadherin-mediated cells contact and Akt downregulation in tumor cells.

A possible explanation of such different results can be that tumor microenvironment influences the behavior of MSCs. Further studies are needed to better understand MSC role in tumor growth (Uccelli et al., 2007).

#### 1.4 Immunomodulatory properties of MSCs

In addition to the regenerative and differentiation potential, MSCs have a *pleiotropic and immunomodulatory activity* both in vivo and in vitro. These stem cells are involved in mechanisms that promote tissue homeostasis and regulate inflammation processes. They are able to interact with the components of the innate immunity, with a dual effect: anti-inflammatory or pro-inflammatory. They are also called sensors of inflammation, depending on the environment they can acquire either a pro- or an anti-inflammatory phenotype which in turn influences the activity of the immune cells (Bernardo and Fibbe, 2013).

Innate immune cells express the Toll like receptors (TLRs). These receptors recognize specific molecules expressed by pathogens or associated with tissue damage. TLRs activation triggers the innate immune response that is mediated by the activation of phagocytic cells, such as macrophages and neutrophils, and the adaptive response. TLRs are also expressed by MSCs, where they exert an important regulatory role on their immunomodulatory activity. Activation of different TLRs induce specific phenotypes. For example, MSCs that express TLR4 express a pro-inflammatory M1 phenotype (named MSC<sub>1</sub>), while cells that express TLR3 express an anti-inflammatory, immunosuppressive M2 phenotype (named MSC<sub>2</sub>) (Waterman et al., 2010).

MSC<sub>1</sub> phenotype is important in the early response to injury and is characterized by the release of pro-inflammatory factors such as IL6, IL8, Macrophage Inflammatory Proteins 1- $\alpha$  and 1- $\beta$  (MIP1- $\alpha$  and MIP1- $\beta$ ), Chemokine (C-C motif) ligand 5 (CCL5, also known as RANTES), Chemokine (C-X-C motif) ligand 9 and 10 (CXCL9 and CXCL10). In addition, MSC<sub>1</sub> cells recruit lymphocytes at the site of inflammation and stimulate the effector response.

MSC<sub>2</sub> phenotype is involved in the late anti-inflammatory response and the following process of tissue repair. MSC<sub>2</sub> cells releaseIDO, PGE2, Nitric oxide (NO), TGF- $\beta$ , hepatocyte growth factor (HGF) and hemoxygenase (HO), IL4 and IL10. Finally, they inhibit the proliferation of T cells and stimulate the activation of T regulatory cells (Waterman et al., 2010; Yan H. et al., 2014).

The two MSC phenotypes not only differ in term of cytokine and chemokine secretion, but also in their ability to differentiate, to produce extracellular matrix, to modulate lymphocytic activation the TGF- $\beta$  pathway, the PGE2 and IDO expression and the effect on the T lymphocytes activation (Waterman et al., 2010).

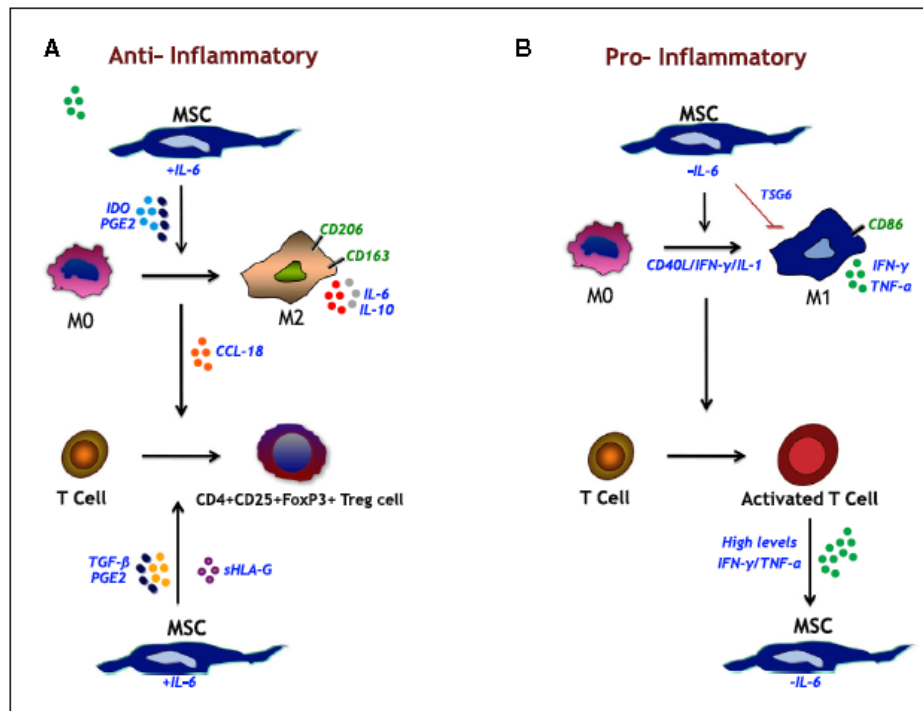


**Figure 3. Interactions between MSCs and macrophages.** A) MSCs constitutively produce IL6, that induces monocytes (M0) differentiation toward macrophages with a M2 phenotype. This polarization is also influenced by cell to cell contact and soluble factors, including IDO and PGE2. The interaction between MSCs and macrophages activates T regulatory cells (Tregs) both directly (via the production of CCL18) and indirectly(via the production of TGF $\beta$ ). B) In the absence of IL6, MSCs induce monocyte polarization towards M1 phenotype macrophages through secretion of IFN $\gamma$  and IL1 and surface expression of CD40L. The interaction between MSCs and macrophages induces T cell activation throughsecretion of IFN $\gamma$  and TNF $\alpha$  and expression of co-stimulatory molecules. High levels of pro-inflammatory signals act as a feedback mechanism and induce the anti-inflammatory pathway shown in fig. A (from Bernardo and Fibbe, 2013).

Depending on the microenvironment, MSCs influence the behavior of innate immunity cells (figure 3), such as macrophages (Bernardo and Fibbe, 2013), that are key players in the inflammatory response. In this context they can acquire two distinct functional phenotypes: the classical pro-inflammatory M1 phenotype or alternative anti-inflammatory M2 phenotype (Mantovani et al., 2013). Therefore, M1 macrophages release pro-inflammatory cytokines such as IL1, IL6, TNF $\alpha$ , and Interferon  $\gamma$  (IFN $\gamma$ ), whereas M2 macrophages secrete anti-inflammatory cytokines, such as IL10 and TGF $\beta$ 1, that promote the tissue regeneration (Mantovani et al., 2013). At the same time, macrophage-derived pro-inflammatory cytokines activate MSCs to release mediators that induce

the ripolarization of macrophages from M1 to M2. Therefore, MSCs and macrophages share a reciprocal regulatory feedback system that controls their ability to switch between pro-inflammatory and anti-inflammatory activities. However, when stimulated by high levels of pro-inflammatory cytokines, MSCs respond by adopting an immunosuppressive phenotype that stimulates macrophages to switch from M1 to M2 to restore the tissue homeostasis. On the other hand, the lack of pro-inflammatory cytokines is a signal for MSCs to promote the M1 phenotype (Bernardo and Fibbe, 2013).

As already mentioned, *MSCs possess immunosuppressive properties* that inhibit the activity of both innate and adaptive immunity cells, such as professional antigen presenting cells (APCs) (including B cells, dendritic cells, macrophages and NK cells) and T cells (figure 4). MSCs also inhibit monocyte maturation and induce a decrease in the expression of major histocompatibility complex (MHC) class II molecules, CD83 and CD11c, thereby limiting the antigen presenting function of dendritic cells.

Moreover, MSCs suppress the cytotoxic activity of NK cells by down-regulating the expression of the receptors involved in their activation. Furthermore, in the early stages of inflammation, when IFN levels are low, MSCs behave as non-professional APCs and express MHC class II antigen in their membrane. Afterwards, the increase in IFN levels induces these cells to switch to the immunosuppressive phenotype (for a comprehensive review see Uccelli et al, 2008).

In conclusion, MSCs represent a promising therapeutic tool suitable for different pathologies. Indeed, they:

- can be extracted from an adult bone marrow and easily cultured and expanded in vitro;
- have immunoregulatory properties;
- secrete factors that stimulate the endogenous neural stem cells in the CNS;
- can be used for autologous transplantation (in which the patient is the donor himself). Therefore avoiding immunosuppressive therapy;
- are less prone to genetic abnormalities during the in vitro culture with respect to other type of stem cells;
- can trans-differentiate and possess neural plasticity (Karussis et al., 2008).

However, the therapeutic use of MSCs may present risks linked to their possible immunogenicity, the safety of the culture medium used to grow the cells in vitro, the neoplastic transformation of the cells or the possible formation of ectopic tissue. Indeed, MSCs are not immunoprivileged. Thus, the transplantation of MSCs into immunocompetent and MHC-mismatched patients may

foster graft rejection. the culture medium used for the in vitro expansion contains fetal bovine (FBS). FBS may be immunogenic itself, or it may serve as a vehicle for pathogen transmission. In addition, MSCs proliferation can induce the formation of tissues of mesodermal origin at ectopic site. Finally, the prolonged time of in vitro culture may result in the accumulation of genetic alterations possibly leading to neoplastic transformation of cells (Bernardo and Fibbe, 2012).

Notwithstanding the need for further investigations concerning their biological properties and effectiveness, MSC administration in several diseases seems to be safe, without serious complications and ethical issues. For this reason, MSCs represent a promising therapeutic strategy (Pountos and Giannoudis, 2005).

## **2. Microvesicles (MVs)**

Cells in resting state or upon activation by soluble factors generated by chemical or physical stress conditions (such as oxidative stress or hypoxia, or serum deprivation in cultures), are known to release extracellular vesicles (EVs) as Apoptotic Bodies, Microparticles (MPs) and Microvesicles (MVs) and Exosomes (Exo) (Ratajczak et al., 2006<sup>2</sup>; Smith J. A. et al, 2014) (figure 4).

These vesicles mediate a paracrine action, are involved in both physiological and pathological mechanisms and are released by cells into the microenvironment and the biological fluids (Chaput and Théry, 2011; Tetta et al., 2011).

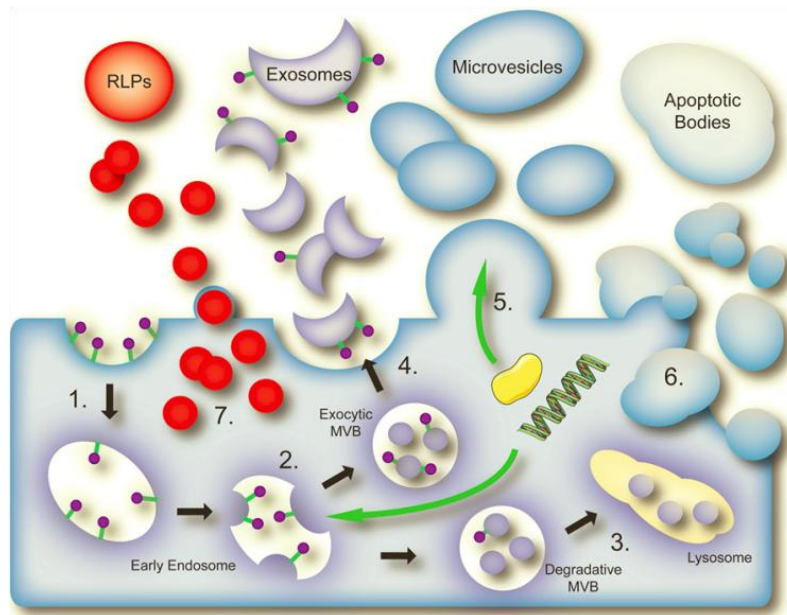


**Figure 4. Representation of extracellular vesicles (EVs) released by cells and the four possible general pathways of membrane vesicle biogenesis.** EVs include Exosomes, Microvesicles (MVs) and Apoptotic Bodies and Retrovirus-like particles (RLPs). 1 Exosomes arise from an endocytic pathway that begins with the invagination of receptor-coated plasma membrane to form an endosome and (2) Intraluminal vesicles bud off into the endosome. (3) The endosome matures into a MVB, which is subsequently destined for either degradation within a lysosome, or (4) exocytosis whereby exosomal EVs are released into the extracellular milieu. (5) Microvesicles (shedding vesicles) arise from direct budding and fission of portions of the plasma membrane, encapsulating a cargo of cytoplasmic proteins and nucleic acids from the cytosol as they do so. (6) The shrinkage and fragmentation of apoptotic cells gives rise to so called apoptotic bodies or blebs, (7) while an unknown mechanism believed to involve transcription of endogenous retroviruses leads to the formation of RLPs. (from Smith et al, 2014).

EVs were described for the first time by Chargaff and West in 1946, who characterized a “*precipitable factor*” present in the plasma with the potential to generate thrombin (Chargaff et al., 1946).

EVs are structurally, biochemically and functionally different depending on the mechanism of secretion, the cell type from which derive and its physiological condition, and the site of origin. Other factors, such as sex, age, circadian rhythms, exposure to drugs and physical activity can affect the number and nature of the released vesicles.

Nowadays, most of the research in this field focuses on the study of EVs from plasma and serum, but vesicles can be isolated also from pleural effusions, ocular effluent and aqueous humor, milk, tumoral effusions, ascites, amniotic or bronchoalveolar fluid, bile, sperm, saliva, urine and cerebrospinal fluid (Quesenberry et al., 2014).

EVs can originate from the most cell types, including placental, stem cells (Tetta et al., 2011), intestinal, epithelial cells, Schwann or oligodendroglial cells, tumor cells, reticulocytes, mast cells,



dendritic cells, platelets, B and T lymphocytes, microglia, neurons, astrocytes, fibroblasts, keratinocytes and endothelial cells (Chaput and Théry, 2011; György et al., 2011; Lai et al., 2013). Based on the source, the size and the content (Biancone et al., 2012), EVs can be classified into three main classes: Apoptotic Bodies (size range 1- 5  $\mu\text{m}$ ), Shedding Vesicles (size range 0,1- 1  $\mu\text{m}$ ) and Exosomes (size range 0.5- 0.1  $\mu\text{m}$ ) (György et al., 2011). The table in figure 5 (figure 5C) describes the main features of exosomes and shedding vesicles. Variables such as the nature or pathological state of the parent cell will influence the type and contents of EVs ( Smith J.A., et al, 2014).

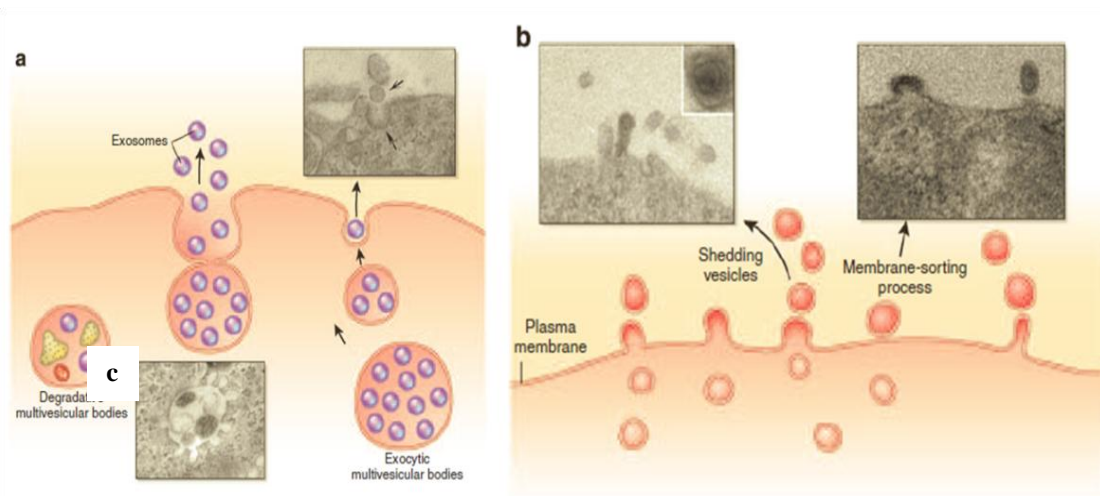


**Table 1** Key features of membrane vesicle populations

	Exosomes	Microvesicles	Apoptotic bodies
Size range	Approximately 50–100 nm	100–1,000 nm (~ 100–400 nm in blood plasma) [2, 22, 38]	1–5 $\mu\text{m}$ [61]
Mechanism of generation	By exocytosis of MVBs	By budding/blebbing of the plasma membrane	By release from blebs of cells undergoing apoptosis
Isolation	Differential centrifugation and sucrose gradient ultracentrifugation [25], 100,000–200,000g, vesicle density is 1.13–1.19 g/mL	Differential centrifugation [39] 18,000–20,000g	Established protocols are essentially lacking; most studies use co-culture with apoptotic cells instead of isolating apoptotic bodies
Detection	TEM, western blotting, mass spectrometry, flow cytometry (bead coupled)	Flow cytometry, capture based assays [38, 52]	Flow cytometry
Best characterized cellular sources	Immune cells and tumors	Platelets, red blood cells and endothelial cells	Cell lines
Markers	Annexin V binding, CD63, CD81, CD9, LAMP1 and TSG101 [23, 24]	Annexin V binding, tissue factor and cell-specific markers	Annexin V binding, DNA content
Recent review articles	[2, 22, 23, 26–35]	[2, 24, 35, 53–57]	

**Figure 5. Representation of biogenesis of exosomes and shedding vesicles formation.** A | Release of exosomes from the multivesicular bodies. B | Formation of shedding vesicles from budding of the plasma membrane. C | The table describes the main differences between exosomes and shedding vesicles (adapted from Camussi et al., 2010 and György et al., 2011).

## 2.1 Isolation of EVs

There are several methods for isolating EVs. Most of them are based on a series of differential centrifugations and ultracentrifugations with or without separation by density gradient. Other approaches employ techniques based on size or immunoaffinity separation as *Western Immunoblot*, *Mass Spectroscopy*, *Dynamic Light Scattering* analysis (DLS), *Atomic Force Microscopes* (AFM) or *Flow Cytometry* (FACS).

However, the gold standard technique the determination of vesicle size is *Transmission Electron Microscopy* (TEM): this is the only technique that permits to achieve a reliable identification of EVs both in terms of size and structure. On the other hand, the Flow Cytometry Allows to characterize EVs on the basis of the expression of surface antigens. Nonetheless FACS presents a limit of resolution of 200 nm making impossible the detection of vesicles smaller than this size (György et al., 2011).

An innovative technique that allows to study the smallest EVs is the *Nano-Plasmonic Exosome Assay* (nPLEX), a *Surface Plasmon Resonance* (SPR)-based assay for label-free, high-throughput exosome protein analyses that has a higher sensitivity than the above mentioned techniques. It consists of arrays functionalized with antibodies able to recognize both surface and intravesicular (lysate) proteins expressed on/in EVs. Thus, nPLEX is a very useful method for the quantitative analysis of EV content, in particular for Exo (Im et al., 2014).

## 2.2 Exosomes (Exo)

Exosomes (Exo) are vesicles derived from the endosomal membrane, with a variable size from 30 to 120 nm (Tetta et al., 2011), a cup-shaped morphology and a density between 1.13 and 1.19 g/mL, depending on the producing cell type (Chaput and Théry, 2011). Due to the small size, exosomes can be hardly visualized by fluorescence, transmitted light microscopy or flow cytometry.

### **2.2.1 Origin and molecular composition of Exo**

Exo originate from the endosomal compartment that sorts multiple small intraluminal vesicles (ILVs) and targets them to their destinations, including lysosomes and cell surface membranes for

degradation, recycling or exocytosis (Akers et al., 2013). Endosomal compartment consists of several vesicular organelles, such as the primary endocytic vesicles, the early endosomes, the recycling endosomes, the late endosomes and the lysosomes.

The late endosomes that contain ILVs are also called multivesicular bodies (MVBs). MVB formation is coordinated by the endosomal sorting complex required for transport (ESCRT), a multiprotein complex consisting of four protein complexes called ESCRT-0, ESCRT-I, ESCRT-II and ESCRT-III. These multi protein systems recruit ubiquitinated proteins and assemble them to form MVBs (Wollert and Hurley, 2010). MVBs are formed by budding of membrane the ILVs, that contain the cargo protein. MVBs can fuse with lysosomes to degrade their protein content. Alternatively, they can fuse with the plasma membrane and release ILVs in the extracellular space. Extracellularly –released ILVs are called exosomes. (figure 4). Exosome secretion and release is mediated by the activity of several Rab-GTPases, including Rab 5, 11, 27 and 35 that regulate the vesicular transport between the organelles (Ludwig and Giebel, 2012; Raposo and Stoorvogel, 2013) and by the activation of the cytoskeleton and the p53 protein (Yu et al., 2006).

Exo contain a defined set of cellular proteins. Some of them are common to all the exosomes, whereas other are cell type-specific (Chaput and Théry, 2011). Examples of common proteins are *tetraspanins* (CD63, CD81, CD9 and CD82) (Ludwig and Giebel, 2012), *cytoskeletal proteins* (actin and tubulin), *surface peptidases* (CD13 and CD23), *lipid-binding protein MFGE8* (milk fat globule-EGF/factor VIII), *GPI-anchored molecules* (CD55 and CD59), *clathrin*, *heat-shock proteins* (Hsp, such as Hsp60, Hsp70 and Hsp90).

Exosomes also contain endosome-associated proteins, such as *Rab GTPases*, *SNAREs*, *Annexin*, *Alix*, *Tumor susceptibility gene 101* and *flotillin* (Tsg101), some of which are involved in MVB biogenesis (Théry et al., 2001; Van Niel et al., 2006).

### 2.3 The shedding vesicles (SV)

Shedding vesicles include Ectosomes, Microparticles or Microvesicles (MVs). Unlike exosomes, they originate from small protrusions of the plasma membrane and include vesicles with a irregular shape and heterogeneous size, from 100 nm to 1 µm (Ratajczak et al., 2006<sup>1</sup>; Tetta et al., 2011; Biancone et al., 2012).

Few techniques allow to accurately separate MVs, for example the flow cytometry. One of the most popular techniques for isolating the shedding vesicles is the immuno-precipitation, that

involves the use of antibodies against antigens present on the outer side of the vesicle (Cocucci et al., 2007 and 2009).

### ***2.3.1 Biogenesis and molecular composition of shedding vesicles***

Vesicles form as the result of dynamic interplay between phospholipid redistribution and cytoskeletal protein contraction. Shedding vesicles formation occurs through budding of cytoplasmic protrusions which detach from the cell membrane (Cocucci et al., 2009). The plasma membrane has an asymmetric protein and phospholipid distribution, that forms micro-domains. This asymmetric distribution is regulated by aminophospholipid translocases, including flippases and floppases, that transfer phospholipids from one leaflet of the plasma membrane to the other. Vesicle formation is promoted by translocation of phosphatidylserine to the outer-membrane leaflet. The process is completed by the contraction of cytoskeletal structure (Akers et al., 2013). MV release occurs constitutively in resting cells but the rate of the process increases upon stimulation. In the latter case, MV release depends on calpain, cytoskeleton reorganization and intracellular calcium concentration (Tetta et al., 2011). Secretion indeed, can be induced by different kinds of stimuli, including the increase of intracellular calcium and activation of protein kinase C (PKC) and purinergic receptors of ATP (Cocucci et., 2009).

MVs express a some ubiquitous proteins, such  $\beta$ 1 integrin (Cocucci et al., 2009). Their lipid content includes phosphatidylserine, which is abundant in the plasma membrane, cholesterol, sphingomyelin, ceramide and membrane lipid raft -associated proteins (Camussi et al., 2010; Biancone et al., 2012). Another common marker of MVs is Annexin V (Garzetti et al., 2014).

In spite of a common secretion process, shedding vesicles of distinct cells can be molecularly different from each other and may be enriched with metalloproteinases and other proteolytic enzymes, integrins, cytokines, growth factors and plasma membrane glycoproteins Specific for each cell type (Cocucci et., 2009).

## **2.4 Interaction with target cells**

Once they have been released into the extracellular space, exosomes and shedding vesicles communicate with target cells upon a specific interaction (Cocucci et., 2009). The effects of EVs in

both physiological and pathological processes depend on their ability to interact with cells and to deliver their content, including proteins, lipids, and RNAs.

Vesicles interact with their target cells by binding to specific receptors that induce fusion of the vesicle with the plasma membrane of the recipient cell or by a process of endocytosis that is regulated in different ways depending on cell type (figure 6) (Raposo and Stoorvogel, 2013).

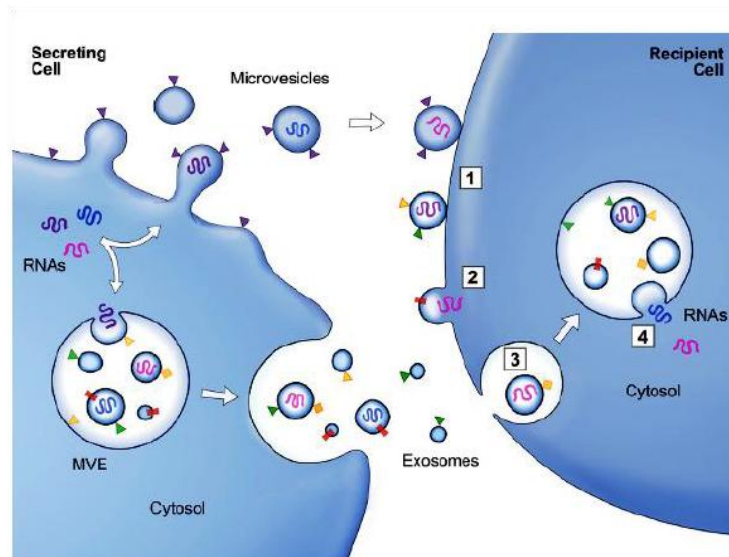


**Figure 6. Interaction between EVs and recipient cell.** Shedding vesicles (MVs) and exosomes interact with target cells by contact (1) and direct fusion with the plasma membrane (2) or endocytosis (3). Once internalized, vesicles may fuse with an endocytic compartment and finally, deliver proteins and RNAs to recipient cell (4). MVE: multivesicular endosome (from Raposo and Stoorvogel, 2013).

Vesicle fusion has been documented in different cell types through fluorescence microscopy associated with cell live-imaging (Tian et al., 2010; Montecalvo et al., 2012).

EVs content can influence the behavior of the recipient cell in multiple ways: by direct stimulation, by delivery proteins and receptors or by a horizontal transfer of genetic information (Ratajczak et al., 2006<sup>1</sup>).

## 2.5 EV content and biological role

EVs contain surface receptors, proteins, lipids and RNA, in particular messenger RNAs (mRNAs) and micro RNAs (miRNAs), that contribute to regulate the epigenetic and proteomic properties of the target cell (Hunter et al., 2008; Biancone et al., 2012). Among the receptors and surface molecules expressed by many types of vesicles are the tissue factor (TF), TNF $\alpha$ , the chemokine receptors CCR5 or CXCR4, the intercellular adhesion molecule 1 (ICAM1) and the delta-like 4 (Dll4,

a transmembrane Notch ligand). EVs may also contain growth factors and proteases (Biancone et al., 2012). In addition, they express specific molecules of the cell types of origin (Chaput and Thèry, 2011). Exosome content was studied in more detail, compared to shedding vesicles (Raposo and Stoorvogel, 2013).

EVs play an important role in intercellular communication by transferring Proteins and genetic material between cells to modulate their function. In this manner they may extend or amplify to the surrounding environment or other cells, a typical effect of the cell of origin (Chaput and Thèry, 2011). In spite of their small size, EV content may have striking effects on fundamental processes such as cell growth, differentiation and cancer progression (Hunter et al., 2008).

EVs are also involved in antigen presentation, And immunomodulation (Chaput and Thèry, 2011). Moreover, EVs can be used as natural drug delivery vehicles since they could be loaded with specific molecules (Lai et al., 2013).

Ratajczak and colleagues (2006<sup>1</sup>) were the first to describe EV effects on target cells. They demonstrated that MVs derived from embryonic stem cells (ESCs) are able to reprogram hematopoietic progenitors through a mRNA-dependent mechanism and protein delivering.

Moreover, EVs may alter the expression of genes in target cells by transferring miRNAs (Tetta et al., 2011), which are important regulators of protein translation.

## 2.6 BM MSC-derived microvesicles

BM-MSC derived MVs (hereafter MVs will indicate both exosomes and shedding vesicles, as widely accepted) express several adhesion molecules present on the cell of origin, such as: CD44 and CD29 involved in the internalization of the vesicles to the target cell (Bruno et al., 2013<sup>1</sup>); CD73, the enzyme responsible for the formation of extracellular adenosine from released adenine nucleotides (Arslan et al., 2013; Bruno et al, 2009), CD105, an endoglin (Barry et al., 1999; Bruno et al., 2013<sup>1</sup>), CD90 that mediates cell-cell interactions (Haeryfar et al., 2004; Kim et al., 2012), CD13, a surface peptidase. They also express CD107a, an intracellular protein located on the lysosomal/endosomal membrane, a lysosome-associated membrane protein 1 (LAMP-1) usually expressed on endosomal and lysosomal membranes (Conforti et al., 2014).

The RNA content depends on the cell of origin and includes several mRNAs associated with the MSC mesenchymal differentiative phenotype and with many other functions such as gene transcription, proliferation, regulation of the immune system (Bruno et al., 2013<sup>1</sup>), angiogenesis

(Eirin et al., 2014), cell adhesion and migration and actin cytoskeleton organization (Kim et al., 2012).

MVs are also enriched in mRNAs that regulate the p53 dependent apoptotic pathway, such as the p53-negative regulators MDM4 and the paternally expressed-3 (PEG3). They contain transcription factors involved in pro-angiogenic pathways, like the hepatocyte growth factor (HGF), that stimulates the proliferation and migration of endothelial and vascular smooth muscle cells, and proteins of TGF- $\beta$  family, that regulate proliferation, differentiation, extracellular matrix production and apoptosis (Eirin et al., 2014).

The main proteins contained in MVs can be classified into four groups (Kim et al., 2012):

- *surface receptors*:  $\beta$ -type platelet-derived growth factor receptor (PDGFR $\beta$ ), involved in tissue repair, the epidermal growth factor receptor (EGFR), that stimulates proliferation and differentiation, and the plasminogen activator urokinase receptor (PLAUR), that stimulates mobilization, migration and differentiation of MSCs;
- *signaling molecules*: RRAS/NRAS, MAPK1, GNA13/GNG12, CDC42 and VAV2, Involved in MSC recruitment, proliferation and differentiation;
- *cell adhesion molecules*: fibronectin (FN1), that regulates the migration of MSCs, integrins and their associated molecules (CD47, ITGA1/2/3/5/7/10/11/V and ITGB1/3/5), involved in fibronectin-mediated MSC migration, galectin-1 (encoded by LGALS1 gene) that regulates embryogenesis, cancer metastasis, proliferation, differentiation, migration, adhesion, angiogenesis and immunomodulation; finally EZR and IQGAP1 that regulate proliferation and angiogenesis of the endothelial cell;
- *MSC-associated antigens*: CD9, CD63, CD81, CD90, CD109, CD151, CD248 and CD276, that play roles in neurogenesis, anti-inflammation, apoptosis, adhesion, migration, tumor suppression and fibroblast proliferation.

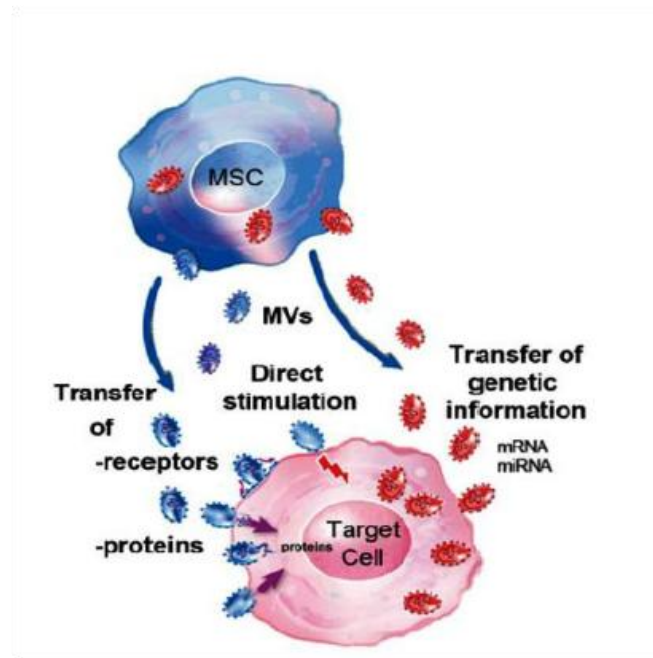


**Figure 7. BM MSC communication to the target cells.** MVs can interact with cells by direct or by transfer of receptors, proteins or genetic information (from Biancone et al., 2012).

As previously mentioned, after being released into the extracellular space, MSC-derived MVs can interact with the target cell through different mechanisms (figure 6 and 7):

- *by direct stimulation of the target cell through surface expressed receptors;*
- *by fusion with the cell membrane and transfer of receptors and bioactive factors;*
- *by horizontal transfer of genetic material, such as mRNAs and microRNAs that induce functional changes into the target cell (Biancone et al., 2012).*

Camussi's group (Collino et al., 2010) demonstrated that MVs derived from MSCs contain specific patterns of miRNAs. Some of them (for example miR-103-1, -140, -143-5p and -340) are also present in the cell of origin, but some other (miR-223, miR-564 and miR-451) are MV-specific. These findings support the theory of a specific and organized package of miRNAs in MVs before their secretion. The authors also demonstrated that miRNAs shuttled by MVs are able to down-regulate their specific target. These data suggest that MVs may interact with target cells also through miRNA delivery.

## 2.7 Therapeutic applications of BM-MSc derived MVs

By a therapeutic point of view, MSC-derived MVs are attractive tools for harnessing the clinical benefits of MSC through a natural product that possesses the same biological properties of the cell



of origin without the issues regarding engraftment of MSCs, immune rejection following allogeneic cell administration and the development of ectopic tissue (Mokarizadeh et al., 2012; Akyurekli et al., 2015). However, safety and efficacy of therapeutic MV administration requires a molecular characterization of their content, that can be loaded or change with specifically bioactive factors to suit therapeutic needs (Akyurekli et al., 2015; Conforti et al., 2014).

For the reasons, MVs represent a promising alternative therapeutic strategy to MSC infusion even if this technique has been already experimented in a number of animal models of organ injury, tumor and immune modulations (Akyurekli et al., 2015; Conforti et al., 2014).

One of the first in vivo studies in this field was published by Camussi and colleagues (Bruno et al., 2012). Previous studies (Morigi et al., 2004; Bi et al., 2007; Bruno et al., 2009) demonstrated that MSC treatment reduces mortality in an animal model of cisplatin-induced lethal acute kidney injury (AKI), by promoting functional and morphological recovery of renal cells. Based on this evidences, Camussi and colleagues (Bruno et al., 2012) demonstrated that also MSC derived-MVs are able to rescue kidney functions by inducing the expression of anti-apoptotic genes and down-regulating pro-apoptotic genes.

Therapeutic administration of MVs was also studied for *autoimmune disease* treatments. Mokarizadeh and colleagues (2012) studied MSC-derived MVs in a murine model of EAE. They demonstrated that MVs express mediators of peripheral tolerance, including Programmed Death Ligand-1 (PD-L1), galectin-1 and TGF- $\beta$  and are also able to suppress auto-reactive T lymphocyte proliferation, inhibit tissue damages and prompt these cells to secrete anti-inflammatory cytokines.

Moreover, in the *oncology field*, it was observed that MVs, both in vitro and in vivo, inhibit the cell cycle of tumor cells, inducing apoptosis or necrosis, thereby blocking the growth and survival of the tumor. One of the reasons of this effect is that the substitution of MSCs with MSC-derived MVs avoids the risk of the former differentiating into stromal fibroblast, that would promote the tumor growth (Bruno et al., 2013<sup>2</sup>).

Furthermore, Lee JK and colleagues (2013) were the first to demonstrate that miRNAs transported in MVs can reprogram the tumor microenvironment: their work shows that MVs inhibit angiogenesis both in vitro and in vivo by down-regulating the expression of vascular endothelial growth factor (VEGF) in cancer cells and consequently, inhibiting the proliferation and migration of endothelial cells. MV effect seems to be associated with the down-regulation of miR-16, that is shuttled to cancer cells by vesicles.

On the other hand, in an in vitro model of Graft Versus Host disease (GVHD) Conforti and colleagues (2014) demonstrated that the effect produced by MVs is not as incisive as that produced by MSCs: MVs in fact, seem to induce only a mild inhibition of the activation of T lymphocytes, suggesting that they might not induce a clinically significant response in vivo.

To date, few clinical trials have tested MV efficacy in patients and these trials have been mainly realized in late-stage cancer patients (Escudier et al., 2005; Dai et al., 2008). Phase I trials that involved the administration of MVs to elicit an immune response against established tumors, demonstrated the safety and the good tolerability of the treatment (Chaput and Théry, 2011). One of the first phase I clinical trials was guided by Dai and colleagues (2008), who co-administered MVs and granulocyte macrophage colony-stimulating factor (GM-CSF) in patients with colorectal cancer. MV treatment was well tolerated by patients and induced a tumor specific cytotoxic T cell response causing a minimal toxicity.

Starting from these assumptions, phase II clinical trials based on MV administration have been set up. In particular exosomes have been employed in oncology with diagnostic and/or therapeutic purposes (<http://clinicaltrials.gov>) (Chaput and Théry, 2011).

In conclusion, despite MVs have been tested in different animal models for several diseases with promising results, their biodistribution, cellular uptake and pharmacokinetic properties have yet to be fully investigated (Chaput and Théry, 2011). Hence, there is still a great need of understanding the mechanisms responsible for the benefits induced by MVs in regenerative medicine.

### **3. Microglia**

Brain has long been considered an immune privileged organ, because of its reduced ability of antigen presentation (Galea et al., 2007) and above all, for the presence of blood-brain barrier (BBB) (Block and Hong, 2005). Nevertheless, despite a different immunological capacity from other peripheral tissues, the brain is able to set a substantial immune response when it is required. This evidence is supported by the existence of several neurodegenerative diseases that are characterized by activation of brain-resident cells following an inflammation insult and leukocyte infiltration from the periphery (Block and Hong, 2005).

Immune response of Central Nervous System (CNS) is mediated by specialized cells of innate immunity, such as microglia, macrophages and dendritic cells (DC). Macrophages and DC are responsible for the local immune surveillance and are located in the meninges, choroid plexus and perivascular spaces (Nayak et al., 2012); on the other hand microglial cells, that perform many functions, are localized in parenchyma.

Microglial cells represent 10-15% of the total glia and are often referred to as CNS tissue-resident macrophages. Unlike macrophages though, microglial cells originate from the yolk sac and populate the CNS even before the vasculogenesis (Ginhoux et al., 2010; Greter et al., 2013).

Microglial cells are morphologically different from neurons and astrocytes and for this reason, in 1913, were classified by Santiago Ramon y Cajal as the third CNS element (Harry, 2013).

Microglial cells reside in all the major brain regions, with differences in density and distribution and, depending on the region where they are located, microglial cells differ in terms of ramification and surface antigen expression (Harry GJ et al, 2013).

Microglial cells are involved not only in CNS development and homeostasis, but also in the pathogenesis of diseases. Indeed, alterations in the phenotype, morphology and function of microglial cells are present in different disorders, such as degenerative diseases, infection, stroke, tumors and brain injury (Nayak et al., 2014).

### 3.1 Microglia development

Owing to phenotypic similarities with macrophages, scientists originally supposed that microglial cells had hematopoietic origin and derived from circulating monocytes (Ginhoux et al., 2013). In 1990, Cuadros and colleagues (1993) generated chimeras between chick embryos and quail yolk sac (YS) to establish that primitive myeloid cells invade the brain despite the hematopoietic system is still developing. Their study was the first to suggest the embryonic yolk sac origin of microglial cells (Nayak et al., 2014). Subsequently, other studies supported this hypothesis. The definitive evidence was given by the study of Ginhoux and colleagues (2010), who demonstrated that microglial cells derived from CD45-c-kit<sup>+</sup> erythroid myeloid progenitor cells (the primitive macrophages) arise from embryonic YS during the development (Kierdorf et al., 2013). Then, the progenitors invade the rudimentary BBB by the action of matrix metalloproteinases (MMPs), including MMP-8 and MMP-9, and colonize the brain (Nayak et al., 2014).

The differentiation of myeloid progenitors into microglial cells is regulated by several molecules, including transcription factors, growth factors, chemokines, MMPs and microRNAs, some of which are involved in the development of the hematopoietic system (Nayak et al., 2014). On the other hand, in adult CNS homeostasis is preserved by a fine balance among mitosis and apoptosis of microglial cells (Wirenfeldt et al. 2007).

### 3.2 Microglia phenotypes

In the adult brain, microglial cells play many roles and undergo not only functional, but also morphological changes. In particular, Del Rio Hortega identified three types of microglial morphology: ramified, intermediate and ameboid. Each morphology was then associated to a specific function (figure 8) (Lynch, 2009).

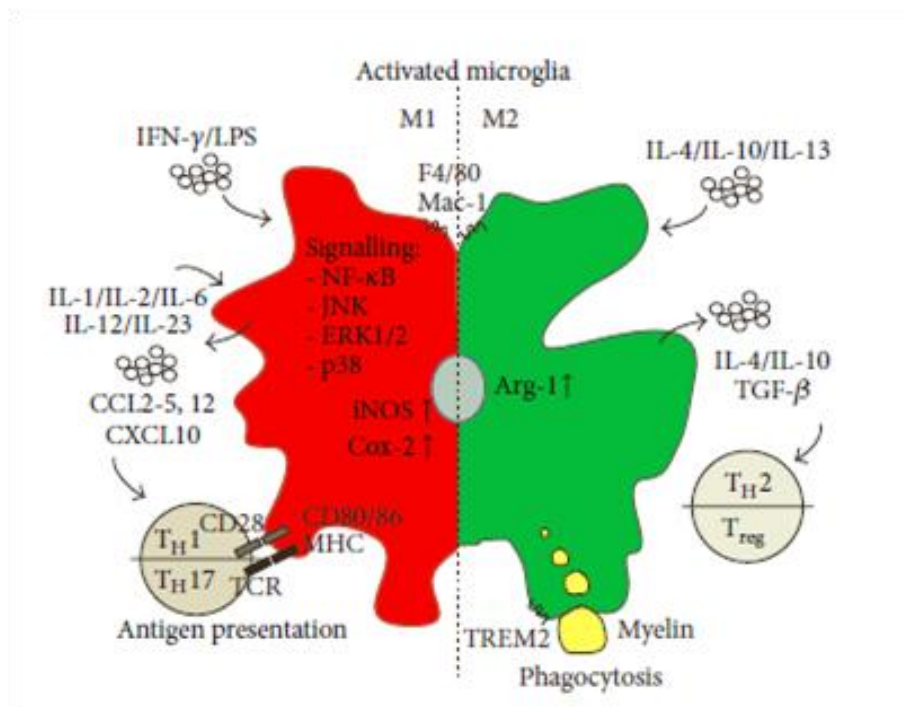


**Figure 8. Activated microglial cells display two possible phenotypes: pro-inflammatory M1 or anti-inflammatory M2.** M1 phenotype is induced by inflammatory molecules and is involved in Th1/Th17 response. M2 phenotype stimulates T regulatory cell functions and the release of anti-inflammatory cytokines (from Goldman and Prinz, 2013).

In homeostatic conditions, microglial cells present a resting phenotype characterized by a ramified morphology, a small amount of perinuclear cytoplasm and a dense and heterochromatic nucleus. Their processes are active and continuously interact with the surrounding microenvironment for

immune surveillance: for this reason they are also called monitoring microglia (Nimmerjahn et al., 2005). Apart from processes, cells are not motile and do not display phagocytic activity. They express minimal levels of surface marker and constitutively release low levels of cytokines and chemokines (Lynch, 2009).

In response to an immunological stimulus or to brain damage, microglial cells become activated: they retract their processes, migrate to damaged site and switch to an amoeboid macrophage-like morphology, characterized by somal expansion and enlargement of the processes (Harry GJ et al., 2012).

This phenotype responds not only to changes in brain structural integrity (mechanical and chemical trauma), but also alterations in the microenvironment (as alteration of ionic homeostasis) or exogenous or endogenous insult (like infection, ischemia, inflammation, cell death, accumulated debris, aberrant proteins or pathogens) (Kreutzberg, 1996).

The main functions of amoeboid microglial cells are: proliferation, migration, phagocytosis, antigen presentation and up-regulation of innate immune system (Vilhardt et al., 2005).

The concept that also microglia, like other immune peripheral cells, can be divided in activation phenotype subclasses is recent and the original classification become very simplistic. In fact for microglia a deeper understanding of the heterogeneity and different phenotypes is needed since immunomodulation and regulation in CNS is very complicated and it has yet to be unravelled (Cherry et al. 2014).

To simplify, activated microglial cells can be divided into two main phenotypes that are identified by the expression of cell surface antigens (figure 8): "classical" M1 or "alternative" M2, based on the nature of the stimulus and the effect produced, either neurotoxic or neuroprotective (Goldmann and Prinz, 2013).

M1 microglia are non-phagocytic cells secreting pro-inflammatory and cytotoxic soluble factors, including cytokines, such as IL1 $\alpha$ , IL1 $\beta$ , IL6, IL12, IL23, prostaglandins, chemokines, monocyte chemoattractant (MCP) protein, such as MCP-1 and CCL2, IFN $\gamma$  inducible protein 10 (IP-10), macrophage inflammatory protein 1 $\alpha$  (MIP-1 $\alpha$ , also called CCL3), fractaline like CX3CL1, proteases, reactive oxygen species (ROS), superoxid, TNF $\alpha$ , nitric oxide synthase (iNOS) (Lynch, 2009). In particular M1 microglia increase the crosstalk with other immune cells through MHC II, CD86 and Fc $\gamma$  expression and the production of reactive oxygen species and reactive nitrogen species by iNOS, (Cherry et al. 2014).

The alternatively activated M2 macrophage phenotype was initially classified on the basis of the expression of the mannose receptor (CD206); Through the years a variety of different markers has been identified as 'M2' specific (Cherry et al. 2014).

M2 phenotype is characterized by motile and phagocytic cells, that secrete anti-inflammatory factors, such as IL10 and TGF $\beta$ , Arginase 1 (Arg1), mannose receptor (MRC), and Chitinase-3-like-1 (YM1 in rodents). These molecules promote neuronal survival, tissue repair and the resolution of inflammation (Harry GJ, 2013). In addition, cells express surface scavenger receptors, purinergic receptors, Toll-like receptors (TLRs) 1-9, CD40 and the triggering receptor expressed on myeloid cells (TREM-2) (Lynch MA, 2009).

Three distinct alternative activation states have been identified: *pro-regenerative M2a*, *immunoregulatory M2b* and *deactivated M2c phenotype*.

- *M2a phenotype* is promoted by Th2 lymphocytes and is characterized by high expression levels of the macrophage mannose receptor (CD206), Arginase 1 (Arg1), Chitinase-3-like-1 (also known as YM1, Zanier et al., 2014) CD36, Stabilin-1 and heparin-binding lectin (Fizz1) (Pepe et al., 2014). Cells in this activation state possess a reduced phagocytic ability, play a pro-regenerative function and secrete anti-inflammatory cytokines, such as IL4 and IL13 (Zanier et al., 2014).
- *M2b phenotype* is characterized by an immunomodulatory action and the expression of specific markers, such as suppressor of cytokine signalling 3 (SOCS3), SphK1 and IL-1RN (Chhor et al., 2013).
- *M2c phenotype* is promoted by regulatory T lymphocytes and is characterized by high levels of CD68 expression, a marker of the lysosomal phagocytic activity (Lynch MA, 2009) and by expression of molecules related to tissue repair and immunosuppression. These cells secrete anti-inflammatory cytokines, including IL10 and TGF $\beta$  and express high levels of IL-4R $\alpha$ , Arg1, scavenger receptor A, scavenger receptor B, CD14, CCR2, fibrinogen, collagen and CD206 (Varnum and Ikezu, 2012; Chhor et al., 2013).

In conclusion, it is not possible to classify microglia only on the basis of their neurotrophic or neurotoxic effects, but is necessary to consider all the different functions they are able to perform, according to the type of stimulus (Lynch, 2009).

### 3.3 Microglia functions and disease

Microglial cells are essential for a correct development of brain. Studies conducted in recent years demonstrated that microglial cells actively interact with neurons both during CNS development (microgliogenesis and neurogenesis occur simultaneously) and in adulthood.

Alterations of this interaction may have serious consequences for the CNS development and function (Nayak et al., 2014).

Microglial cells contribute to the homeostasis of the CNS by the phagocytosis of apoptotic neurons but also by supporting neuronal differentiation via direct cell-to-cell contact or the release of the extracellular matrix components and trophic factors, (Vilhardt, 2005), such as insulin-like growth factor-1 (IGF-1, Ueno et al., 2013), neuronal growth factor (NGF), brain derived neurotrophic factor (BDNF), neurotrophin-3 (NT3), glial derived neurotrophic factor (GDNF) and cytokines with neurotrophic activity, that support the formation of neuronal circuits and promote neuronal survival (Harry et al., 2012).

On the other hand, neurons maintain microglia in a quiescent state by ligand-receptor interactions, such as the interaction between the neuronal membrane protein CD200 with the myeloid cell receptor CD200R and the release of neurotransmitters and neurotrophins (Vilhardt, 2005).

In addition, microglial cells can induce programmed cell death of neurons following in response to aberrant differentiation, by releasing reactive oxygen species (ROS) and removing cell debris by phagocytosis (Marin-Teva et al., 2004). Moreover, when neurons die release factors, including fractaline/CX3CL1, that recruit microglial cells and stimulate their phagocytic activity, that is important not only in CNS development, but also in adult brain for the surveillance of neural networks (Noda et al., 2011).

Microglial cells are also involved in synaptogenesis, myelination and protection from glutamate toxicity (Noda et al., 2011).

Finally, microglial cells represent the first line of defense of CNS immune response (Kettenmann et al., 1993): in fact, they they respond to any type of change that occurs in the surrounding environment and immediately switch their phenotype, performing a specific function for each type of insult and interacting with other cells, including astrocytes and T lymphocytes (Lynch, 2009).

Given the important role played by microglial cells in development and surveillance of CNS homeostasis, it is not unexpected that some important neurological disorders are linked to their dysfunction, such as autism, schizophrenia (Harry et al., 2012), Huntington's disease, Amyotrophic Lateral Sclerosis (ALS), Rett Syndrome (Nayak et al., 2014), HIV-associated dementia (HAD), Parkinson's (PD) and Alzheimer's disease (AD). A deregulation or over-activation of microglia in fact, can have several neurological consequences for the individual, because microglial cells may contribute to establish a chronic neuro-inflammatory environment (Vilhardt et al., 2005).

Moreover, during senescence microglial cells become more activated and neurotoxic and their phagocytic activity is compromised. As result accumulation of aberrant proteins may occur, such as  $\beta$ -amyloid ( $A\beta$ ),  $\alpha$  synuclein and apolipoprotein E (ApoE) that are associated with neurodegenerative diseases and impairment of synaptic activity (Harry, 2013).



## 4. Alzheimer's Disease

Alzheimer's disease (AD) is a chronic, progressive and neurodegenerative disorder that affect more than 35 million of individuals worldwide (Parkinson et al., 2013). It is the most common cause of age-related cognitive impairment and dementia (Gotz et al., 2004) and its prevalence increases exponentially with age. Approximately 13% of people over the age of 65 and 45% over 85 years are affected by AD (Liu C.C. et al., 2013).

The disease can onset with a *sporadic* or *familial form*.

Around 90-95% of patients are affected by a *sporadic form* of the disease (Selkoe, 2001), called Late onset AD (LOAD) (Adlard et al., 2014), that occurs in the old age, characterized by a multifactorial etiology (Bhojak et al., 2000). Several susceptibility genes, including amyloid precursor protein (APP), apolipoprotein E, presenilin 1 and 2, CD2-associated protein (CD2AP), ATP-binding cassette subfamily A member 7 (ABCA7), membrane-spanning 4 domains subfamily A, CD33 (Nayak et al., 2014), Cathepsin D (Cat D), an intracellular aspartyl protease, and IL6, a marker of inflammation implicated in the early stages of AD, have been described to be involved in the pathogenesis of AD (Bhojak et al., 2000). Recently also some cytokines such as interleukin- 1 (IL1) and interleukin- 10 (IL10) are shown implicated in AD predisposition, because of polymorphism presence in relation of specific individual genotype (Sardi et al, 2011).

Familial forms of AD, called Early-onset familial AD (EOAD), have an early onset and affect only 5-10% of patients. Despite their differences, clinical manifestations of AD are similar in familiar and sporadic forms, although some families may show distinctive clinical signs, such as myoclonus, seizures, early and prominent extrapyramidal signs (Selkoe, 2001).

Regardless the etiology, all AD patients exhibit the same clinical features and the same lesions in brain. AD is a complex disease that affects many brain areas: entorhinal cortex, hippocampus, parahippocampal gyrus, amygdala, frontal, temporal, parietal and occipital association cortices (Selkoe, 2001). The neurological damage usually starts in temporal and parietal lobes of cerebral cortex and progresses with time to hippocampus and amygdala (Braak and Braak, 1994). Many physiological processes seem to be altered in the development of AD: tau and  $\beta$ -amyloid deposition, cholesterol metabolism, inflammation, oxidative damage and lysosomal dysfunction. The results of these pathological processes are neuronal death and brain atrophy (McGhee et al., 2014), that appear to precede the onset of clinical symptoms (Mattsson et al., 2009).

Such pathological picture leads progressively to behavioral disturbances, loss of memory, cognitive deterioration, neuropsychiatric symptoms, impairment of activities of daily living and loss of independent function (Salloway et al., 2008).

#### 4.1 Pathological hallmarks of AD

The main hallmarks of AD consist of the formation of neurofibrillary tangles and neuritic plaques. *Neurofibrillary Tangles* are non membrane-bound bundles of fibers that occupy the perinuclear cytoplasm of neurons of the regions typically affected by AD. The abnormal fibers are mainly formed by pairs of 10 nm filaments wound into a helix with a helical period of 160 nm. In general, the tangles are composed of microtubule-associated tau protein that, in physiological conditions, is involved in microtubules modeling (assembling and stabilization), signal transduction, organization of the actin cytoskeleton, intracellular transport of vesicles and anchoring of phosphatases and kinases (Gotz et al., 2004).

On the other hand, during the development of disease tau becomes hyperphosphorylated, adopts an altered conformation and relocalizes itself from axonal to somatodendritic compartment. Such hyperphosphorylation induces the dissociation of the protein from microtubules (Gotz et al., 2004). Different kinases that can phosphorylate tau in serine and threonine residues have been identified (Illenberger et al., 1998; Selkoe, 2001). Nevertheless, it is still unclear if one or more kinases begin the process of tau hyperphosphorylation leading to the dissociation from microtubules favouring aggregation into insoluble paired helical filaments (Selkoe, 2001). Among possible kinases, cyclin-dependent kinase 5 (cdk5) seems to be involved in the process of tau hyperphosphorylation, as result of a dysregulation, becoming constitutively active in AD (Patrick et al., 1999).

*Neuritic plaques* (NPs) are extracellular deposits with a core of insoluble fibrillar  $\beta$ -amyloid protein ( $A\beta$ ), present mainly in cerebral cortex, associated to axonal and dendritic damage (Dickson, 1997). There are two major isoforms of  $A\beta$ : the 42-residue  $A\beta_{42}$  that is the most hydrophobic form (Jarrett et al., 1993), and the 40-residue  $A\beta_{40}$ , the more abundant form in the brain (Gu and Guo, 2013). Apparently, the only difference between the two peptides are the additional C-terminal residues present on the  $A\beta_{42}$ . The plaques in AD brains consist mostly of  $A\beta_{42}$ , that seems to be the isoform more toxic (Gu and Guo, 2013) and prone to aggregation (Jarrett et al., 1993).

Plaques develop gradually over the years and display variable features: the diameter varies greatly, from 10 to 120  $\mu\text{m}$ , but also the density and the degree of aggregation of the fibrillar protein exhibit great variability (Jarrett et al., 1993; Selkoe, 2001). In addition, the plaques are associated to the activation of microglial cells and astrocytes: microglial cells are usually located adjacent to or within plaque core; while the astrocytes surround the plaque and their processes extend centripetally towards the core (Jarrett et al., 1993).

The two typical hallmarks of AD previously described may develop at different times and independently from each other. In addition, neurofibrillary tangles can occur also in other neurodegenerative diseases in most of which  $\text{A}\beta$  deposits and neuritic plaques are not observed. This evidence suggests that the neurofibrillary tangles may arise secondarily in several neurological disorders, including the AD. In particular, in the development of AD they can be a neuronal response to  $\text{A}\beta$  accumulation (Selkoe, 2001).

#### **4.1.1 $\beta$ -Amyloid protein**

The  $\beta$  Amyloid is a protein that derives from the proteolytic cleavage of its precursor, Amyloid Precursor Protein (APP). APP, is a single type 1 transmembrane polypeptide ubiquitously expressed that includes three major isoforms, arising from alternative splicing: APP695, APP751 and APP770 (Selkoe, 2001). In particular, the APP695 isoform is mainly displayed in neurons (Haass et al., 1991).

Although APP function has been not totally clarified yet (Zolezzi et al., 2014), few hypothesis have been proposed: it is involved in neurite outgrowth, synaptogenesis, calcium metabolism, cell adhesion and neuronal protein trafficking (Zhang Y.W. et al., 2011<sup>1</sup>).

The protein is synthesized in the endoplasmic reticulum (ER) and subsequently, transported to the cell surface (Zhang Y.W. et al., 2011<sup>1</sup>). During the cellular trafficking APP is modified with the addition of N- and O- linked sugars (Weidemann et al., 1989). The protein undergoes also a series of proteolytic cleavages by the secretases, leading to the release of protein fragments in the extracellular space (Zhang Y.W. et al., 2011<sup>1</sup>).

The first cleavage can be operated by the  $\alpha$ -secretase, a membrane-bound zinc metalloproteinase or the  $\beta$ -secretase ( $\beta$  site APP converting enzyme, BACE) (Selkoe, 2001). Two  $\beta$ -secretase isoforms have been identified: BACE1, a membrane-bound aspartyl protease specifically present in the

brain and considered the major  $\beta$  secretase isoform, and BACE2, ubiquitously distributed (Harada et al., 2006).

The first cleavage is followed by a further cleavage at the COOH, performed by the  $\gamma$ -secretase complex, composed of presenilin 1 and 2 (PS1 and PS2), anterior pharynx-defective-1 (APH- 1), nicastrin and presenilin enhancer-2 (PEN-2) (Zhang Y.W. et al., 2011<sup>1</sup>; Selkoe, 2001).

Depending on which secretase is involved in the process of APP cleavage, there are two different pathways: the non-amyloidogenic pathway, in which are involved  $\alpha$  and  $\gamma$  secretases, and the amyloidogenic pathway, in which act  $\beta$  and  $\gamma$ -secretases (Gotz et al., 2004).

The non-amyloidogenic pathway leads to the formation of soluble  $\alpha$ -APPs peptide.  $\alpha$ -APPs (or sAPP $\alpha$ ) plays an important role in neuronal survival and is protective against the excitotoxicity. In addition, it regulates the neural stem cell proliferation and CNS development (Zhang YM et al., 2011<sup>1</sup>). In the amyloidogenic pathway instead, the action of  $\beta$  and  $\gamma$ -secretases causes the release of  $\beta$ -APPs and the neurotoxic A $\beta$  peptides (Gu and Guo, 2013).

When an increase of production, a decrease in the activity of the degradative enzymes or a reduced activity of the A $\beta$  removal mechanism occur, senile plaques are formed, caused by accumulation and deposition of intracellular A $\beta$  (Parkinson et al., 2013).

#### 4.2 Hypothesis for explaining AD pathogenesis

*The amyloid hypothesis* (also called the amyloid cascade hypothesis), emerged in 1980s, has been considered the main theory regarding AD pathogenesis until few years ago. According this theory a close relationship between the onset of the disease and accumulation of senile plaques in the brain exists: this in turn would lead to the damage of neuronal circuits and synaptic dysfunction (Ferreira and Klein et al., 2011).

Interestingly, this hypothesis suggests that fibrillar A $\beta$  is also related to tau hyperphosphorylation and assembly. It has been suggested in fact, that the presence of A $\beta$  could facilitate the phosphorylation of tau protein. There are some indications that support the amyloid cascade hypothesis, including the evidence that A $\beta$  increases the formation of aberrant tau aggregates. More detailed studies have suggested that tau phosphorylation in dystrophic neurites of senile plaques, but not necessarily phosphorylation of tau in neurofibrillary tangles is related with amyloid accumulation (Pérez M. et al., 2005).

In recent years, growing evidences support the hypothesis that the soluble A $\beta$  oligomers, rather than A $\beta$  fibrils deposits, trigger the synaptic dysfunction and deterioration of cognitive functions (Bao et al., 2012). Among these, there is the study of Mucke and colleagues (2000), who demonstrated that synapse loss does not require the presence of fibrillar A $\beta$  deposits. Lambert and colleagues (1998) instead, demonstrated that A $\beta$  oligomers inhibit the functional synaptic plasticity.

These findings have led to *the oligomer hypothesis*, according to which memory loss is attributed to oligomer-induced disruption of synaptic plasticity, while the dementia that occurs in later stages of AD is attributed to oligomer-induced cellular degeneration and death.

Oligomers assemble from soluble A $\beta$  monomers that are abundant in normal brain tissue, and accumulate early in the disease progression. The reason for which the oligomers accumulate remains unknown, but the alteration of the clearance of A $\beta$  could be involved in the accumulation of toxic oligomers (Ferreira and Klein, 2011).

Is still unknown, however, which of the different A $\beta$  assembly states is responsible for neurodegeneration: some groups have suggested that dimers are most critical, while others have suggested that higher order oligomers are most relevant, including 12mers and 24mers (Ferreira and Klein, 2011).

Interestingly, a study from Giuffrida and colleagues (2009) demonstrated that A $\beta$  monomers, are able to support the survival of developing neurons and protect mature neurons against excitotoxic death.

#### 4.3 The role of microglial cells in the pathogenesis of AD

It has long been known that inflammation is a prominent factor in AD. Several evidences, in fact, demonstrated the involvement of the inflammatory processes in the development of AD, including elevated levels of pro-inflammatory cytokines (TNF $\alpha$  and IL6) in the serum and in the brain tissue of AD patients, activated microglial cells surrounding senile plaques in the cerebral cortex, T cells, and astrocytes co-localization to A $\beta$  deposits (Varnum and Ikezu, 2012). Finally, dystrophic neuritis are present, characteristic signal of neuronal degeneration processes (figure 9, Meraz Rios et al., 2013).

AD has been one of the first neurodegenerative disorders to be associated with neurotoxic activation of microglial cells (Block and Hong, 2005).

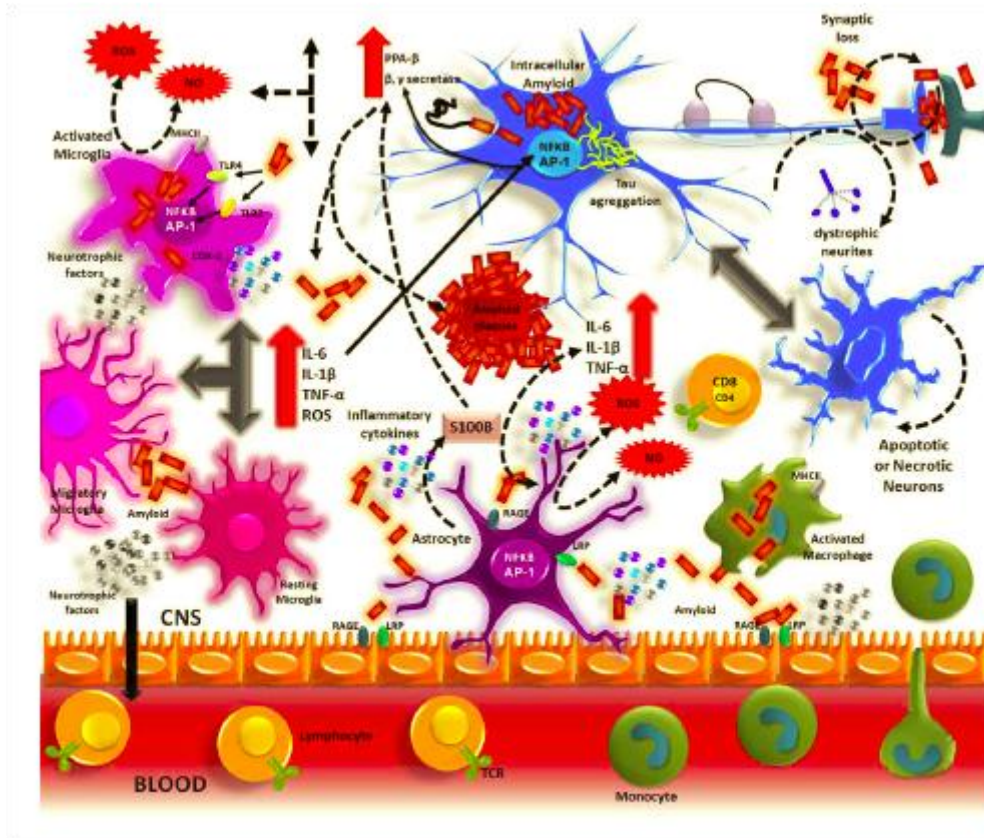


**Figure 9. Inflammation process in Alzheimer's disease.** Aβ aggregates activate microglial cells through TLRs and RAGE receptors. Once activated, cells produce pro-inflammatory cytokines, such as IL6, IL1β and TNFα and the reactive oxygen species (ROS). These inflammatory factors act directly on neurons and stimulate astrocytes activation, that amplifies the inflammatory process. The inflammatory mediators induce the production of adhesion molecules and chemokines that recruit peripheral immune cells (from Meraz Rios et al., 2013).

Microglial cells in physiological conditions, participate in phagocytic activities from development to adulthood. During conditions of long term inflammation besides could be a shift away from reparative responses, due to a failed M2 response. This could be induced by M2 microglia lack and failed inflammation control or by a decrease of neuroprotective factors and or brain derived neurotrophic factor, which microglia produce (Cherry et al, 2014).

This function maintains the overall health of the brain and may delay the onset of AD; when the phagocytic activity declines, the CNS can rapidly deteriorate. Inflammation and decline of microglial phagocytosis could contribute to AD pathogenesis.

On the other hand, studies on microglial phenotype demonstrated that the anti-inflammatory M2 phenotype plays a protective role in AD pathogenesis: cells with M2a phenotype stimulate neural differentiation and act on Aβ deposits reducing them, while cells with M2c phenotype suppress the inflammatory response and promote the neurogenesis and the restoration of spatial learning.

An interesting therapeutic strategy thus, might be to promote the switch of the microglial phenotype from M1 to M2 (Varnum and Ikezu, 2012).

Microglial cells can play an important role in the early stages of AD by reducing the A $\beta$  toxic effects, while are less involved in the late stages, in which their phagocytic function decreases. In the final stage of the disease, instead, microglial cells play a pro-inflammatory role, characterized by the production of pro-inflammatory cytokines that exacerbate the inflammation and promote the cognitive decline (Nayak et al., 2014).

In the final stage of the disease microglial cells undergo to a phenotypic change from M2 to M1 phenotype and begin to secrete pro-inflammatory cytokines, stimulating the amyloid peptide accumulation (Varnum and Ikezu, 2012).

Many factors are implicated in activating microglial cells and directing them toward sites of A $\beta$  deposition: the Toll-like receptors (TLRs), the scavenger receptors A and B, fractalkines, the receptor for the vascular endothelial growth factor 1 (VEGFR-1) and proteolytic enzymes, such as the insulin-degrading enzyme (IDE), the neprilysin (NEP), matrix metalloproteinase 9 (MMP9) and plasminogen (figure 10) (Hickman et al., 2008; Mosher and Wyss-Coray, 2014).

The interaction between A $\beta$  and microglial cells involves also other receptors, such as RAGE, CD14,  $\beta$ 1-integrin receptor,  $\alpha$ 6- $\beta$ 1 integrin and CD47 (integrin-associated protein). In particular, CD47 is involved not only in the A $\beta$  internalization through a non-traditional pathway, but also in the production of superoxide by microglial cells (Block and Hong, 2005). RAGE is involved in the A $\beta$ -induced microglial migration, cytokine induction and impairment of the mechanism of A $\beta$  clearance (Fang et al., 2010).

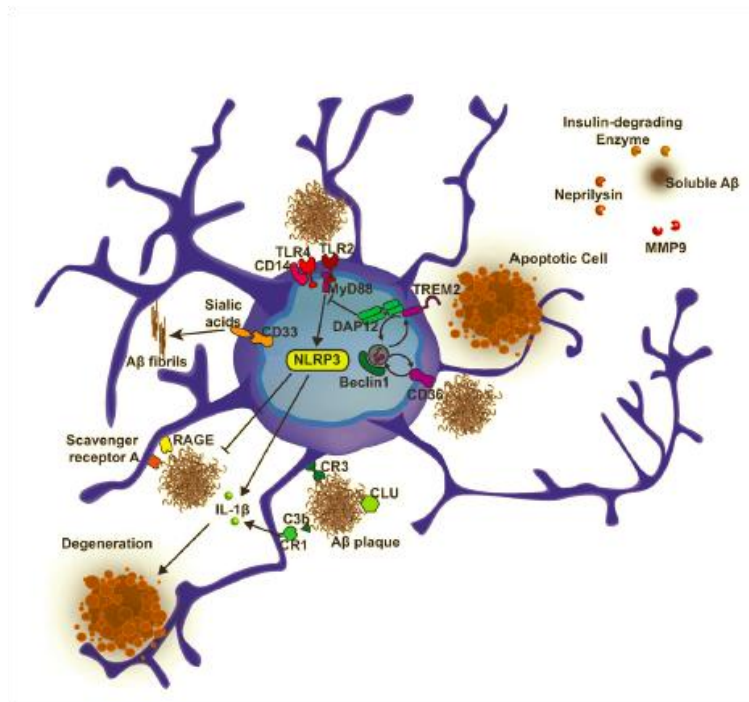


**Figure 10. Microglial cells in the pathogenesis of the Alzheimer's disease.** Microglial cells interact with the A $\beta$  peptide through many receptors, such as RAGE, TLRs, CD36, TREM2, CR1, CR3 and the scavenger receptor A. Once activated, cells release pro-inflammatory cytokines and enzymes, including neprilysin (NEP), matrix metalloproteinase 9 (MMP9) and insulin-degrading enzyme (IDE) that are involved in the clearance of the toxic peptide (Mosher and Wyss-Coray, 2014).

Recently it was observed that microglia might display two different proliferating phenotypes involved in neuroprotective effects. These are designated as “Proliferating Amoeboid Microglia” (PAM) and “Differentiated Process-bearing Microglia” (DPM). It has been assessed, *in vitro*, that the two different phenotypes show different responses to neurons or A $\beta$ - mediated neurotoxicity (Tsay et al. 2013). In particular there was evidence that the proliferating microglia (PAM), but not the differentiated microglia (DPM), protected neurons against A $\beta$ -mediated neurotoxicity.

In conclusion microglia is deeply involved in the homeostasis of healthy brain and in the resolution of pathological states of CNS. AD is a neurodegenerative condition, whose gradual development is favored by persistent inflammation status. Thus, regulating microglia recruitment into the brain represents a great potential as novel therapeutic strategy to delay or stop the progression of AD (El Khoury and Luster, 2008). Neuroprotective effects or immunomodulator strategies might be increased and developed to enhance the recruitment of mononuclear phagocytes and microglia precursors into the brain, to induce a positive resolution of inflammatory status.



## **5. Genetics of AD**

The Early-onset familial AD (FAD) is an autosomal dominant disorder that affects only a small portion (<5%) of AD cases (Adlard et al., 2014). Typically the disease occurs before 65 years old and is associated to APP and presenilin genes mutations (Liu C.C. et al., 2013).

The first genetic cause of familial AD identified is a missense mutation in the APP gene (Goate et al., 1991), located on the chromosome 21. Mutations affecting this gene alter the proteolytic process of the protein corresponding to the secretase's cleavage sites. The overproduction of A $\beta$ 40 and A $\beta$ 42 neurotoxic peptides and early age formation of senile plaques are the result of changes in the APP gene (Selkoe, 2001).

The main genetic risk factor for the disease is the Presenilin 1 (PS1) (Chau et al., 2012) gene, located on chromosome 14 (Selkoe, 2001). It is a membrane protein that forms the catalytic subunit of  $\gamma$ -secretase. Alterations in PS1 cause a conformational change in the  $\gamma$ -secretase active site, leading to APP incorrect processing and the massive formation of A $\beta$ 40 and A $\beta$ 42 (Chau et al., 2012). In addition, Presenilin 2 (PS2) gene mutations on chromosome 1 are also associated with AD (Chau et al., 2012; Selkoe, 2001).

Another form of AD is the Late-onset AD (LOAD), with a sporadic onset (Ferri et al., 2005). The main genetic risk factor of this form is the  $\epsilon$ 4 allele of the apolipoprotein E (APOE) gene, located on chromosome 19. This gene is involved in the regulation of lipid homeostasis, metabolism of A $\beta$  (aggregation and clearance) and modulation of the  $\gamma$ -secretase activity (Liu C.C. et al., 2013). In addition, recent studies demonstrated that the expression of APOE $\epsilon$ 4 is different between man or woman: a single copy of the allele in a woman induce an increase risk to develop AD pathology, because amyloid or tau-related pathology onsets early in women compared to men (Altmann et al., 2014).

### **5.1. Animal Models of Alzheimer's disease**

Animal models of AD have been created to mimic one or more abnormalities characteristic of the disease and to test any therapeutic strategies. They allow to study in detail the molecular mechanisms that cause the onset of the disease and are responsible for the decline of cognitive functions (Higgins and Jacobsen, 2003).

Currently the best model of AD, the more similar to the human disease, is the aged monkey, such as the Caribbean vervet monkey, lemur, cotton-top tamarin, rhesus monkey and squirrel monkey (Philipson et al., 2010). Nevertheless, because of the time and the costs associated with this model, most of the studies on AD have focused on the development of other animal models, such as rats, rabbits, dogs, the *Drosophila melanogaster*, the nematode *Caenorhabditis elegans* and two types of fish, the *Petromyzon marinus* and the Zebrafish (Götz et al., 2004 and Götz and Götz , 2009; Crews et al., 2010; Murphy and LeVine, 2010; Philipson et al., 2010).

Until few years ago rodent models of AD were essentially focused on drug or CNS lesion-induced behavioural deficits. The problem with these approaches is that, unlike human and other species, A $\beta$  deposition has not been reported in rodents. With the advent of the transgenic technology and the identification of AD-associated genes has been possible to create a model of AD more similar to the human pathology (Higgins and Jacobsen, 2003).

The first generation of transgenic models of AD was based on the expression of wild-type human APP (hAPP) cDNAs. It is a single transgenic model in which the production of A $\beta$  is not sufficient to produce the senile plaques (Marx, 1992). Over-expression of the hAPP gene in combination with the Swedish (APPK670N, M671L) or the London mutation (APPV717F), in order to produce a more realistic model of the human disease, is proved to be essential. The Swedish mutation affects the  $\beta$ -secretase cleavage site and makes the APP a better substrate for this enzyme. The London mutation instead, affects the  $\gamma$ -secretase cleavage site. As for the human disease, in this model the A $\beta$  deposits increase with the age and occur mainly in the cerebral cortex and the hippocampus (Higgins and Jacobsen, 2003).

More recently, double transgenic animals expressing both mutant human presenilin cDNA and hAPP cDNA, have been generated in order to enhance the production of A $\beta$ 42 at early stage of development. Transgenic mice expressing the presenilin cDNA alone do not show A $\beta$  deposition at any age due to the low propensity of endogenous mouse A $\beta$  to form fibrillar aggregates (Higgins and Jacobsen, 2003).

### **5.1.1 Single APP transgenic models**

Over the years several APP transgenic models have been created, among these the NSEAPP, PDAPP, Tg2576 and TgAPP23 (Higgins and Jacobsen, 2003).

In 1991 Quon and colleagues (1991) described for the first time the NSEAPP mouse, a transgenic mouse carrying the human APP751 isoform. Nevertheless, only in a small subset of animals (approximately 5%) neuritic plaques formed (Higgins and Jacobsen, 2003).

Subsequently, a PDAPP mice model with the mutated human APP 695, 751 and 770 isoforms (with the London mutation) was generated. It is a more realistic model of the human disease with many of the pathological hallmarks of AD, including neuritic plaques surrounded by dystrophic neurites, astrogliosis, microgliosis and synapse loss, but not neurofibrillary tangles. In this model the disease onsets in the cingulate cortex at 8 months of age and is characterized by plaques deposition in the entorhinal/hippocampal areas at 10-12 months, with cognitive impairment from 6-9 months of age (Games et al., 1995; Higgins and Jacobsen, 2003).

In 1996 the Tg2576 transgenic model with APP695 isoform, carrying the Swedish mutation, was described (Hsiao et al., 1995). This model presents A $\beta$  accumulation at 6/9 months of age, astrogliosis, microgliosis, hyperphosphorylated tau, but no loss of synaptic function. In addition, animals show a decline in cognitive function from 7 months of age (Higgins and Jacobsen, 2003).

Another model, the TgAPP23, presents the mutation K670N/M671L in the APP751 isoform (Sturchler-Pierrat et al. 1997). In these animals the plaques onset from 6 months of age. The mice show neurodegeneration in the hippocampal region at 14-18 months of age with an apparent correlation with the plaque load. In addition, this model is characterized by the presence of cerebral amyloid angiopathy (CAA), microgliosis, astrocytosis, dystrophic neurites, loss of synapses, cholinergic deficits and hyperphosphorylated tau proteins, but not neurofibrillary tangles (Richardson and Burns, 2002; Higgins and Jacobsen, 2003; Kobayashi and Chen, 2005).

### ***5.1.2 APP/PS double transgenic models***

In addition to single transgenic models, double APP/PS1 transgenic models have also generated (Higgins and Jacobsen, 2003).

Duff and colleagues (1996) generated a transgenic model carrying the M146L mutation of the PS1 gene (hPS1M146L) in which mice do not develop senile plaques. Subsequently they crossed the Tg2576 mice with the hPS1M146L model and obtained a new double transgenic mouse model, the PSAPP. This model is characterized by the plaques onset from 3 months and cognitive deficits at 6-9 months.

Moreover another model, the APP<sup>swe</sup>/PS1<sup>dE9</sup> mouse that co-expresses the mutated Swedish APP gene and the exon-9-deleted variant of the presenilin-1 (PS1) has been studied. This animal model is characterized by earlier and aggressive onset of A $\beta$  amyloidosis (between 2 and 6 months of age), dysfunctional neuronal networks, microgliosis and loss of synaptic function and functional deficits. The amyloidogenic process is age-dependent. Cognitive decline onsets from 6 months of age. Mice show a stronger correlation between cognitive performance and A $\beta$  total load (Perez et al., 2009). In addition, Zhang W. and colleagues (2012<sup>1</sup>), suggested that APP<sup>swe</sup>/PS1<sup>dE9</sup> mice at the age of 3,5 month old exhibit spatial memory impairment correlated with soluble A $\beta$ , cholinergic dysfunction and oxidative damage. For the reasons mentioned, the APP<sup>swe</sup>/PS1<sup>dE9</sup> mouse constitutes the ideal model to study the amyloidogenic process and its role in the pathogenesis of AD (Zhang et al., 2012<sup>1</sup>).

### ***5.1.3 Tau-based transgenic models***

Few models carrying tau protein mutations have generated. One of these is the JNPL3, in which mice express the P301L mutation. In this model symptoms of the disease begin from 6-7 months of age but the animals die before the appearance of cognitive deficits. Moreover, at physiological level mice exhibit neurofibrillary tangles but not amyloid plaques (Lewis et al., 2000). Later, Lewis and colleagues (2001) described also a double transgenic mouse model, the TAPP, resulting from the cross between JNPL3 and Tg2576 mice. It is the first animal model characterized by the onset of both amyloid plaques and neurofibrillary tangles.

### ***5.1.4 Triple transgenic models***

Moreover, triple transgenic mouse models have generated. The 3xTg-AD model was described by LaFerla and colleagues (2007). It is characterized by the presence of three mutations in the key genes involved in the pathogenesis of AD: Swe APP, P301L Tau and M146V PS1. The animals manifest aged-related neurological deficits and exhibit both amyloid deposition and neurofibrillary tangles. The extracellular deposits of A $\beta$  are formed before neurofibrillary tangles, according to the amyloid cascade hypothesis. In addition, mice show deficits in the synaptic plasticity. For the

reasons mentioned above, this is a very useful animal model for the study of the role of tau and A $\beta$  on synaptic plasticity (Oddo et al., 2003<sup>1</sup> and 2003<sup>2</sup>).

## **6. Drug treatment for Alzheimer's disease**

Currently no effective therapy in the treatment of AD exists since all clinical trials based on the manipulation of the many identified disease pathways, including A $\beta$  and tau deposition processes, inflammation and oxidative stress have failed (Higgins and Jacobsen, 2003).

For these reasons, today AD therapy consists of symptom-based drugs, such as acetylcholinesterase inhibitors (AChEIs) and the N-methyl-D-aspartate (NMDA) antagonist. These drugs however, do not affect significantly the course of the disease (Higgins and Jacobsen, 2003).

Donepezil, Rivastigmine, Galanthamine and Memantine are among the drugs currently most used for AD treatment (Wilkinson, 2011; Singh et al., 2013). The first three are acetylcholinesterase inhibitors and act by increasing the activity of acetylcholine, trying to restore the cholinergic function and thus, cognitive dysfunctions (Singh et al., 2013). Moreover, another drug used today for AD therapy is the Memantine, that acts on the NMDA glutamate receptor, a ionotropic receptor. The Memantine acts as an NMDA antagonist receptor and restores the neuronal memory, improving cognitive functions (Wilkinson, 2011). To date the best AD treatment is a combination therapy with Memantine and Donepezil (Wilkinson, 2011).

### **6.1 New therapeutic targets for AD**

Due to the fact that the disease occurs long time before the onset of symptoms, the ideal therapeutic strategy would be a treatment that prevents the neurodegenerative process.

Several therapeutic approaches for AD are directed to modulate the pathway of A $\beta$  or the tau aggregation. Drugs inhibitors of  $\beta$  and  $\gamma$  secretases have been studied. Nevertheless, no one has been successful, because secretases act on different proteins, not only on APP (Parkinson et al., 2013).

Given the new findings concerning the involvement of A $\beta$  oligomers in the neurodegenerative process that leads to the cognitive decline of subject affected by AD, studies for targeting directly A $\beta$  oligomers or post translational modifications that predispose to the oligomer formation have been developed (Rowan et al., 2005).

One of the most studied approaches is the immunization: the synthesis of a vaccine directed against A $\beta$  and tau proteins. Anti-A $\beta$  antibodies have been synthesized. They can be administered by active immunization, through direct removal of A $\beta$  oligomers or passive immunization that stimulates microglial-mediated clearance. The result is a reduction in A $\beta$  brain levels and an improvement of cognitive function (Rowan et al., 2005). Clinical trials using two murine anti-A $\beta$  monoclonal antibodies (mAbs), bapineuzumab and solanezumab, were performed, but at the phase III failed to reach their primary endpoints: improving or stabilizing cognitive functions (Moreth et al., 2013; Salloway et al., 2014).

Moreover, Dodel and colleagues (2002) reported that intravenous immunoglobulin (IVIG, a mixture of polyclonal antibodies that contains most of the IgG found in the human immune repertoire) contain elevated levels of antibodies against A $\beta$  monomers that can be used as treatment for AD. Since then, several clinical trials have been performed to test IVIG but to date none has had a major impact on the progression of AD symptoms (Relkin, 2014).

In recent years, researchers are interested to the study of nanoparticles, a new potential therapeutic strategy for diseases that affect the CNS, including AD (Balducci et al., 2014).

Currently liposomes (LIPs) are the best known type of nanoparticles used in clinic as a drug vehicle. Interesting, Balducci and colleagues (2014) functionalized LIPs with a peptide receptor binding domain of APOE-derived (mAPOE), that allows them to cross the BBB and with phosphatidic acid (PA), that allows them to bind A $\beta$  aggregated in different forms.

## 6.2 Therapeutic potential of Bone Marrow-derived Mesenchymal Stem Cells in the treatment of Alzheimer's disease

Owing to the increasing importance of stem cells as a new potential therapeutic strategy for different types of diseases, several studies showing the beneficial effects derived from MSC's administration are currently in progress. In a murine model of AD, Lee JK and colleagues (2009) for instance, used an acute AD model by direct injecting A $\beta$  in the hippocampal dentate gyrus. Their results showed a reduction in A $\beta$  deposits and activation of microglial cells towards

neuroprotective and phagocytic phenotype. Subsequently, the same group (Lee JK et al., 2010) studied the intracerebral BM-MSc transplantation into a double transgenic model, the APP/PS1. They observed in brain a reduction of amyloid load and tau phosphorylation, an increase of A $\beta$  clearance and an improvement in spatial learning, memory and neuronal survival.

In 2012, the same group of researchers (Lee JK et al., 2012) examined MSC transplantation focusing on the evaluation of MSC paracrine effects. The results demonstrated that MSCs release in brain soluble factors that attract microglial cells stimulating their migration near plaques and activation into the phagocytic phenotype. Chemotactic activity of MSCs is mediated by the secretion of CCL5, a chemokine that induces dendritic, natural killer (NK) and T cells, granulocytes and macrophages migration to the sites of inflammation. In addition, transplanted MSCs secrete A $\beta$  degrading enzymes, including neprilysin (NEP), that contribute to A $\beta$  clearance.

Therefore, Lee JK and colleagues' studies (2012) confirmed that BM-derived MSCs represent a promising therapeutic strategy for the treatment of AD.

In recent years the attention of researchers has focused on another characteristic of MSCs: their ability to secrete microvesicles (MVs) with therapeutic potential. The therapeutic potential of MVs has already been tested in animal models and clinical trials of several diseases, with very promising results. Investigating the mechanisms by which MSCs promote their positive effects on AD, it has been hypothesized a role even for MVs: Katsuda and colleagues (2013), in fact, demonstrated that MVs released from adipose tissue-derived MSCs (ADSCs) express NEP on their membrane. They thus suggested a role for MV in the processing of A $\beta$ . The study illustrated that MVs may act preventing the extracellular plaque formation and removing the pre-existing plaques. In conclusion, MVs, owing to the advantages that possess compared to parental cells, can be an ideal candidate for AD treatment.

## MATERIALS and METHODS

### **1. IN VITRO EXPERIMENTS**

#### **1.1 Isolation and culture of murine Bone Marrow-derived Mesenchymal Stem Cells (BM-MSCs)**

Isolation of mononuclear cells and in vitro expansion of BM-derived MSCs were performed from the bone marrow of 4-12 week old female C57BL/6 mice.

After the sacrifice of the animal, femur and tibia bones were isolated from the hind limbs and placed in 1X phosphate buffered saline (PBS, Lonza®) at 4 °C. Under sterile hood these bone segments were cleaned, through gauze sterile, of muscles and connective tissues surrounding and deprived of the symphysis. Cells were isolated from bone marrow by flushing method: alpha Eagle's minimum essential medium ( $\alpha$ MEM, Lonza®) was injected in the medullary canal using an insulin syringe with 29 G needle and cells were collected in a petri dish. This procedure was repeated 3 times for each end of the bone. Subsequently, cells were mechanically dissociated, transferred into a tube and centrifuged at 430x g for 10 minutes. Following centrifugation, the supernatant was discarded and the cell pellet was resuspended in 0,84% ammonium chloride (NH<sub>4</sub>Cl) to lyse red blood cells and incubate for 2-3 min at room temperature (RT), occasionally shaking manually. After incubation, the complete medium composed of  $\alpha$ MEM supplemented with 20% Fetal Bovine Serum defined (FBS, HyClone™), 2mM L-ultra glutamine (Lonza®), 100 U/mL penicillin (EuroClone®) was added to cells to stop the lysis reaction and centrifuged at 430x g for 10 min. The supernatant was discarded and the cell pellet resuspended in  $\alpha$ MEM complete medium. Finally, cells were plated at 4\*10<sup>4</sup> cells/cm<sup>2</sup> on T25 flask. At this time the culture was considered as passage 0 (p0).

Cells were incubated at 37°C with 95% humidity and 5% CO<sub>2</sub>. After 48 hours, non-adherent cells were removed and fresh medium replaced. The medium was changed every three days until cells reach the confluency.

Cells were detached after reaching subconfluency (~80%). At this time, the cell culture was rinsed twice with 1X PBS and harvested by incubation with Trypsin-EDTA [200 mg/L Versene (ethylenediaminetetraacetic acid, EDTA), 170000 U Trypsin/L; Lonza®] for a few minutes (this step is called trypsinization). Then, the complete medium was added to stop the trypsin reaction and the cell suspension centrifuged at 122x g for 10 min. Finally, cells were cultured (p1).



From p4, the culture was amplified by plating cells at a density of  $2,5 \cdot 10^4$  cells on T25 flask (10000 cells/cm<sup>2</sup>) or  $4 \cdot 10^4$  cells (5300 cells/cm<sup>2</sup>) on 75 cm<sup>2</sup> (T75) flask. For our experiments cells were used from 9 to 14 passages (p9-p14).

## 1.2 Osteogenic and Adipogenic differentiation assay

Culture-expanded MSCs were tested for their ability to differentiate into osteogenic lineage and adipogenic lineage at passages 6th and 15th. BM-derived MSCs were plated at a density of  $1 \cdot 10^4$  cells in a 6-well tissue culture plate (1000 cells/cm<sup>2</sup>) and maintained in growth medium (containing  $\alpha$ MEM, 10% FBS, 2mM L-ultra glutamine and 100 U/ml penicillin/streptomycin) for 24h. The day after, cells were cultured in respective media of growth medium and differentiation medium added with differentiating factors at final concentration of:

- Osteogenic differentiation: 10nM dexamethasone (Sigma), 50  $\mu$ g/ml ascorbic acid (Sigma), 10mM  $\beta$ - glycerophosphate (Sigma);
- Adipogenic differentiation: 10nM dexamethasone (Sigma), 5  $\mu$ g/ml insulin (Sigma).

Both differentiating cell cultures were cultured at 37°C as usually and the medium was replaced twice weekly for 14 days.

After 21 days, differentiated cells were rinsed with 1X PBS and fixed.

Visualization of osteogenic differentiation:

- Fixation with 70% cold ethanol (in distilled water) for 1h at RT and analyzed for osteogenic differentiation. To observe calcium deposition, cultures were rinsed once with distilled water and stained for 10 min at RT with Alizarin Red S (Sigma Aldrich®) at pH 4,1-4,3. Excess staining was removed by rinsing with distilled water. Finally, calcium deposition was quantified by extraction of the dye by solubilization of Alizarin Red in a solution containing 5% Sodium Dodecyl Sulphate (SDS) and 0,5M Hydrochloric Acid (HCl) and subsequent absorbance reading at 425 nm. The absorbance was evaluated using the Synergie H4 spectrophotometer (Bio-Tek®).

Visualization of adipogenic differentiation:

- Fixation in PFA 4% upon two washes in PBS1x for 20 minutes. To observe fat droplets, cultures were stained for 10 minutes at RT with Red Oil (Sigma Aldrich®) at 0,5% in isopropanol. The quantification of fat formation in cells by measuring absorbance was not performed.

### 1.3 Determination of BM-derived MSC surface antigen profile

MSC phenotype was characterized for a selection of surface antigens by flow cytometry analysis from 4 to 14 passages. The cells were trypsinized and counted. Then, MSCs were resuspended in a tube in complete medium supplemented with 2mM EDTA to facilitate the dissociation. After trypsinization to restore antigens at the cell surface is necessary the recovery (McCLAY et al., 1977). For this reason, cells were kept in recovery by shaking in the bath at 37 °C for 1h, to favor the return of the antigens to the membrane. Later, cells were centrifuged at 122x g at 4 °C for 10 min, resuspended in FACS buffer [1x PBS supplemented with 2% Fetal Bovine Serum (FBS, EuroClone®) and 2mM EDTA]] and plated approximately 200000 cells/well (31250 cells/mm<sup>2</sup>) in a 96-well tissue culture plate. Cells were rinsed twice with FACS buffer at 430x g at 4 °C for 5 min, each time removing the supernatant and resuspending the cells by vortexing. After rinsing, cells were stained for 20 min on ice in the dark: antibodies were diluted to the optimal concentration in 1X PBS with 2% FBS.

Cells were stained with the following antibodies at a concentration of 0,2 or 0,5 mg/ml (according to the product data sheets):

- Fluoroisothiocyanate (FITC) Mouse Hematopoietic Lineage Cocktail (Lin, eBioscience™)
- Peridinin Chlorophyll Protein (PerCP™)/Cy5.5-conjugated Rat anti-mouse CD117 (c-kit, BioLegend®)
- Brilliant Violet™ (BV) 510-conjugated Rat Anti-mouse CD31 (BD Pharmingen™),
- Phycoerythrin (PE) conjugated Rat Anti-Mouse Ly-6A/E (Sca1, BD Pharmingen™),
- Alexa Fluor® 647-conjugated Hamster Anti-Rat/Mouse CD49a (BD Pharmingen™),
- FITC-conjugated Rat anti-mouse CD9 (BioLegend®)
- Alexa Fluor® 647-conjugated Rat anti-mouse/human CD44 (BioLegend®)
- Pacific Blue™-conjugated Armenian Hamster anti-mouse/rat CD29(BioLegend®)
- Alexa Fluor® 647-conjugated Rat anti-mouse CD73 (BioLegend®)
- PE/Cy7™-conjugated Rat anti-mouse CD105 (BioLegend®)

After that, cells were rinsed as previously described. For FACS reading, cells were resuspended with FACS buffer in FACS tubes, after filtering (with a 70µm filter) to remove cell aggregates from the suspension. Eventually, cells were fixed after the last rinse with 2% paraformaldehyde (PFA) in 1X PBS for 20 min on ice, when the staining was not performed the same day of the experiment. Finally, the cells were rinsed twice with FACS buffer and 1X PBS, respectively. Then, cells were

resuspended in 1X PBS supplemented with 2mM EDTA and stored at 4 °C (in the dark) until the time of reading.

For all the stainings we used as negative controls Fluorescence Minus One (FMO) and unstained samples. A FMO control contains all the fluorochromes in the tube, except the one that is being measured. This control ensures that any spread of the fluorochromes into the channel of interest is improperly identified. Unstained control instead, ensures to exclude the auto fluorescence of the cells. We used  $2 \times 10^5$  cells both for each sample.

Samples were acquired at the LSR Fortessa™ FACS (BD Biosciences®) and the data analyzed with FlowJo® software.

#### 1.4 Isolation of BM-MSC derived MVs

Microvesicles (MVs) were obtained from supernatant of BM-MSCs adapting the Théry's protocol (Théry et al., 2006). Briefly, MSCs at the appropriate passage were cultured overnight at  $4 \times 10^4$  cells/cm<sup>2</sup>. The day after, cells were starved for 3h in serum free-  $\alpha$ MEM. Then, the culture medium, that contained MVs, was collected and subjected to a series of centrifugation at 4 °C:

- 300x g for 10 min to remove death cells;
- 1000x g for 15 min to discard any remaining debris;
- 110000x g for 70 min to separate the pellet, containing MVs, from supernatant: both will be kept to perform the experiments.

Finally, the resultant pellet containing MVs, was resuspended in physiological saline solution (Sodium Chloride –NaCl- Baxter 0,9%) or  $\alpha$ MEM medium. For experiments that investigate the modulation of cytokines release in vitro, MVs were resuspended in  $\alpha$ MEM medium. For in vivo experiments and flow cytometric analysis they were resuspended in physiological saline solution. However, a portion of MVs was diluted in RIPA buffer [(TRIS 0,05M pH 7.4 + 0,25M NaCl+ 1% Triton + 0,05M EDTA)] supplemented with 1/25 of protease inhibitor (Roche®) in order to perform protein quantification. Total protein concentration of MVs preparation was quantified by micro-BCA assay following the manufacturer's protocol (ThermoScientific Promega®).

## 1.5 Characterization of BM MSC-derived MVs

MSC-derived MVs were characterized by flow cytometry for the expression of both MSCs (CD29, CD49a and CD73) and exosomes (CD9) surface markers.

Resuspended MVs in physiological saline solution were stained with Phalloidin Tetramethylrhodamine (TRITC)-conjugated (0,5mg/ml; Sigma Aldrich®), CD9, CD29, CD49a and CD73 (at the same concentration used at par 1.3 Mat&Meth) for 40 min at 4 °C in the dark. After incubation, labeled MVs were ultra-centrifuged to remove the excess antibody and then, resuspended with physiological saline solution for flow cytometric analysis. Moreover, a part of MVs were incubated with 5µl of latex beads of 0,79 and 1,34 µm size. Calibration beads were employed to gate MVs by dimension parameters.

FACS analysis for MVs was performed with FACS CANTO II (BD Biosciences®) and the data analyzed with FlowJo® software and with Diva software.

## 1.6 Microglial dissection and culture

Primary cultures of microglial cells were prepared from brains of postnatal 1-2 days old C57BL/6 mice. After the sacrifice of the animals, brains were extracted and maintained in cold and sterile Hank's Balanced Salt Solution (HBSS) [Balanced Salt Solution (BSS, Gibco®), supplemented with Hepes 0.3M (Sigma Aldrich®), 100µg/ml streptomycin and 100 U/ml penicillin (EuroClone®)]. After the removal of meninges, cortices and hippocampi were isolated from brainstem, striatum and substantia nigra. Brain tissues were collected in HBSS and crumbled with the scalpel for mechanical digestion; the homogenate was collected in HBSS and residues of meninges eliminated. This procedure was followed by a doubled enzymatic digestion in digestion buffer: HBSS supplemented with 0.3% Trypsin (Sigma Aldrich®) and 0.25% DNase (Sigma Aldrich®). The homogenate was incubated twice in digestion buffer for 15 min at 37°C (inverting manually the tube in the incubator 3 times every 5 min or shaking in the bath). The supernatant obtained from the first digestion was collected in a tube and an equal volume of glial medium [(Eagle's minimal essential medium (MEM, Gibco®) supplemented with 20% FBS, 33mM Glucose, 2mM L-ultra glutamine, 100µg/ml streptomycin and 100U/ml penicillin] was added in order to inactivate the digestion. The second digestion was made on the residual pellet. At the end of the second incubation in digestion buffer, the pellet was mechanically dissociated and harvested in the tube

already containing cells from the first digestion. The obtained cell suspension was filtered with 70µm nytex membrane and centrifuged 10 min at 800x g at RT. Finally, cell pellet was resuspended in glial medium and cells were seeded into poly-L-lysine (0.02mg/ml, Sigma Aldrich®) pre-coated (2h at 37 °C) flasks in complete glial medium. After seeding, cells were left grow without changing the medium in order to let microglial cells to grow on the top of the astrocyte monolayer. After 10 days microglial cells were harvested after shaking the flasks at 230rpm for 45min at RT. Then, the medium from each flask was collected in a tube and centrifuged at 800 x g for 10 min.

This procedure allows isolating microglial cells and at the same time to leave astrocyte monolayer adhering to the flask, to be used for a possible second shaking (waiting at least 10 days). The microglial pellet obtained by centrifugation was resuspended in glial medium and cells seeded about 150000 cells/ml on the appropriate plate, pre-coated with 0.05 mg/ml poly-Ornithine (Sigma Aldrich®).

### 1.7 Microglial treatment with the β-amyloid peptide and MVs

For experiments that investigate the modulation of cytokines release (TNFα, IL6 and IL10) by microglial cells, cells were seeded at a density of about 150000 cells/ml and treated with the β-amyloid(1-42) peptide (Aβ42) (0.44µM American Peptide Company), MVs (4,5µg/ml) or the supernatant obtained from the last ultracentrifuge to isolate MVs (in equal volume to that used for MVs). The treatment was carried out for 12, 24, 48 and 72h; at the end of each time points the supernatant was collected and stored at -80 °C until ELISA was performed (see par. 1.8 Mat&Meth).

Preparation of the β-amyloid (Aβ) peptide or 488 fluorophore conjugate Aβ (488 Aβ) provides that it is dissolved in the Aβ aggregation buffer [50mM Disodium hydrogen phosphate (Na<sub>2</sub>HPO<sub>4</sub>) and 100mM NaCl in water; pH 7.4] at a final concentration of 0.44µM, sonicated for 20 seconds in order to break up the amyloid aggregates and administered to cells after 20 min. for 488 Aβ was not performed sonication but it was ready to use after dilution in aggregation buffer.

## 1.8 Cytokine profiles

Microglial cells not treated, treated with A $\beta$ 42 or BM MSC derived-MVs and co-treated both with A $\beta$ 42 and MVs or A $\beta$ 42 and MVs supernatant, were incubated for 12, 24, 48 and 72 hours to evaluate cytokines production in different conditions.

Levels of interleukin 6 (IL6) and 10 (IL10) and tumor necrosis factor  $\alpha$  (TNF $\alpha$ ) released by microglial cells were measured from culture-derived medium, analyzed with a commercially available kit of enzyme-linked immunosorbent assay (ELISA, R&D Systems) following the manufacturer's protocol. This system measures the amount of antigen between two layers of antibodies. The antigens to be measured must contain at least two antigenic sites, capable of binding to antibody, since at least two antibodies act in the sandwich. The plate is coated with a capture antibody. Sample is added to plate and any antigen present (the cytokines) is bound by the capture antibody. A detection antibody is added to the plate and also binds to antigens present in sample. The plate is then, incubated with Streptavidin conjugated to horseradish peroxidase (HRP). Finally, substrate solution is added and converted by Streptavidin-HRP to a detectable (colorimetric) form. The colorimetric reaction is read as absorbance that is proportional to the concentration of the cytokines present in the sample. Cytokines production is quantified after interpolation of Abs values with the calibration line (obtained from the linear portion of the standard curve)

## 1.9 Immunofluorescence staining of cultured N9 and microglial cells

Cultured N9 line cells and microglial cells are treated with 4% paraformaldehyde (4% paraformaldehyde, 4% sucrose, phosphate buffer 240mM) for 10 minutes to fix them and then washed three times with D-PBS. Thus, cells are washed three times with a low concentrated salt solution (phosphate buffer 10mM, NaCl 150mM) and then three times with a high concentrated salt solution (phosphate buffer 20mM, NaCl 500mM). In this protocol blocking step is required and to reduce background staining, samples are incubated with a buffer that blocks the reactive sites to which the primary or secondary antibodies may otherwise bind. In this protocol I used Goat serum dilution buffer as blocking buffer. Therefore, neurons are incubated for 30-45 minutes with Goat serum dilution buffer 1x (GSDB 2x: Goat Serum, Tryton 10%, Phosphate Buffer 40mM, NaCl 0,9M). Afterwards, fixed cells are incubated for 2h30-3h with primary antibody diluted in GSDB. Then, coverslips are rinsed three times with high concentrated salt solution and are incubated

with secondary antibody for 45 min–1 hour. Subsequently, coverslips are washed 3 times with high concentrated salt solution, 3 times with low concentrated salt solution and 1 time with Phosphate buffer 5mM for 5 minutes each. Finally, coverslips are mounted on glass with the nuclear dye Hoechst® (LifeTechnologies®) at a concentration of 1: 10000 slides and stored at –20°C. Immunofluorescence was detected with Olympus confocal microscope.

## **2. IN VIVO EXPERIMENTS**

### **2.1 Animals**

In the present study a double transgenic mouse model of AD was used for the evaluation of BM MSCs derived-MVs intracranial transplantation. We used APP/PS1 mice (from the Jackson Laboratory) that express a chimeric human amyloid precursor protein (APP<sup>swe</sup>) and a mutant human presenilin 1 (PS1<sup>dE9</sup>). Transgenic mice were used in the age range of 3 to 6 months. Given the existence of gender differences in A $\beta$  deposition in this model (Wang et al., 2003), in the present study we used only males.

All experiments were performed according to the guidelines of World Health Organization (WHO). Animals were housed at the Humanitas Research Hospital in a room maintained under controlled temperature and on a 12 hour/12 hour light/dark cycle in Specific Pathogens Free (SPF) condition.

### **2.2 Injection of BM-MSC derived MVs in APP/PS1 Double Mutant Mice**

BM-MSC derived MVs suspension or physiological saline solution (as vehicle) were transplanted at 3 and 5 month old mice for 25 days.

Animals were anesthetized intraperitoneally with a combination of 80mg/kg ketamine and 5mg/kg xylazine. With a scalpel, an incision to access to the cranium was made. Then, at cranium visible, two access points were made through 21G needle for the intracranial injection, one for hemisphere. BM-MSC derived MVs suspension (5.6 $\mu$ g/ $\mu$ l, ) and the vehicle (physiological saline solution) were administered by a Hamilton precision syringe in a total volume of 4 $\mu$ l/hemisphere per mouse: eventually 8 $\mu$ l of MVs suspension (approximately 45 $\mu$ g of proteins) and 8 $\mu$ l of vehicle (as control) were injected bilaterally into the cortex.

Mice were injected at 3 and 5 month old. Twenty-five days after the injection, both groups of APP/PS1 animals, control and treated, were sacrificed according to the guidelines of WHO. Briefly, under general anesthesia, mice were subjected to intracardiac perfusion with 1X PBS or 4% Paraformaldehyde in Phosphate Buffer solution (4% PFA in PB) to perform biochemistry and immunoistochemical analysis. The blood was collected from each animal.



### 2.3 Preparation of tissue for immunohistochemical staining

For immunohistochemical analysis, mice were subjected to perfusion with 4% PFA to allow the tissues fixation. Before perfusion, the blood was collected from the right atrium. After perfusion, brains were removed, by beheading the carcass and removing the organ from its cranial location. Brains were then, post-fixed overnight (O/N) in 4% PFA at 4 °C. In the following days, they were treated in sucrose solutions at different concentrations (7% and 20% sucrose in 1X PBS) at 4 °C until equilibrated, to prepare them for the immunohistochemical analysis.

Sequential 30µm sagittal sections were taken from one hemisphere for each animal with the Vibrating blade microtome Leica VT1000 S. Other hemispheres were stored at -80 °C after inclusion in Cryobloc (Diapath®). Brain slices were stored at -20 °C in antifreeze solution (0,1 M Phosphate Buffer solution supplemented with 30% Glycerol and 30% Ethylene Glycol) after treatment with sucrose solutions at different concentrations (7% and 20%).

### 2.4 Immunohistochemical staining

Immunohistochemical analysis was performed on free floating 30µm brain sections obtained from male mice at different age (4 and 6 month old). Brain slices have been transferred, using a paintbrush, from the antifreeze solution to a well containing 20% sucrose. After 30 min, they have been rinsed once for 5 min with 4% sucrose and three times in 1X PBS to remove all residues of the antifreeze solution. Subsequently, they have been left in cold 1X PBS supplemented with 3% Methanol (MeOH), 3% Hydrogen Peroxide (H<sub>2</sub>O<sub>2</sub>) and 0,1% Triton (X-100) for 30 min to permeabilize, dehydrate the tissue and deactivate the endogenous peroxidases all in one. Following incubation, they have been rinsed again three times as previously described. Brain sections have been then, treated with 90% formic acid (in water) for few minutes (slices must become transparent) at RT. Then, slices have been rinsed twice in 1X PBS and once in 1X PBS containing 0,1% Triton (X-100). After rinsing, sections have been incubated for 1h in 1X PBS containing 0,1% Triton and 10% goat serum at RT to block unspecific antibody binding. Subsequently, all brain sections have been incubated in primary antibody 6E10 (Beta Amyloid, 1-16 Monoclonal Antibody, Covance®) 1mg/ml in 1X PBS supplemented with 0,1% Triton (X-100) and 1% goat serum O/N at 4 °C.

The next day, all brain slices have been rinsed twice in 1X PBS supplemented with 0,1% Triton (X-100) and incubated for 15 min in MAC1 Mouse Probe (Biocare Medical). Then, they have been rinsed once in 1X PBS and incubated 20 min in MAC1 Universal HRP-Polymer (Biocare Medical). After rinsing three times in 1X PBS brain slices have been stained with 3, 3'-diaminobenzidine (DAB) [40µl (0,9mg) of DAB cromogen and 1ml of Betazoid DAB Substrate Buffer (Biocare Medical)] until the reaction occurred. The reaction was stopped when the signal background ration was optimal with distilled water to eliminate all the DAB residues.

Finally, slices have been gently positioned on microscope slides, left to dry and then rinsed twice in Alcool 100% and three times in Xilene for 5 min. Eventually, slices have been covered with cover glass slipped and left to dry into the stove at 37 °C for 24h.

## 2.5 Tissue homogenation for biochemical assay

For biochemical analysis, mice were perfused with 1X PBS. Before this procedure the blood was collected from each animal. One hemisphere of each removed brain was placed directly on dry ice, the other one was fixed in 4% PFA by immersion O/N and processed for immunohistochemistry experiments (par. 2.3 Mat&Meth). Frozen hemispheres were immediately processed for ELISA.

Tissues were homogenized by glass potter, in Tris Lysis Buffer [TLB: 20mM Tris pH 7.4, 137mM NaCl, EDTA pH 7.4, 1% Triton (X-100) and 25mM Beta-glycerol phosphate. TLB was filtered and stored at 4 °C] in ice. Each hemisphere was processed in 1ml of TLB supplemented with phosphatase (1:1000, Sodium orthovanadate) and protease (1:25) inhibitors until it was totally smashed. The homogenate was sonicated for 2 sec and subsequently, centrifuged at 15700x g for 20 min at 4 °C. Finally, the supernatant that contained the soluble Aβ42 present in the tissue was collected for ELISA and the pellet (that contained the insoluble Aβ42) was stored at -80 °C until use (either for ELISA or WB analysis). The protein content of supernatant was quantified by BCA assay. For Aβ42 and cytokine isolation from blood, after collection centrifugation at 9300x g for 15 min at 4 °C was carried out, in order to separate plasma from serum, that were then kept at -80 °C for cytokine and human Aβ42 detection by ELISA.

## 2.6 Biochemical assay

A $\beta$ 42 ELISA: to evaluate the amount of soluble human A $\beta$ <sub>42</sub> in brain tissue and blood (plasma and serum) of each animal, injected or not with MVs, we used a commercially available ELISA kit (IBL International): Amyloid-beta (x-42) ELISA. The assay was performed following the manufacturer's protocols.

Cytokine profiles in the blood was determined as described in par. 1.8 Mat&Meth valuating TNF $\alpha$  and IL10 content in both plasma and serum.

## 3. ACQUISITIONS and DATA ANALYSIS

### 3.1 Analysis of the immunohistochemistry stain

For the acquisition of brain slices processed for immunocytochemistry, we used Olympus VS DotSlide microscope endowed with a 10X objective, connected to a computer equipped with Olyvia<sup>®</sup> software. Analysis of data was performed with the ImageJ<sup>®</sup> software.

To examine the distribution and quantify the amount of A $\beta$ 42 each experimental condition (mice injected with vehicle and mice treated with MVs) about 10 slices for animal have been analyzed. In each slice three areas of interest were manually selected: cortex, hippocampus and cerebellum. Within the area of interest total number of plaques has been counted. An arbitrary threshold has been fixed and maintained for all the experimental conditions.

Using the ImageJ<sup>®</sup> software for each plaque have been obtained the area of selections ( $\mu\text{m}^2$ ) and the solidity, calculated as [Area]/[Convex area]]. In addition, also the area of each region analyzed has been obtained. The data were averaged and analyzed with Graph Pad Prism 6<sup>®</sup> software. All values were expressed as the mean  $\pm$  SEM.

The graphs represent the average area, the solidity and the density (given by the ratio between the average of the number of plaques and the mean area of brains' region analyzed) of plaques for each experimental condition.

Statistical analysis was performed using the unpaired Student's t-test with Welch's correction. P value lower than 0,05 was considered statistically significant. In the graphs \* corresponds to  $p < 0,05$ , \*\*  $p < 0,005$ , \*\*\*  $p < 0,0005$  and \*\*\*\*  $p < 0,00005$ .

### 3.2 Analysis of the immunofluorescence

For the acquisition of fixed cells processed for immunofluorescence, we used Olympus confocal microscope endowed with a 40X objective, connected to a computer equipped with Olyvia® software. Analysis of data was performed with the ImageJ® software.

To examine the amount of revealed marker through immunofluorescence of each experimental condition (treated microglia cells with 488 fluorochrome conjugated human Abeta<sub>1-42</sub> and/or BM MSC- derived MVs) we acquired for each slice almost 10 fields.

Using the ImageJ® software, an arbitrary threshold has been fixed and maintained for all the experimental conditions, to set minimum and maximum value to analyzed fluorescence intensity, after the image transformation at 8 bit. For each field have been obtained the AREA, MEAN GRAY VALUE and INTEGRATED DENSITY, a parameter that is the product of the area and the mean gray value. The obtained data were averaged and analyzed with SigmaPlot software analysis. All values were expressed as the mean ± SEM if N=3 or with SD if N<3.

Statistical analysis was performed using the unpaired One Way ANOVA test, with all Pairwise Multiple Comparison Procedures (Dunn's Method). P of value lower than 0,05 was considered statistically significant. In the graphs \* corresponds to p<0,01, \*\* p<0,001, \*\*\* p<0,0001 and

### 3.2 Analysis of results obtained by FACS

The graphs representing data obtained by FACS from MSC and MV characterization, have been created with the FlowJo® software or DIVA® software.

The dot plots show the frequency of recorded events and the squares identify the viable cell population of interest or the percentage of positive cells for each surface marker. The percentage of positive cells is calculated starting from the FMO of each fluorochrome.

### 3.3 Analysis of ELISA results

For the analysis of data obtained by ELISA, absorbance (Abs) values were interpolated on the calibration curve obtained from the standard curve of the assay, in order to extract the values of

concentration of the different cytokines (TNF $\alpha$ , IL6 and IL10) or proteins (human A $\beta$ 42). The values were expressed in pg/ml or ng/ml (for A $\beta$ 42 quantification in brain).

Statistical analysis was performed by using the Two-way ANOVA test (Tukey's multi-comparison test) for TNF $\alpha$ , IL6 and human A $\beta$ 42 and a Multiple T-test using the Holm-Sidak method for IL10 with Graph Pad Prism 6<sup>®</sup> software. All values were expressed as the mean  $\pm$  SEM. P value lower than 0,05 was considered statistically significant.

## **1. Immunophenotypical characterization of Bone Marrow isolated Mesenchymal Stem Cells and own released Microvesicles**

### **a. Characterization of immune- phenotypical markers of Mesenchymal Stem Cells**

Cultured primary Mesenchymal Stem Cells (MSCs) show in culture the typical immune-phenotypical markers reported by literature. After their isolation from Bone Marrow (BM), MSCs are first selected in culture for their adhesion properties and can be recognized for the fibroblast-like spindle-shaped morphology.

In our experimental settings, primary MSC cultures were obtained according to the protocol shown by *Lennon and Caplan in 2006*, which is still widely used.

At early passages (P), P0 and P3 cells were morphologically heterogeneous; hematopoietic cells were also usually found in culture. Only after few days in culture, MSCs could be recognized for their ability to grow as small colonies, called colony-forming units (CFU). Among the passages 10<sup>th</sup> - 15<sup>th</sup>, we assessed the multipotent stemness of our cultures, meaning their ability to differentiate in two out of three possible lineage they can give rise to: OSTEOGENIC and ADIPOGENIC lineages. Cells were cultured for 21 days in specific differentiation medium and untreated cultures were grown in parallel as control (figure 1, column A)

In MSCs treated to reveal a possible *osteogenic* differentiation, the deposition of calcium salts – typical of bone matrix – started to appear about 13 days after the beginning of the differentiation protocol. Calcium deposits were detected by staining with Alizarin Red S, a chromogenic dye with forms a long- term complex of typical red colour in the presence of calcium (figure 1, column B). At higher passages, osteogenic differentiation did not occur as easily.

In order to assess the MSC adipogenic commitment, cells were cultured for 21 days in *adipogenic* differentiation medium. After 15 days in the presence of differentiation medium, treated MSCs showed the presence of intra-cytoplasmatic lipid droplets which could be visualized by staining with the lipophilic Red Oil dye, after binding to triglycerides (figure 1, column C). Lipid deposits were not observed in untreated cultures, unless at higher cell passages (over p14<sup>th</sup>, data not shown).

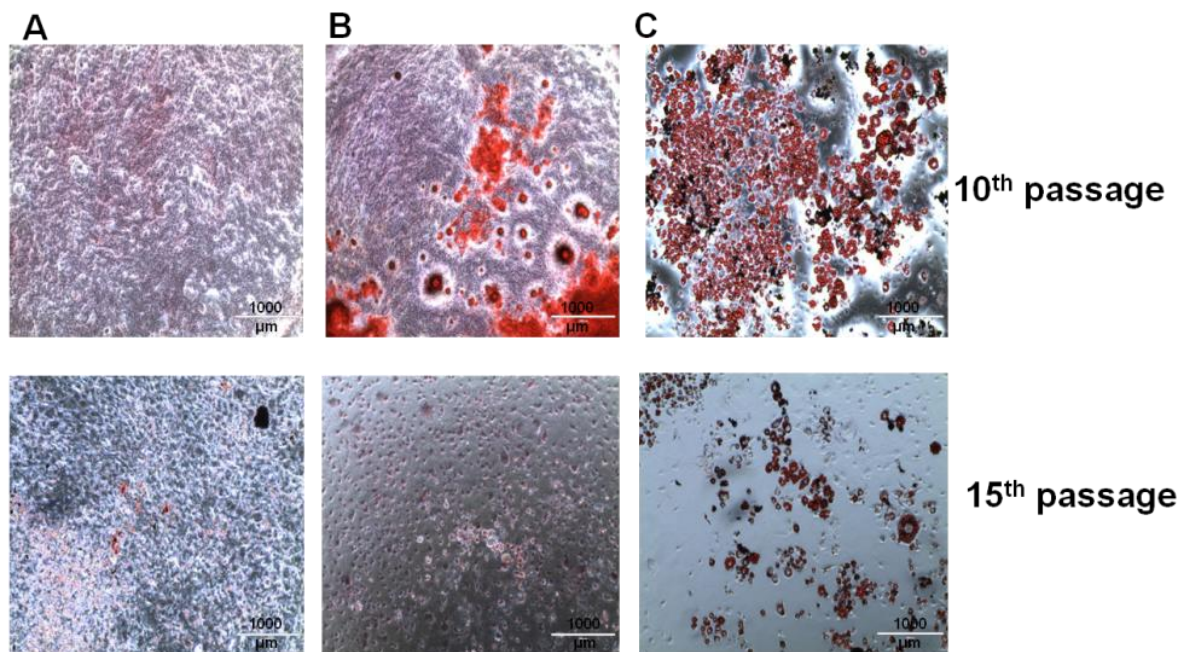


**Figure1. MSC cultures at 10<sup>th</sup> and 15<sup>th</sup> passages, subjected to osteogenic and adipogenic differentiation. Column A)** Controls were stained respectively with Alizarin Red and Red Oil staining. **Column B)** Osteogenic differentiation visualized by Alizarin Red staining of 10<sup>th</sup> and 15<sup>th</sup> passage MSC cultures. **Column C)** Adipogenic differentiation visualized by Red Oil staining of 10<sup>th</sup> and 15<sup>th</sup> passage MSC cultures. Scale bar= 1000 µm.

Furthermore, to confirm the cell phenotype, the expression of membrane molecules or antigens typical of MSCs in vitro, was assessed through Fluorescent-Activated Cell Sorting (FACS). This approach allowed us to identify the expression of typical mesenchymal markers according to different cultures' passages (from p6 to p15) and to monitor their stemness by the time.

Data from literature provide a list of typical MSC-linked positive markers (CD73, CD105, Sca1) as well as negative markers (CD3, CD19, Ly6c CD45, together reported as Lineage markers (Lin), CD117 (c-Kit) and CD31). The expression of additional MSC membrane markers, such as CD106, CD44, CD9, CD29, CD49a (Da Silva Meirelles et al., 2003), will be assessed.

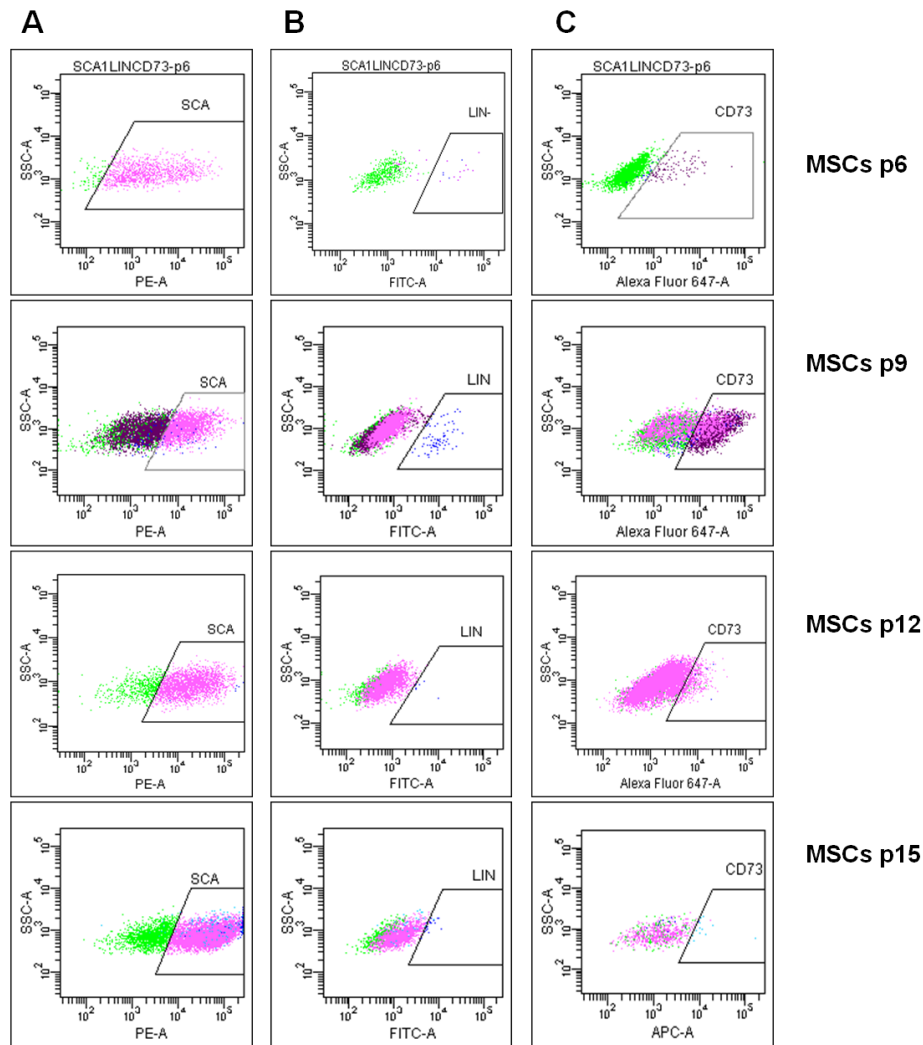


**Figure 2. Representative panels of flow cytometric analysis for Sca1, Lineage and CD73 markers.** Comparison of MSC cultures at different passages, showed as characteristic membrane molecule changes in culture. **Column A)** Sca1 marker; **column B)** Lineage markers (CD3, CD19, Ly6c CD45); **column C)** CD73 marker, each one showed for different passage of cultures. FACS representative plots for each marker was performed by analysis with DIVA software (N=3).

As shown by FACS analysis panels (column A, figure 2), MSCs maintain high levels of Sca1, a marker of various types of stem cells, for different passages. In addition, MSCs were also positive for CD73 and CD105 (figure 2, column C and figure 3, column A, respectively), which represent two out of three fundamental markers for mesenchymal stemness, together with CD90, which is not always present in murine cells (Schurgers, E. *et al.* 2010). Figure 2 (column C) and figure 3 (column A) show that CD73 and CD105 were reduced on MSC surface at high passages (p15), with characteristic modulation for each one: CD73 (figure 2, column C) increased in the first passages while decreasing at p12; CD105 (figure 3 column A) increased up to p12 and almost disappeared at p15.



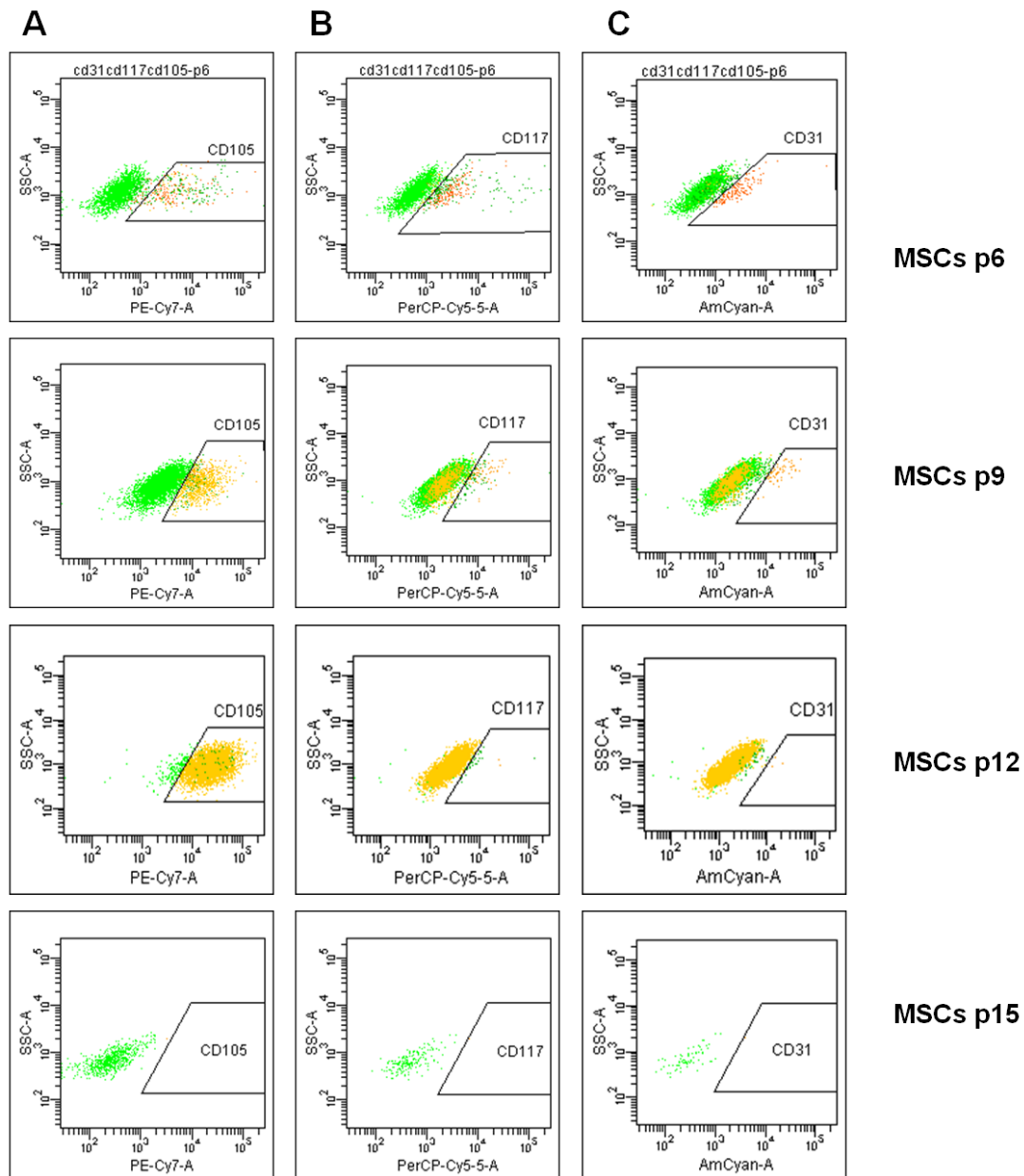


**Figure 3. Representative panels of flow cytometric analysis for CD105, CD117 and CD31 markers.** Comparison of MSC cultures at different passages showed as characteristic membrane molecule changes. **Column A)** CD 105 marker; **column B)** CD 117; **column C)** CD 31 marker, each one showed for different passages in culture. FACS representative plots for each marker was performed by analysis with DIVA software. (N=3).

As expected, cells were negative at the selected passages for lineage markers (Mouse Hematopoietic Lineage –Lin), for CD117 and for CD31, thus excluding, respectively, leukocytes (B cells and T lymphocytes) presence and a possible contamination of MSC cultures by hematopoietic stem cells or endothelial cells (showed in figure2, column B). It is interesting to note that CD117 and CD31 decreased during in vitro passaging, highlighting the purification of the cultures by contaminating cells.

Considering CD73 and CD105 fundamental markers for mesenchymal cells endowed with stemness properties, and the CD117 and CD31 absence important to guarantee MSC cultures purity, we can conclude that cell cultures obtained presented heterogeneity in the cell population composition, up to 6<sup>th</sup> passage (figure 2, columns B-C). Moreover BM-MSCs are usually isolated and purified through their physical adherence to the plastic cell culture plate (Dominici et al., 2006.), hence we used for our experiments those cultures that showed high levels of CD73 and CD105, in association with low presence of CD117 and CD31. These cultures were therefore stimulated to release MVs from *in vitro* passage the 9<sup>th</sup> up to the 14<sup>th</sup>, in which CD73 and CD105 showed higher expression.

### b. Characterization of MSC-released Microvesicles (MVs)

In order to isolate Microvesicle (MV) pool from BM-derived MSCs, we used a protocol accepted and widely used by the scientific community (Théry et al., 2006) which, by multiple centrifugation and ultracentrifugation steps, allows to isolate cellular  $\mu\text{m}$  and  $\text{nm}$  sized particles.

For our experiments, we decided to isolate the extracellular vesicle population indicated as “p3p4” which includes the larger vesicles released by shedding from plasma membrane (100- 1000 nm sized) and the exosome population (usually called p4), which is released by exocytosis of Multivesicular Bodies (MVB). The exosome size is included into 30-100 nm range (Théry et al., 2006; Kenneth W. Witwer et al., 2013). We named this p3p4 pool of isolated vesicles as MVs.

The secretion of MVs was induced after plating MSCs at high density ( $4 \times 10^4$  cells/cm<sup>2</sup>) and subjecting them to serum deprivation for 3h. We then performed multiple centrifugation and ultracentrifugation passages, isolating heterogeneous populations of MVs.

The first centrifugation was performed at 400x g to eliminate P1 population, consisting in broken membrane and dead cells. The second centrifugation was performed to isolate P2 vesicle pool: it consists in all that vesicles with a size range of 1 $\mu\text{m}$  -2 $\mu\text{m}$ . In this population, were described the *Apoptotic Bodies*, that are released by dying cells during starvation stimulus. Then we isolated p3p4 MV population by an ultracentrifugation of 110 000xg, that allowed to isolate microvesicles and exosomes together.

In order to visualize MVs and to obtain a quantification of the samples, we used the NanoSight® Viewer Technology, that allowed an accurate analysis of the MV presence in the ultracentrifuged

pellet. This technology allows to both visualize and characterize nanoparticles from 10 nm - 2000nm in solution.

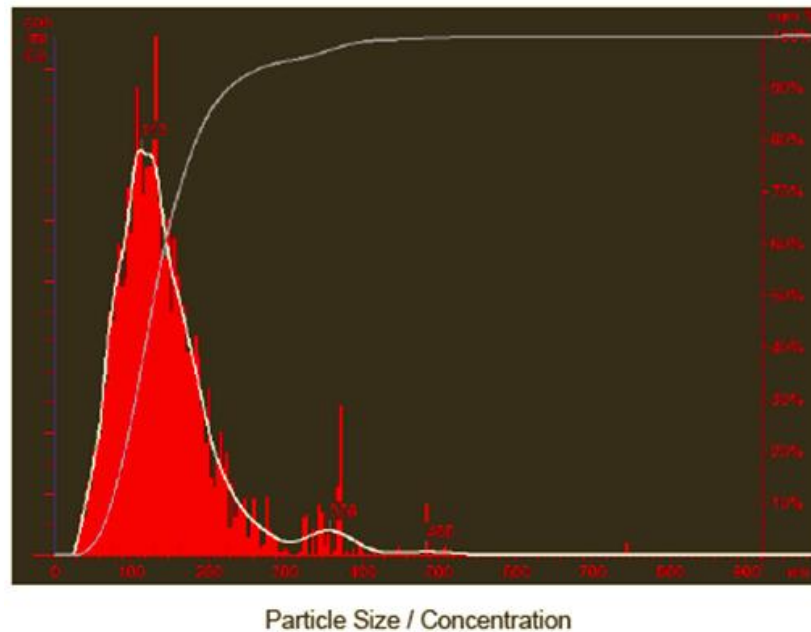


**Figure5. Representative image from NinoSight®analysis.** Histogram shows that isolated MVs revealed particles mainly placed between 50nm and 300nm size,: MVs (p3 and p4 pool), according to Théry's protocol of separation (*Théry et al,2006*).

of the Nanosight® analysis allowed us to detect isolated extracellular vesicles which, according to the isolation protocol used, ranged mostly between 100 nm and 300 nm (figure 5).

In order to visualize the MV associated proteins we run the MV lysates on a polyacrilamide gel and subsequently stained them with the Coomassie Blue, which gave us an initial idea of the total protein amount which can be obtained from a final cellular density of plated cells of  $3 \times 10^6$  cells, cultured for different passages. Although FACS analysis is not the most suitable technique, since the resolution limit does not allow to accurately discriminate microparticles smaller than 200 nm, nevertheless it represents the most widespread technique used to characterized MVs for the expression of some surface markers. Therefore, we investigated the expression of CD9, CD29, CD49a and CD73 on MV membrane, combining to Phalloidin (Ph) staining, a fungal toxin that binds to F-actin stabilizing actin filaments (figure 6b), in order to discriminate between fragments of cell membranes, Ph<sup>+</sup> labeled, and MVs, that must be Ph<sup>-</sup>, because excluded from their lumen. Standard beads with a size of 0,79-1,34  $\mu$ m, respectively, were used as reference points of size.

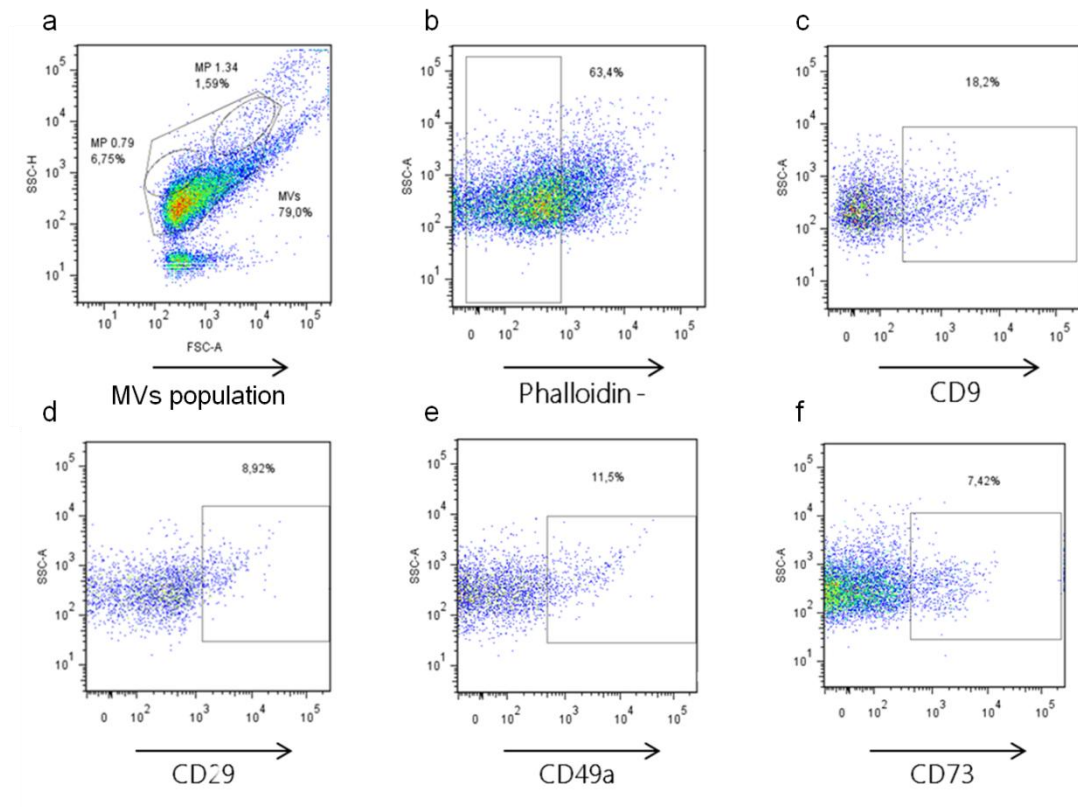


**Figure 6. Representative panels of BM-MSC derived MV FACS analysis .** The “a” scatter plot shows the total population of isolated and stained MVs. Two different dimension beads, with a size of 0,79-1,34  $\mu\text{m}$ . Respectively, were used to determine the dimension range and to exclude the close to resolution limit noise due to instrument.

“b” scatter plot shows Phalloidin negative gate, excluding fragmented membrane particles. Inside Phalloidin negative gate, MV population shows presence of CD9 (exosome marker), CD29 and CD49a (Integrins) and CD73 (Ecto-5'-nucleotidase) typical markers of MV population (c- d- e-f scatter plots). (N=2).

Figure 6 shows the MV immune phenotype obtained through FACS technique using typical markers reported in literature (Suresh Mathivanan et al., 2010): CD9 as exosome marker, CD49a and CD29 integrins as markers of shed microvesicles and CD73 as marker of MSC – derived MVs (Stefania Bruno et al, 2009). This preliminary MV membrane molecule characterization showed that within the total population, more than 50% is represented by Ph<sup>-</sup> MVs (figure 6, b). Overall, these findings made us confident that the cell stimulus and isolation protocol used, yielded to obtain an enriched MV population that includes exosomes, positive for CD9.

Western Blot (WB) analysis using MV- typical markers, is still needed to characterize MV pool in a semi- quantitative manner, in order to investigate the MV protein components specifically released upon starvation stimulus. We expect to find classical proteins both characteristic “p3” pool – such as Selectins, Integrins, CD40 and Metalloproteinases (typical of shedding MVs) and

typical of exosomal population such as CD9, CD63, CD81, Alix, TSG101 and HSC70 as indicated by literature (Suresh Mathivanan et al., 2010).

## **2. In vitro evaluation of cytokine release by cells treated with human-Abeta1-42 and BM MSC-derived MVs**

### **a. Experimental Design.**

After characterization of both MSCs and MSC-derived MVs, we decided to test the MV pool p3p4 in a simplified *in vitro* experimental model of Alzheimer's disease (AD) to investigate their possible anti-inflammatory role in the inflamed environment, followed by Beta Amyloid<sub>1-42</sub> (A $\beta$ <sub>1-42</sub>) administration.

Alzheimer's disease involves most of brain cells: in fact in response to inflammatory stimuli neurons are induced to overproduce A $\beta$ <sub>1-42</sub> and its neurotoxic fragments (Walsh DM et al., 2007.). In turn, astrocytes become reactive upon neuronal injury. This process is usually described as reactive astrogliosis (Lian H et al., 2015). Also microglia, the resident immune cells of the brain, turn out to be activated and play a pivotal role for the cerebral neuroinflammation progress (Rubio-Perez JM et al., 2012).

Since in literature the MSC ability to promote microglial cells to secrete cytokines has been extensively demonstrated (Giunti et al., 2012; Rahmat et al., 2013), we decided to verify whether MSC-derived MVs might affect the release of cytokines, possibly endowed with anti-inflammatory properties, from cultures exposed to A $\beta$ <sub>1-42</sub>. We focused on microglia, the immune cell population of the brain. We performed a first set of experiments with N9 cells, an immortalized murine primary microglia, to set stimulation conditions and, subsequently, we investigated the effects in primary microglia.

Both types of cultures were stimulated with human-Amyloid Beta<sub>1-42</sub> peptide (h-Aβ<sub>1-42</sub>), and simultaneously exposed to either MSC-derived MVs or the supernatant collected after MV isolation (see method section), in order to assess the action of any soluble factors released by MSCs.

We focused our attention on specific molecules: TNFα, which represents the molecular trigger of the inflammatory cascade and maintain the inflammatory response even in AD (Perry et al., 2001) ; IL-6 , a pro-inflammatory cytokine that is heavily released upon the TNFα activation and that is maintained high in different processes involved in inflammation; Interleukin 10 (IL 10), the major anti-inflammatory cytokine (Szczepanik et al., 2001), along with Interleukin 4 (Rubio-Perez JM et al., 2012), that has been described to modulate inflammatory cytokine release by microglia, in the presence of Aβ<sub>1-42</sub> (Szczepanik et al., 2001).

In both types of microglial cultures exposed to h-Aβ<sub>1-42</sub>, we specifically evaluated the pro-inflammatory and the anti-inflammatory cytokine release, during different stimulation times ( N9 cultures at 24h; primary cultures of murine microglia, from 12 up to 72h).

### b. Analysis of cytokine release in N9 cells exposed to h-Aβ<sub>1-42</sub> and MVs- e

As mentioned above, we set up the experimental conditions on the immortalized murine microglial cell line N9. N9 cells were cultured at 150000 cells/mL density and stimulated with 0.44μM h-Aβ<sub>1-42</sub> in the presence of 4.5 μg/mL MVs (calculated as protein contents). Microglial culture supernatant was analyzed by ELISA for TNFα, IL6 and IL10 after 24h of h-Aβ<sub>1-42</sub> /MV stimulation.

A significant release of TNFα from N9 cells was detected after 24 h h-Aβ<sub>1-42</sub> treatment (figure7a, black bars).

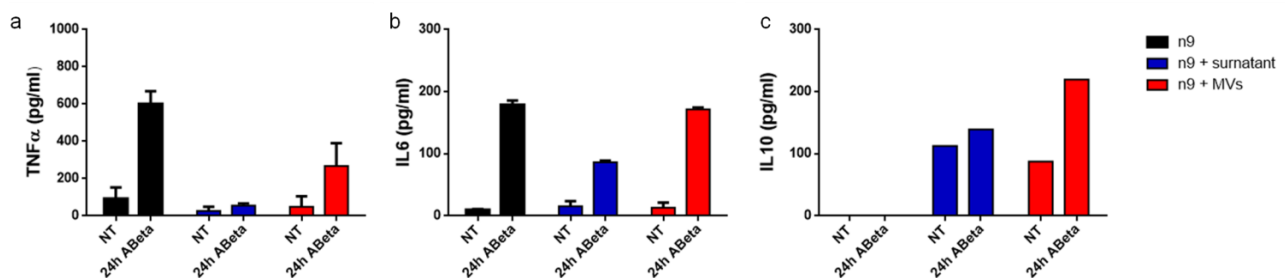


**Figure 7. Cytokine release by N9 upon treatments with h-Aβ<sub>1-42</sub> and BM- MSC derived MVs.** a) Histograms show how the presence of h-Aβ<sub>1-42</sub> induced an increase of TNFα release by N9 during 24h stimulation (black bars). Simultaneous addition of both surnatant

(blue bars) or MVs (red bars) slow down TNF $\alpha$  release. **b)** Histograms show IL6 release by N9. As TNF $\alpha$ , IL6 release occurred following 24h of h-A $\beta$ <sub>1-42</sub> treatment and this effect can be reduced by the addition of the supernatant. Instead MVs appeared not to induce a consistent effect. **c)** Histograms show the release of IL10 by N9 stimulated with h-A $\beta$ <sub>1-42</sub> and ultracentrifugated supernatant or h-A $\beta$ <sub>1-42</sub> and MVs. h-A $\beta$ <sub>1-42</sub> alone administration did not induce IL10 secretion. Note that the presence of MVs led a greater IL10 release with respect to the supernatant. As controls, cultures were treated with any stimulus (NT black bar) or treated only with supernatant (NT blue bar) or MVs (NT red bar). (N<3).

During the 24h-treatment, the presence of MVs contributed to drastically reduce the increase of TNF $\alpha$  (figure 7a, red bars). Interestingly, the addition of the ultracentrifuged supernatant to N9 treated cells, led to a similar effect (figure 7a, blue bars). Addition of either supernatant or MVs to N9 in the absence of amyloid peptide did not impact TNF $\alpha$  release (compare NT black bars with NT blue bars and NT red bars in figure 7a).

In the absence of h-A $\beta$ <sub>1-42</sub>, (fig. 7, NT black bar) or when exposed to MVs or supernatant (NT blue - and NT red bars) N9 cells produced low quantities of IL6. On the other hand, when the amyloid peptide was added to N9 cultures, the release of IL6, strongly increased as for TNF $\alpha$  (figure 7b, black bar). Even in this case, 24 h after the exposure to the MSC supernatant in the presence of the amyloidogenic protein, a remarkable decrease in IL6 production was observed (figure 7b, blue bars). In the absence of h-A $\beta$ <sub>1-42</sub>, the ultracentrifuged supernatant had no effect.

On the other hand, the addition of MVs, did not reduce at appreciable levels A $\beta$ <sub>1-42</sub>-induced IL6 release. Noteworthy, MVs did not induce changes in the basal IL6 secretion (figure 7b, red bars, compare with NT black bars).

These findings indicate that BM-MSC derived MVS, but even more efficiently, the MSC supernatant reduce the release of of proinflammatory cytokine in microglia exposed to h-A $\beta$ <sub>1-42</sub>.

We then investigated the possible release and modulation of anti- inflammatory cytokines, such as IL10 and IL4, which are also released by microglia (Rubio-Perez JM et al., 2012). Although IL10 is generally described playing an important role in the regulation of inflammation, its role in AD is still debated (Sardi et al., 2011; Michaud JP et al., 2015; Guillot-Sestier MV et al.,2015).

Figure 7c (black bars) shows that N9 microglial cells were not able to release IL10 either in basal conditions or in the presence of h-A $\beta$ <sub>1-42</sub>. Interestingly, the addition of ultracentrifuged supernatant- obtained by MV isolation- induced approximately the same release of IL10, both in the absence and in the presence of h-A $\beta$ <sub>1-42</sub> for 24 hours (figure 7c, blue bars).

Noteworthy, MVs induced the release of IL10 already in the absence of h-A $\beta$ <sub>1-42</sub>, but its increase was even higher upon h-A $\beta$ <sub>1-42</sub> treatment (figure 7c, red bars).

These preliminary results, showing a delay in TNF $\alpha$  release and an increase in IL10 following h-A $\beta$ <sub>1-42</sub> and MVs administrations to the N9 cell line, suggest that BM-MSC-derived MVs might participate in the modulation of the *in vitro* inflammatory response in a more specific manner with respect to the supernatant, possibly delaying inflammation.

As next step, we investigated the effects of MVs in primary microglial cultures.

### c. Analysis of cytokine release by treated primary microglia cells

Primary microglial cells were cultured at 150000 cells/mL density and stimulated with 0.44  $\mu$ M h-A $\beta$ <sub>1-42</sub> in the presence of 4.5  $\mu$ g/mL MVs (calculated as protein content). By means of ELISA microglial culture supernatant was analyzed for TNF $\alpha$ , IL6 and IL10 amount after 12h, 24h, 48h and 72h of h-A $\beta$ <sub>1-42</sub>/MV stimulation (figure 8).

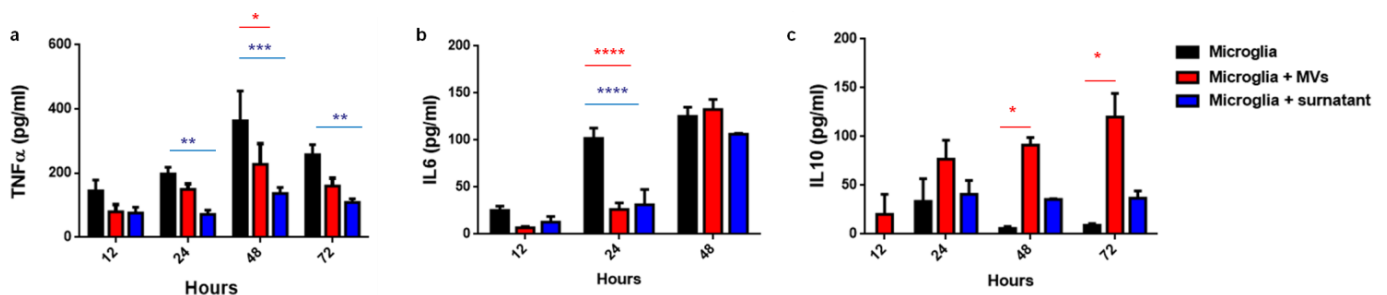


**Figure8. Pro- Inflammatory and anti- inflammatory cytokine release by primary microglia after treatments with h-A $\beta$ <sub>1-42</sub> and BM- MSC derived MVs.** a) Histograms show the time course of stimulation of primary microglia with h-A $\beta$ <sub>1-42</sub> (black bars). It is possible to note that, TNF $\alpha$  increase during time with a maximum peak at 48 hours. Simultaneous treatment with supernatant (blue bars) or MVs (red bars) significantly slow down TNF $\alpha$  release in both cases. MVs show a significant effect at 24h only while Supernatant (blue bars) addition to h-A $\beta$ <sub>1-42</sub> treated cultures show a significant effect at 24h and following time points b) Histograms show IL6 trend under stimulation with h-A $\beta$ <sub>1-42</sub>. At 48h IL6 is higher than previous time point, 12h and 24h and the maximum and significant effect of added MVs was visible at 24 hours, as like as supernatant effect. c) Histograms show that in presence of h-A $\beta$ <sub>1-42</sub>, IL10 is produced weakly and that only added MVs evoked a strong IL10 release. In particular this release became significant at 48 hours of h-A $\beta$ <sub>1-42</sub> stimulation. Supernatant did not induce IL10 release, leading to think that IL10 could be specifically induce by MVs. (N>3).

Primary microglial cells, in the absence of the h-A $\beta$ <sub>1-42</sub> stimulus, did not release TNF $\alpha$  (data not shown); on the contrary, stimulation with h-A $\beta$ <sub>1-42</sub> induced microglial cells to a consistent TNF $\alpha$  release, already at 12 h, with its levels increasing sharply at subsequent time points (figure 8a,



black bars). This effect reached its maximum peak at 48h and then disappeared spontaneously at 72h.

Upon simultaneous treatment of microglial cells with both h-A $\beta$ <sub>1-42</sub> and MVs (figure 8a, red bars), TNF $\alpha$  cytokine secretion appeared to be weakened at 12h with a decreased effect over the time. MV effect became statistically significant only at 48h. Noteworthy, the greatest TNF $\alpha$  attenuation was again induced by the supernatant application, in particular at 48h and at 72h.

IL6 is a cytokine that, with its pro-inflammatory action, appears to be closely related to AD, noticeably in the early stages (Bhojak et al., 2000; Papassotiropoulos et al., 2001). Accordingly, upon h-A $\beta$ <sub>1-42</sub> treatment, IL6 release by microglia cells increased and this was mostly evident at 24 and 48h. MV treatment induced a significant reduction in IL6 levels at 24 h but not at 48h (figure 8b red bars); a similar action was observed after supernatant application (figure 8b). Conversely, primary microglial cells did not produce IL6 in the absence of h-A $\beta$ <sub>1-42</sub>.

MVs in the presence of the inflammatory stimulus, induced a significant increase of IL10 release by microglial cells, starting from 24h up to 72h (figure 8c, red bars). Interestingly, the ultracentrifuged supernatant of MVs only slightly induced the production of IL10 after 24h and this increase in the release was maintained unvaried up to 72h. In conclusion, our results showed that MSC-derived MVs induce a reduction in the levels of pro-inflammatory cytokines TNF $\alpha$  and IL6 and an increase in the secretion of the anti-inflammatory cytokine IL10, both in N9 cultures and in microglia cultures at different time point investigated.

This modulation of inflammatory response in cell cultures exposed to h-A $\beta$ <sub>1-42</sub>, was in line with literature references showing that BM- MSC derived factors can play a modulatory role in the inflammatory status (Bernardo and Fibbe, 2013; Bruno et al., 2012; Mocarizadeh et al., 2012). Moreover these results are in agreement with the data of Giunti and colleagues, (2012) showing the MSC capacity to decrease the release of inflammatory cytokines and increase the expression and the release of neuroprotective molecules from N9 cells and microglia, both stimulated with an inflammatory stimulus (LPS). It is not unexpected that, in our experimental conditions, a greater effect was observed in the presence of the supernatant obtained after the ultracentrifugation of MSC culture medium following starvation, confirming that soluble factors in the MSC culture medium strongly participate in this regulation. However our results suggest that not only soluble factors, but also BM- MSC derived MVs take part in the regulation of microglial response in the presence of  $\beta$  - amyloid peptide, highlighting a specific effect of MVs in IL10 secretion.

### **3. Phenotype assessment of microglia cells upon- Aβ<sub>1-42</sub> and BM- MSC derived MVs treatment**

Recently, some studies have shown that in the presence of MSCs, microglial cells undergo a phenotypic switch from pro-inflammatory to anti-inflammatory state, indicated as M1/M2 phenotypes (Maggini et al., 2010; Cho et al., 2014). In brain under pathological conditions, microglia is activated, and M1 and M2 polarizations are not in balance, being modulated by autocrine and paracrine molecules (Cherry et al. 2014). Furthermore it has been shown that IL-10 is able to decrease the microglial pro-inflammatory state induced by β- amyloid peptide (Lyons et al., 2007 and Szczepanik et al., 2001), which would be relevant in light of our data showing a boost of IL10 release concomitant with TNFα and IL6 decline upon exposure to MSC-MVs.

Therefore, we wondered whether the above mentioned (functional) modifications could induce a phenotypic change in microglia, and in particular the *switch* from a pro-inflammatory to an anti-inflammatory phenotype, involving the change in the expression of specific M1/M2 markers in response to β-amyloid peptide and MV stimuli.

To address this issue, we evaluated, besides the presence of Iba1, a widely recognized microglial marker, the expression of membrane proteins such as MHCII and CD206, the former typical of the pro-inflammatory M1 phenotype, while CD206 (the mannose receptor) being associated with the anti-inflammatory M2 phenotype (Cherry et al. 2014).

Since activated microglia showed phagocytotic features, that are modulated by M2 and reduced by M1 interleukins, we administered to primary microglia cultures 488 fluorochrome conjugated h-Aβ<sub>1-42</sub> (488h Aβ<sub>1-42</sub>) in order to evaluate whether the administration of BM-MSC derived MVs could also modulate phagocytotic capacity.

#### **a. Evaluation of the expression of MHC II, M1 marker, in MV-treated microglia**

In order to investigate whether the treatment with MSC-released MVs could down-regulate the pro-inflammatory activity of h-Aβ<sub>1-42</sub> treated microglia, we assessed the changes in the microglial expression of MHCII, a M1 phenotype specific marker, typical of cell antigen presenting complex (figure 9).

We performed double immunofluorescence for MHCII and Iba1 , the latter being a general marker to identify microglial cells (gray), that also allowed to recognize their gross morphology (red in figure 9).

Figure 9a shows that, in the absence of any treatment, microglia exhibited a branched morphology, as highlighted by Iba1 staining: this morphology is characteristic of the "resting" microglial phenotype. Virtually all cells showed MHCII in the cytoplasm (red, central panel in figure 9 a) .

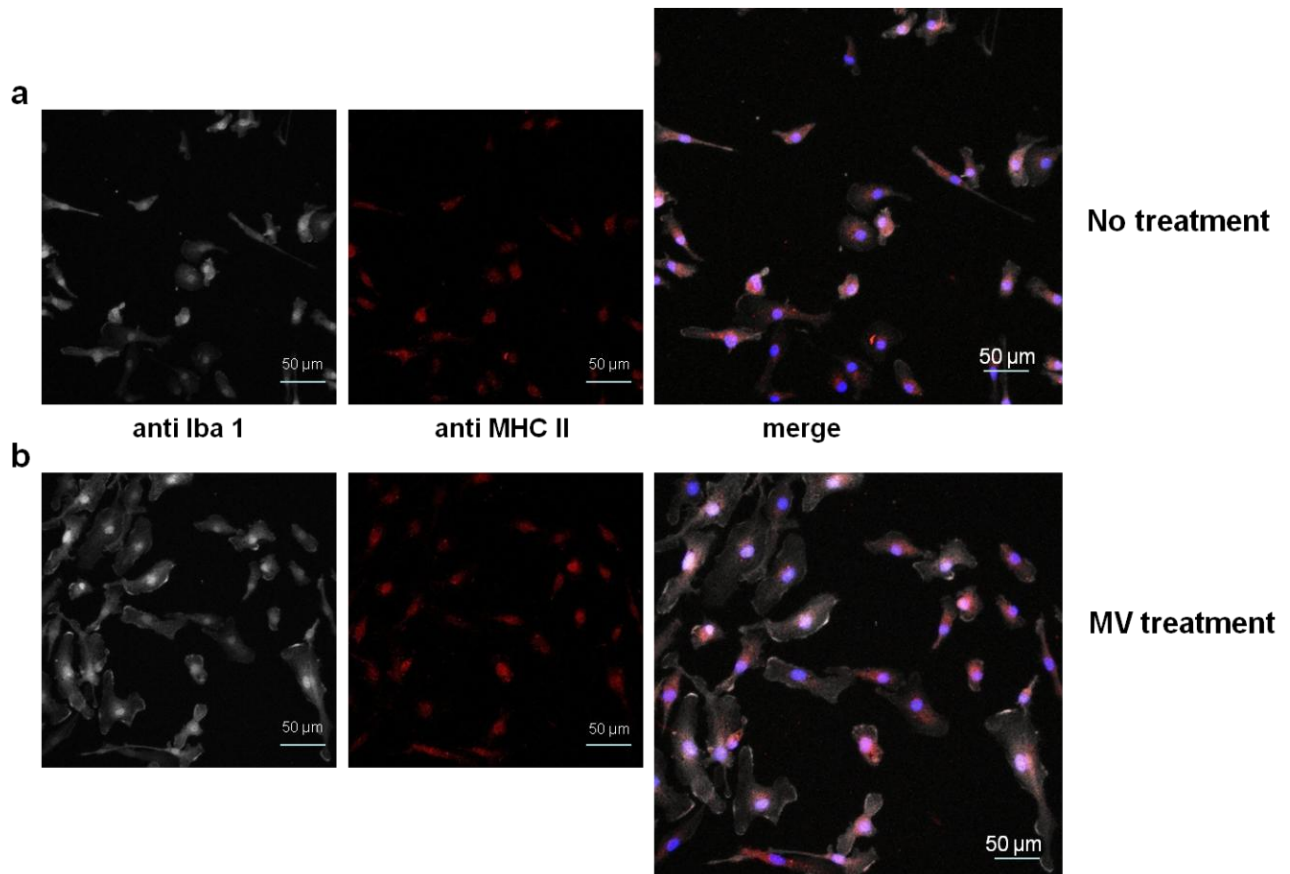


**Figure9. Primary microglia cultures treated with BM- MSC-derived MVs and their controls. a)** control cells **b)** cell stimulated with MVs only. Cultures were stained with antibodies anti Iba1 (gray) and anti MHC II (red), to verify the levels of MHC II expressed by microglia in the absence of any stimulation and whether MV treatment could modify its expression. Notice that microglial shape that assumed an amoeboid morphology, and MHCII expression changes apparently.

Images represent a max projection of the whole Z- stacks, acquired by confocal microscope. In blue the nuclei are stained with DAPI (N=3).

We then analyzed microglial cells treated with MVs only (figure 9b), to verify the possible effects on microglial "resting" state.

No gross changes in the expression of MHCII were observed in microglia following MV addition, although a change in cell shape which frequently assumed an *amoeboid* morphology typical of

“activated” microglia. In literature, this is the state believed to attenuate neurotoxic  $\beta$ -amyloid peptide effects and it is associated with  $A\beta$  phagocytosis, as reported by Tsay (Tsay et al. 2013). The authors in fact distinguished two distinct phenotypes of microglia, designed as proliferating amoeboid microglia (PAM) and differentiated process-bearing microglia (DPM). The PAM phenotype attenuated  $A\beta_{25-35}$ -mediated neurotoxicity through phagocytosis, and produced neurotrophic factors. Phagocytosis, therefore, could be an interesting issue to investigate in order to display microglia function towards  $A\beta$  peptide following MV administration.

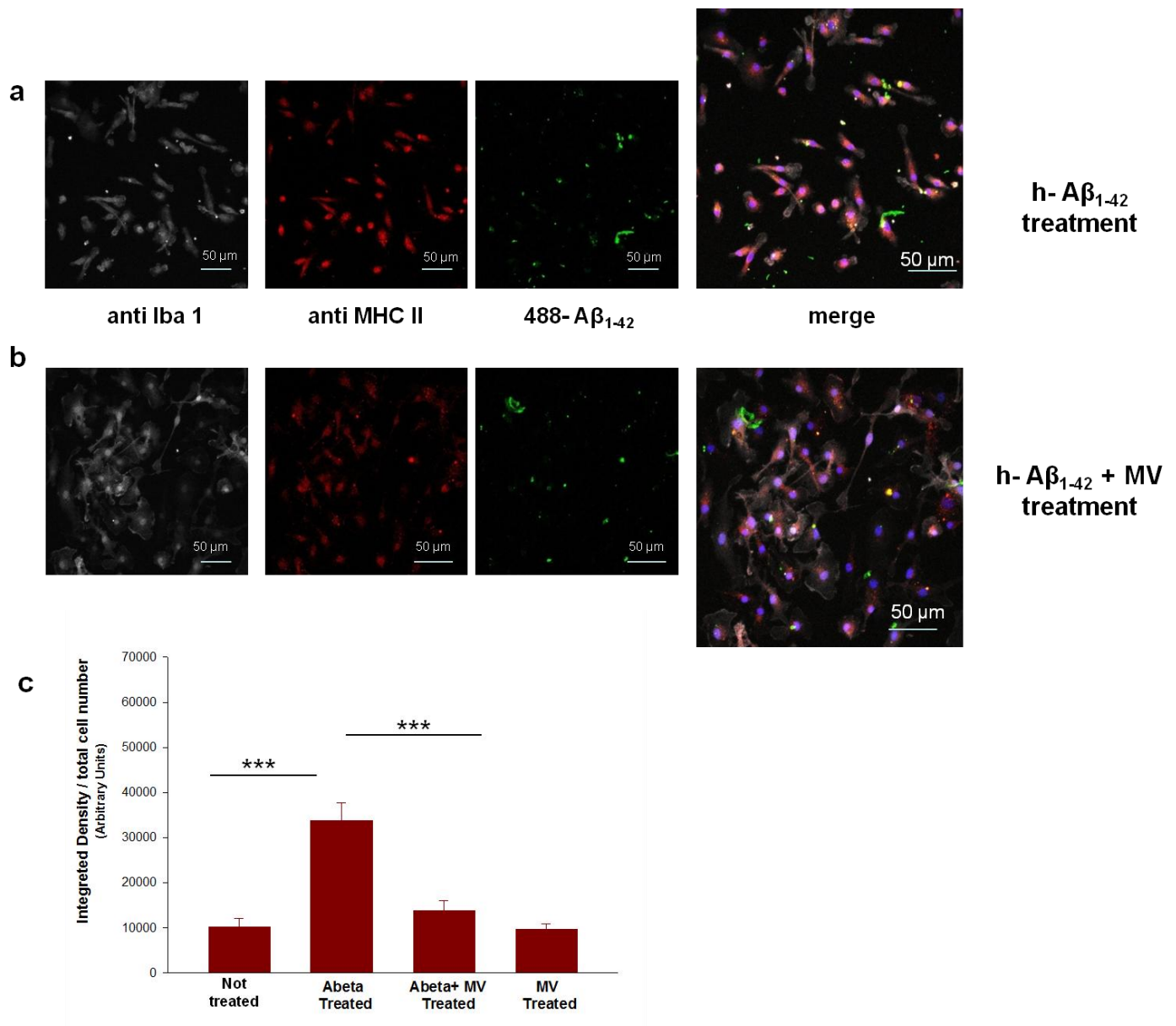


**Figure 10.** Primary microglia cultures treated with BM- MSC derived MVs and h- $A\beta_{1-42}$  488 fluorochrome conjugated to assess MHC II expression. **a- b)** Cultures were stained with anti-Iba1 and anti-MHC II to verify whether MHC II increases under inflammatory condition: **(a)** in 488h- $A\beta_{1-42}$  treated culture is visible a strong MHC II immunoreactivity (red) that is significantly reduced after MV treatment ( $P < 0,001$ , comparing with **c**);

(b) in 488h-A $\beta_{1-42}$  and MVs treated culture is visible a strong reduced MHC II immunoreactivity (red) that is significant comparing with a. The amoeboid morphology can be also observed comparing a and b;

c) Histograms show modulation of MHC II expression by inflammatory stimulus and the decrease obtained by MV treatment. Images represent a max projection of the whole Z- stacks, acquired by confocal microscope In blue the nuclei are stained with DAPI. (N=3).

As expected, 488h-A $\beta_{1-42}$  treatment induced a significant increase in MHCII expression (figure 10a and figure 9a, red). Notably, microglia cells treated with both 488h-A $\beta_{1-42}$  and MVs (figure 10b), displayed a clear reduction in MHC II expression. In order to get a more accurate estimation of the changes in the levels of expression of MHCII in the presence of MVs and h-A $\beta_{1-42}$ , we performed semi-quantitative analysis of the levels of fluorescence (figure 10c), confirming that MV administration down regulate the M1 marker MHCII in an inflammation context.

### b. Evaluation of the expression of M2 marker CD206 by MV treated microglia

We next evaluated the possible modulation of M2 markers by MV treatments of microglia, focusing our attention on the expression of the mannose receptor CD206.

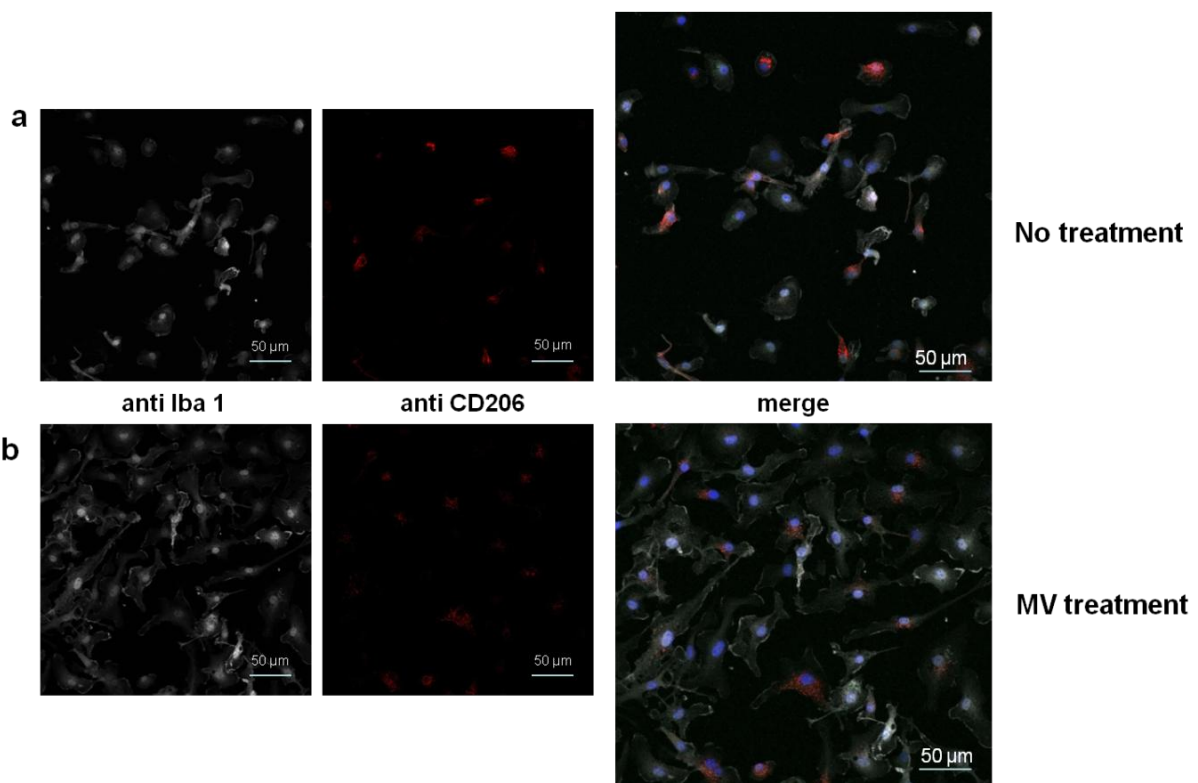


**Figure 11. Primary microglia cultures treated with BM- MSC-derived MVs. a) Control cells b) stimulated cells with MVs only. Cultures were stained with antibodies anti Iba1 (gray) and anti CD206 (red), to verify the level of CD206, expressed by microglia in**

the absence of any stimulation and whether MV treatment could modify its expression. We can observe microglial shape that assumed an amoeboid morphology, and CD206 expression changes apparently.

Images represent a max projection of the whole Z- stacks, acquired by confocal microscope. In blue the nuclei are stained with DAPI. (N<3)

Preliminary staining with anti- iba1 (gray) and anti- CD206 in untreated cultures (Figure 11a) and in cultures treated with MVs only (figure 11b), showed that the presence of MVs increased CD206 expression, as quantified in the graph of figure 12. The comparison between microglia treated only with 488-h-A $\beta_{1-42}$  and microglia exposed to both MVs and 488h-A $\beta_{1-42}$  showed a similar increase in CD206 expression.

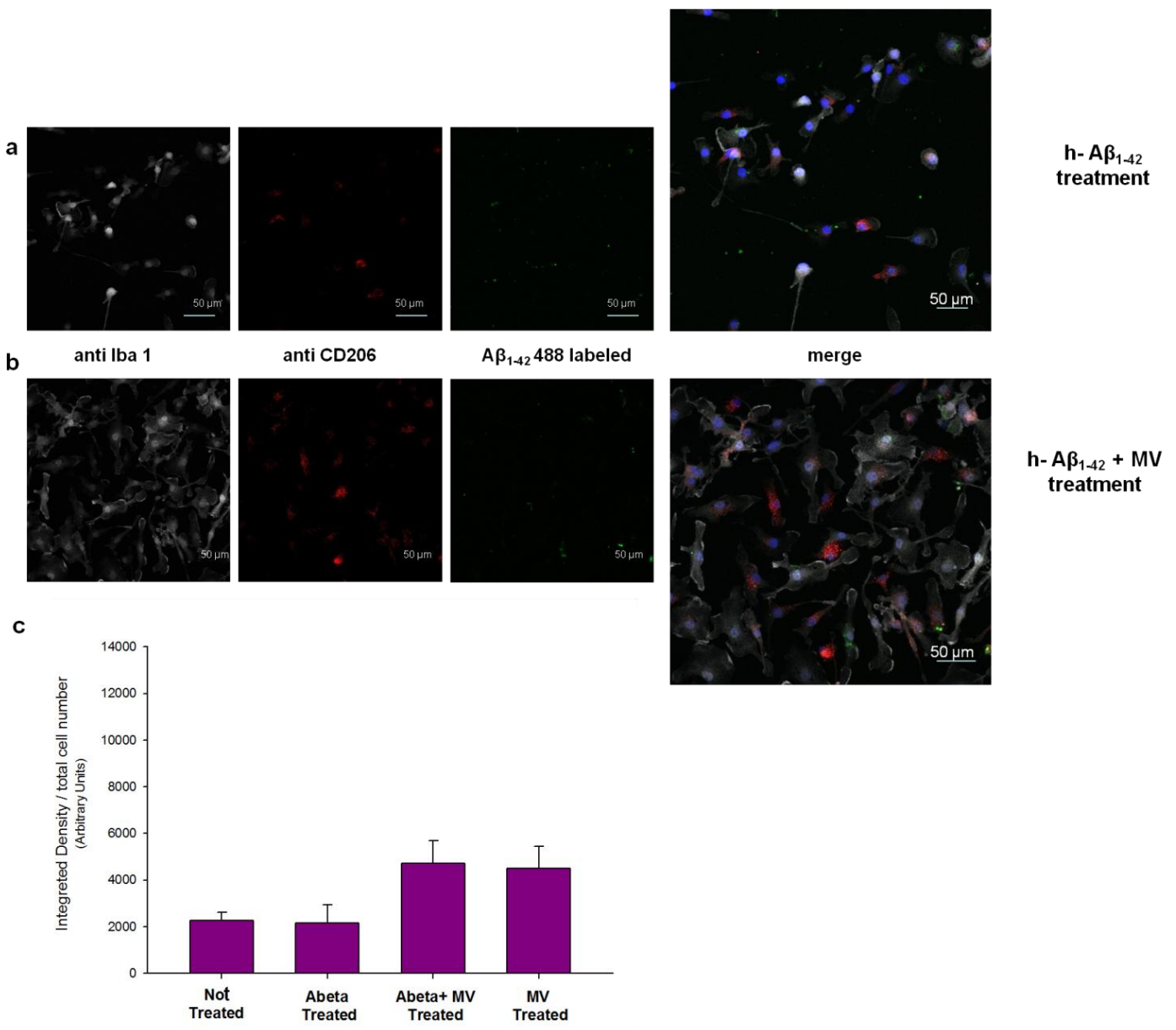


**Figure 12. Primary microglia cultures treated with BM MSC-derived MVs and h-A $\beta_{1-42}$  488 fluorochrome conjugated to assess CD 206 expression. a-b)** Cultures were stained with anti Iba1 and anti CD206 to verify CD206 profile upon both treatment conditions: :

(a) in 488h-A $\beta_{1-42}$  treated culture is visible a low CD206 immunoreactivity (red) that is virtually increased after MV; (b) in 488h-A $\beta_{1-42}$  and MVs treated culture is visible an increased CD206 immunoreactivity (red). The amoeboid morphology can be also observed comparing a and b; c) Histograms show preliminary quantification of CD206 expression in inflammatory condition due to 488h-A $\beta_{1-42}$  stimulus and the upward trend achieved by MV administration. Images represent a max projection of the whole Z- stacks, acquired by confocal microscope. In blue the nuclei are stained with DAPI. (N<3).

Together these data suggest that microglia in cultures stimulated with h-A $\beta_{1-42}$  and BM MSC derived MVs display a decreased release of proinflammatory cytokines and increased IL10 release, which could be at the origin of the phenotypical changes revealed by quantitative evaluation of M1/M2 markers.

Hence we can confirm that MVs extracted from BM- MSCs are endowed with immune modulatory features, which are detectable in the inflammatory context induced by h-A $\beta_{1-42}$  stimulation.

### c. Evaluation of the internalization of $\beta$ -amyloid in MV treated microglia

Generally it has been reported that the presence of TNF $\alpha$  inhibits phagocytic ability of microglia, while IL10 and other factors typical of the M2 phenotype may increase phagocytosis activity (Cherry et al. 2014). Therefore, we evaluated the capacity of MVs to modulate A $\beta$  phagocytosis by microglia. As previously reported, we have observed that MV treated microglia changed its shape, assuming an amoeboid morphology that it is associated with higher phagocytic ability of the cells. We wondered if an increase of microglial phagocytosis of h-A $\beta_{1-42}$  induced by MVs could be assessed.

To test our hypothesis, we first counted the number of microglia cells positive for h-A $\beta_{1-42}$  conjugated to the 488 fluorochrome (488h-A $\beta_{1-42}$ ) in the presence or in the absence of MVs.

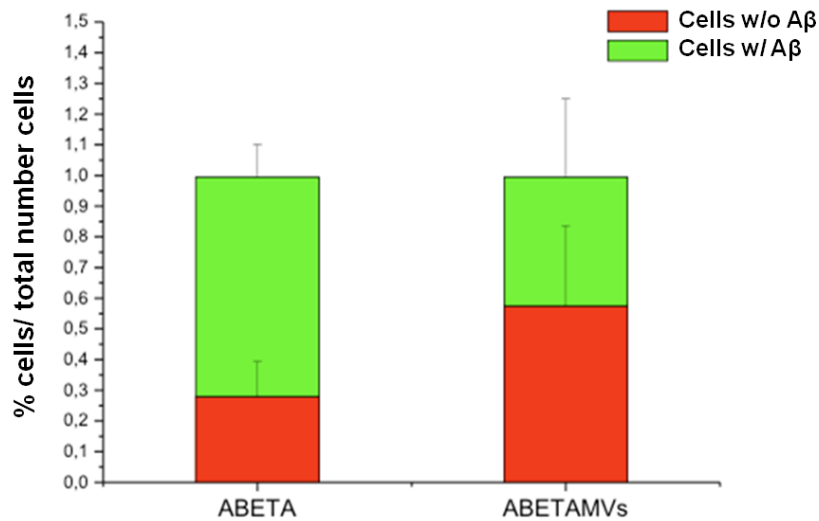


**Figure13. Cell internalization of 488-h-A $\beta_{1-42}$ .**

Histograms show the percentage of 488-h-A $\beta_{1-42}$  positive cells over total cells (counted as positive nuclei in DAPI); the analysis was carried out with the images obtained from the immunocytochemistry. (N=2).

We quantified the number of cells that internalized 488h- A $\beta_{1-42}$ , with respect to the total cells in 488-h-A $\beta$  treated cultures and in cultures exposed to 488h- A $\beta_{1-42}$  together MVs.

About 70% of the cells internalized 488h- A $\beta_{1-42}$  (figure 13, “ABETA”, green), showing high microglial phagocytic activity. Surprisingly, when MVs were added to microglia cultures, the percentage of cells that internalized the fluorescent A $\beta$  decreased up to 40% (Fig. 13, “ABETA MVs”, green), suggesting that the administration of MVs might affect the phagocytosis or the A $\beta_{1-42}$ .

This result is apparently in contrast with in vitro observations showing that microglial cells treated with IL10 before A $\beta$  activation display an increase in microglia phagocytosis (Michelucci, et al., 2009). It is however to be considered that, as described by Mosher and Wyss-Coraya, in a recently review about microglial dysfunctions in AD and in brain aging, phagocytosis process by microglia in CNS include an initial phase of recognition and internalization of external cellular materials and a second phase, indicated as “proteostasis” that comprises the intracellular degradative processes occurring in phagocytic cells (Mosher and Wyss-Coraya, 2014). We can speculate that the 488-h-A $\beta$  presence detected in microglia cells at 24h, is the result of defective “proteostasis” of microglia, and not only of increased phagocytosis. MVs might therefore influence the degradation



of A $\beta$ . The relationship between internalization process (phagocytosis) and degradation of A $\beta$  protein (proteostasis) during the stimulation with BM MSC- derived MVs deserves further investigation.

MSC-derived MVs have a documented role in the modulation of inflammation (S. Bruno et al., 2015) and our results *in vitro* show a possible function in the modulation of cytokine release by h-A $\beta$ <sub>1-42</sub> stimulated microglia, that take part in the the progression of AD in brain environment. MVs *in vitro*, in fact, showed an interesting modulation of both cytokine release and phenotypic changes in microglia cells. Indeed MV treated microglia showed lower expression of MHC II, a typical marker of M1 phenotype, and reduced TNF $\alpha$  release compared to h-A $\beta$ <sub>1-42</sub> treated microglia (figure 7 and 8).

Consistently, a mild increase of mannose receptor (CD206) expression, together the high IL 10 release in culture after MV treatment of microglia insulted with h-A $\beta$ <sub>1-42</sub> could support the view that MVs can modulate the phenotype of microglia cells (*in vitro* results) driving their activation state forward M2 anti-inflammatory phenotype. This is in line with previous reports on the MVs activity, *in vitro* (Bruno, S. et al., 2015) but also with MSC effects, when administered in AD *in vivo* models (Lee et al., 2009; Lee et al., 2010; Lee HJ et al., 2012; Yang et al., 2013). In particular we observed a significant reduction of TNF $\alpha$  and IL6, that play an important role in AD inflammatory process (Perry et al., 2001; Papassotiropoulos et al., 2001) and a significant release of a well known anti-inflammatory cytokine, IL10 (Szczepanik et al., 2001)

Discussing all reported *in vitro* data from quantification of cytokines up to preliminary characterization of microglia phenotype and functional activation, we could speculate that our population of MVs maintained peculiar characteristic of cells origin. Various works recently have shown the beneficial effects of MSC-derived MVs in different inflamed or pathological situations: for instance Camussi's group has recently demonstrated that MVs isolated from human bone marrow MSCs stimulated proliferation *in vitro* and conferred resistance of tubular epithelial cells to apoptosis, while *in vivo*, MVs accelerated the morphological and functional recovery of glycerol-induced AKI in SCID mice, by inducing proliferation of tubular cells (Stefania Bruno, 2009). They showed that RNase abolished the effects of MVs *in vitro* and *in vivo*, and suggested a RNA-dependent modulation mechanism. They also demonstrated that MVs shuttle a specific subset of cellular mRNAs, such as mRNAs associated with the mesenchymal phenotype and with control of transcription, proliferation, and immunoregulation.

We believe that our data are in line with studies that confirmed MVs ability to influence cell behavior, by immune-modulating action. The mechanisms of action by which MVs work are still to be investigated; however literature evidence demonstrated that MVs act through fusion with the cell membrane or horizontal transfer of genetic material, such as mRNAs and miRNAs (Bruno S. et al, 2009; He J et al.,2015; Wang Y et al., 2015). Interestingly, a significant effects, was induced , in our experiments, even by the MSC supernatant, obtained after the ultracentrifugation of MSC culture medium following starvation; this result suggest that soluble factors in the MSC culture medium may perform the predominant role of this regulation. Further experiments are required to assess this possibility.

MVs can be considered a good alternative to MSCs, which also display an anti-inflammatory, immunomodulatory role, since they preserve the characteristics of parental cells but do not involve the risk of transplant rejection or neoplastic transformation (Mokarizadeh et al., 2012). This consideration prompted us to investigate whether MV immunomodulatory effects are maintained in an in vivo AD transgenic model of Alzheimer's Diseases and what could be the consequence of MV administration in vivo.

## **4. In vivo evaluation of MV effects in APP/PS1 transgenic mice**

### **a. Experimental Design.**

Once confirmed the MV immunomodulatory effect through the *in vitro* model of A $\beta$  induced-inflammation, we aimed to assess whether BM-MSC derived MV treatment might ameliorate the  $\beta$ -Amyloid pathology and modulate the inflammatory process *in vivo*, possibly influencing AD development and progression.

Hence we specifically investigated the MV immune-modulatory effect and their ability to affect  $\beta$ -Amyloid deposition *in vivo*, considering that MVs might be the vehicle by which MSCs exert their effects in the  $\beta$ -Amyloid pathology, as demonstrated in the literature (Ma et al., 2013; Yan J et al., 2014).

We have set up experiments *in vivo* using AD transgenic mice models, expressing a chimeric mouse/human Amyloid precursor protein (APP) and a mutant human Presenilin 1 (PS1). This transgenic model allows neurons to secrete human A $\beta_{1-42}$  peptide (A $\beta_{42}$ ) by 6 months of age, A $\beta$  deposits begin to develop in the cortex and hippocampus, without showing neurofibrillary tangles (Iván Carrera et al, 2013). The APP<sup>swe</sup>/PS1<sup>dE9</sup> (APP/PS1) mice are characterized by an early onset of the  $\beta$ -Amyloid pathology, that is associated to dysfunctions of neuronal networks, microgliosis, loss of synaptic function and finally, cognitive impairment. For all these reasons, APP/PS1 represents the ideal model to investigate the amyloidogenic process, given cognitive deficits seem to be closely related to A $\beta$  load (Perez et al., 2009; Zhang et al., 2011<sup>2</sup>).

For our study, we considered two mice age groups: 3 and 5 month old mice. We compared APP/PS1 male mice bilaterally injected into the cortex with vehicle or MVs. We chose two different ages to compare the potential different effects of MVs by analysing the cerebral tissue for changes in A $\beta$  plaque load 25 days after the injection. Alternatively, control transgenic mice were injected with physiological solution. We focused our attention on brain areas that have been described to be the first affected by the disease, cerebral cortex and hippocampus, and then the cerebellum, where amyloid pathology occurs later (Savonenko et al., 2004; Garcia-Alloza et al., 2006).

By immunohistochemistry we quantified A $\beta$  deposits, studying three parameters characterizing the plaques: A $\beta$  load into the plaques (referred to as solidity), the plaque area and density.

Furthermore by ELISA, we evaluated the quantity of soluble A $\beta$  and quantity of circulating A $\beta$  in blood and brain at the end of each treatment.

b. MV injection reduces A $\beta$ <sub>42</sub> deposition in APP/PS1 mice.

To investigate the effects induced by MSC-derived MV injection, we compared APP/PS1 male mice of 3 or 5 months of age bilaterally injected with vehicle or MVs into the cortex. At this aim we performed immunohistochemical stainings by using 6E10 antibody (Beta Amyloid, 1-16 Monoclonal Antibody, Covance®) that interacts with the N-terminal domain of human A $\beta$ <sub>42</sub> peptide, to investigate whether changes in amyloid aggregation could be observed in brains of treated mice 25 days after treatments.

Figure 14 shows two representative images of brain slices of 6 month old mice bilaterally injected with BM- MSC derived MVs (C, D) or vehicle (A, B).

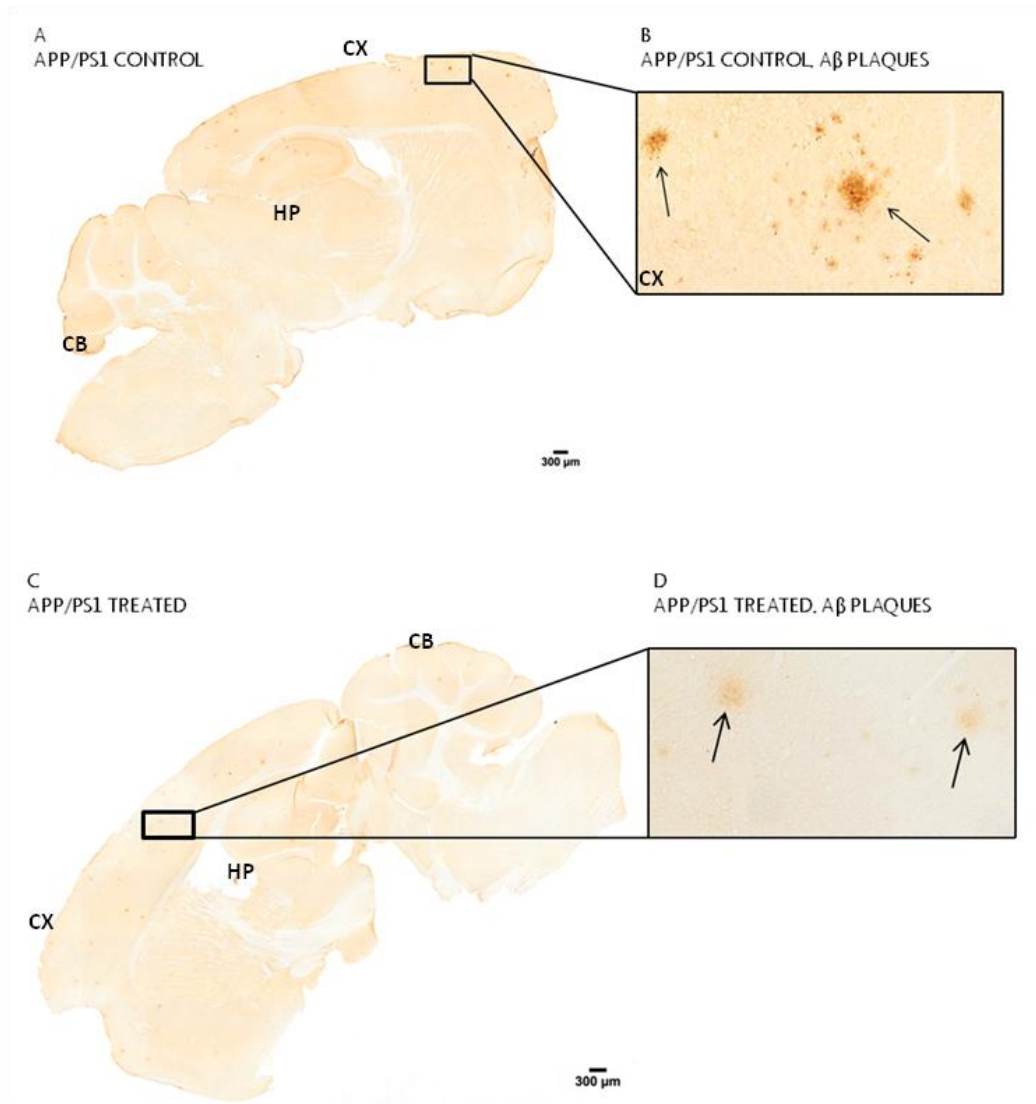


**Figure 14. MV injection reduced  $A\beta_{42}$  plaque load in APP/PS1 mice brains, visualized with 6E10 antibody.** A) Brain slice of a 5 month old mouse subjected to injection with vehicle (control). The three brain areas analyzed are cortex (CX), hippocampus (HP) and cerebellum (CB). In the panel (B), a higher magnification of A, representative of the plaque accumulation. C) Brain slice of a 5 month old mouse subjected to injection of MVs. In the panel (D), a higher magnification of C.

Figure 14 A and B, shows the higher  $A\beta_{42}$  plaque numbers in vehicle treated brains, compared with MV treated brain slices (C and D).

In the higher magnification box, it appears evident that in MV treated brain slices (C), less intense  $A\beta_{42}$  plaques are present compared to the vehicle treated brain (A).

In order to verify and have a quantitative evaluation about the possibility that MV injection might affect plaque size, that increases with age in AD mice, together with the plaque number (Garcia-Alloza et al., 2006), we evaluated the average area occupied by senile plaques (figure 15)

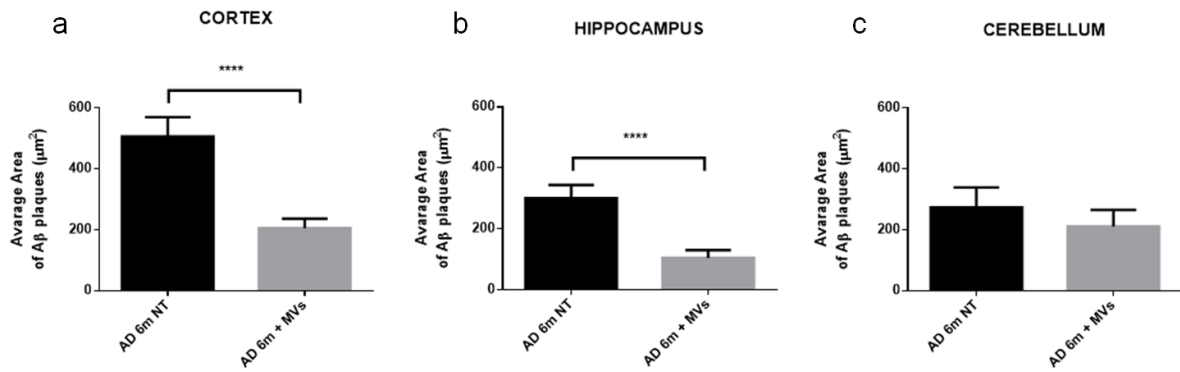


**Figure 15. Quantitative analysis of the averaged area of 6E10 positive plaques in cortex (a), hippocampus (b) and cerebellum (c) of 6 month old mice.** The averaged area occupied by Aβ<sub>42</sub> plaques in APP/PS1 treated mice was significantly reduced, both in cortex (a) and hippocampus (b), by MV treatment. In the cerebellum (c) the effect was milder, although MVs show a trend of reduction. (N=3, 6 mice for control and 5 for treatment).

Histograms in figure 15 show that the plaque area was significantly reduced in MV injected brains, both in the cerebral cortex and hippocampus, compared to control group injected with physiological solution only (vehicle) (figure 15 a and b). The same trend of reduction was observed in the cerebellum (figure 15 c).

The density is the number of plaques per area units and it could change if Aβ<sub>42</sub> decreases. Therefore, in order to assess whether MVs could operate an effect on Aβ aggregation and on accumulation in brain, we have evaluated plaque density.

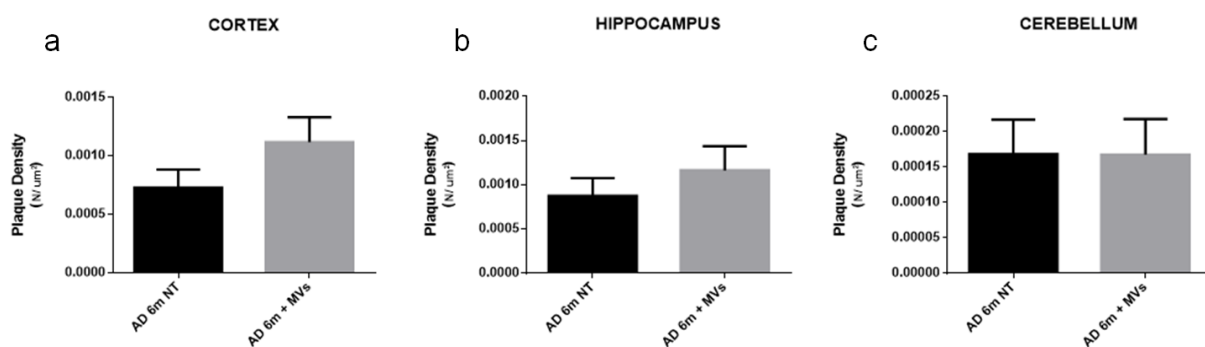


**Figure 16. Quantitative analysis of the plaque density in cortex (a), hippocampus (b) and cerebellum (c) of 6 month old APP/PS1 mice, both treated and controls.** The density appeared to increase both in cortex and hippocampus of APP/PS1 treated mice (fig. a and b), but not significantly. In the cerebellum (Fig. c) any difference between the two groups of animals could be observed. (N=3, 6 mice for control and 5 for treatment).

The analysis of plaque density (number of plaques per area units), showed in figure 16, did not reveal a significant effect in any of the brain areas analyzed. A tendency to increased plaque density in the cortex was detected, although the difference was not statistically significant. We finally evaluated the plaque solidity, a parameter that represents the loading of A $\beta_{42}$  into the plaques. Figure 17 shows that A $\beta_{42}$  into plaques was subjected to a strong reduction, especially in the cerebral cortex and hippocampus when compared to vehicle treated-mice. In the cerebellum, although a trend of reduction could be perceived, a significant effect was not detected.

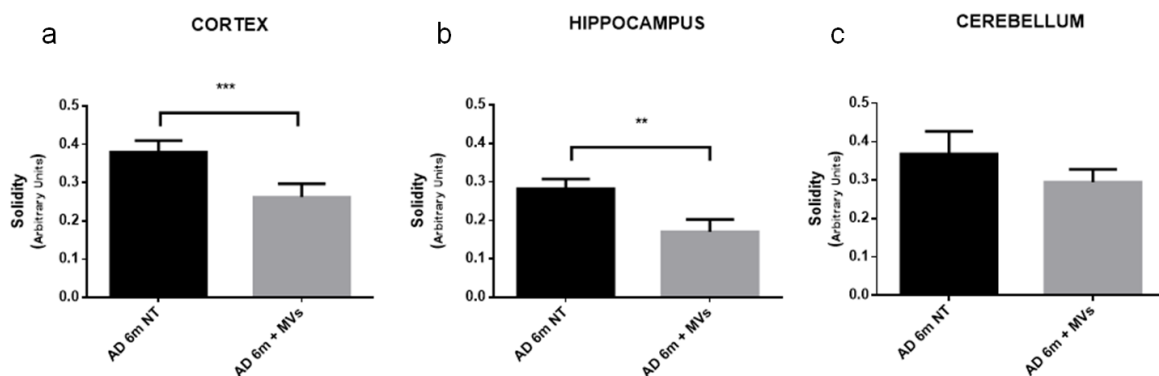


**Figure 17. Quantification of MV effects through evaluation of A $\beta_{42}$  plaque load in APP/PS1 mice brains, visualized with 6E10 antibody.** The graphs show the solidity, defined as plaque load, of 6 month old mice for three brain areas of interesting: CORTEX, HIPPOCAMPUS and CEREBELLUM. Note that in the cortex (a) and hippocampus (b), but not in the cerebellum (c) of MV treated mice significant reduction of solidity parameter was detected. (N=3. 6 mice for control and 5 for treatment).

All together these data suggest that MVs might reduce A $\beta$  aggregation. We can speculate that this can occur in two manners:

- MVs might act directly on the plaques, inducing their disaggregation through interaction between MV lipid membranes and A $\beta$ ; this possibility could be consistent with both decreased area of the plaques and decreased quantity of A $\beta_{42}$  into plaques (solidity) in treated mice. This hypothesis is in line with recent studies, showing that exosomes and MVs are composed by different types of lipids and that A $\beta$  clearance is modulated and conditioned by lipid membrane interactions (Kenji S, 2013; Tofoleanu F., 2012).
- MVs might act on microglia directly, inducing an increase of their functionality and phagocytosis/degradation ability. This possibility may be consistent with our data in vitro that

show a minor number of microglial cell containing  $A\beta_{42}$ , which is possibly in line with an increased degradation ability.

We then performed the same analysis in 3 month old mice, an age in which plaques start to be assembled (D.R. Howlett, 2008; Zhiyong Zhong, 2014). in order to investigate whether MVs could prevent the formation of  $A\beta_{42}$  plaques in younger mice (figure 18).

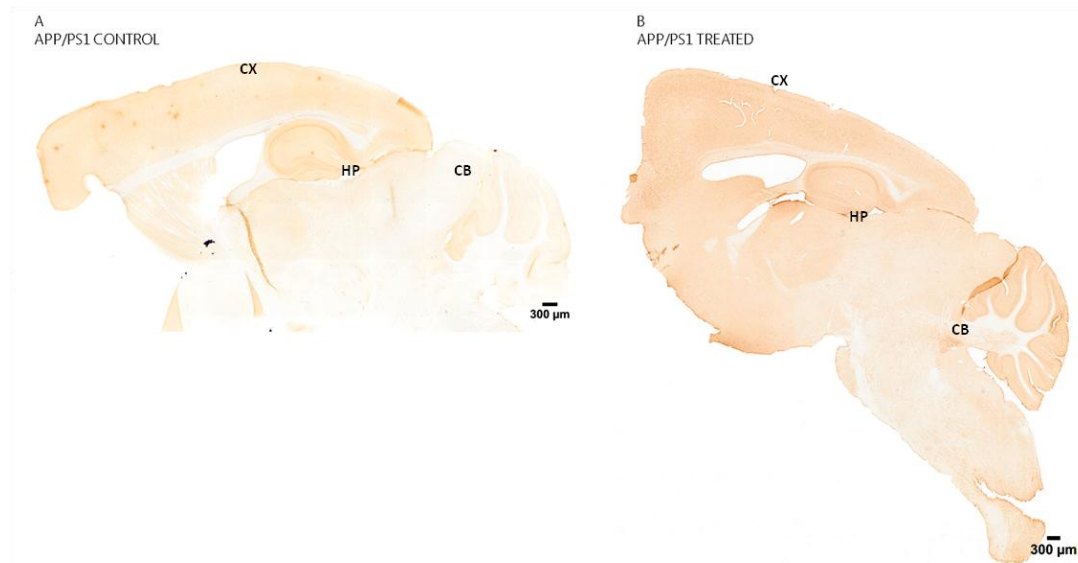


**Figure18. Effect of MV injection in 4 month old APP/PS1 mice.** A) Brain slice obtained from a mouse subjected to injection with vehicle, at 3 month old and sacrificed at 4 months of age. The same three brain areas, cortex (CX), hippocampus (HP) and cerebellum (CB), observed in 6 month old mice were analyzed. Note the lower number of plaques with respect to older animals. B) Brain slice from a mouse subjected to MV injection.

Although mice usually show a very low number of plaques at this age -as noticeable in figure 18, in which not treated group (A) showed visible plaque only in the cortex, both the plaque solidity (figure 19c) and the average area (figure 19a) tend to decrease in all the analyzed regions in MV treated APP/PS1 mice with respect to the age-matched controls, in line with what observed in 6 month old mice. On the other hand, as regards plaque density (figure 19b), differently from what observed in 6 month old treated mice, 3 month old mice showed a significant reduction in all the areas upon injection with MSC MVs (figure 19b).



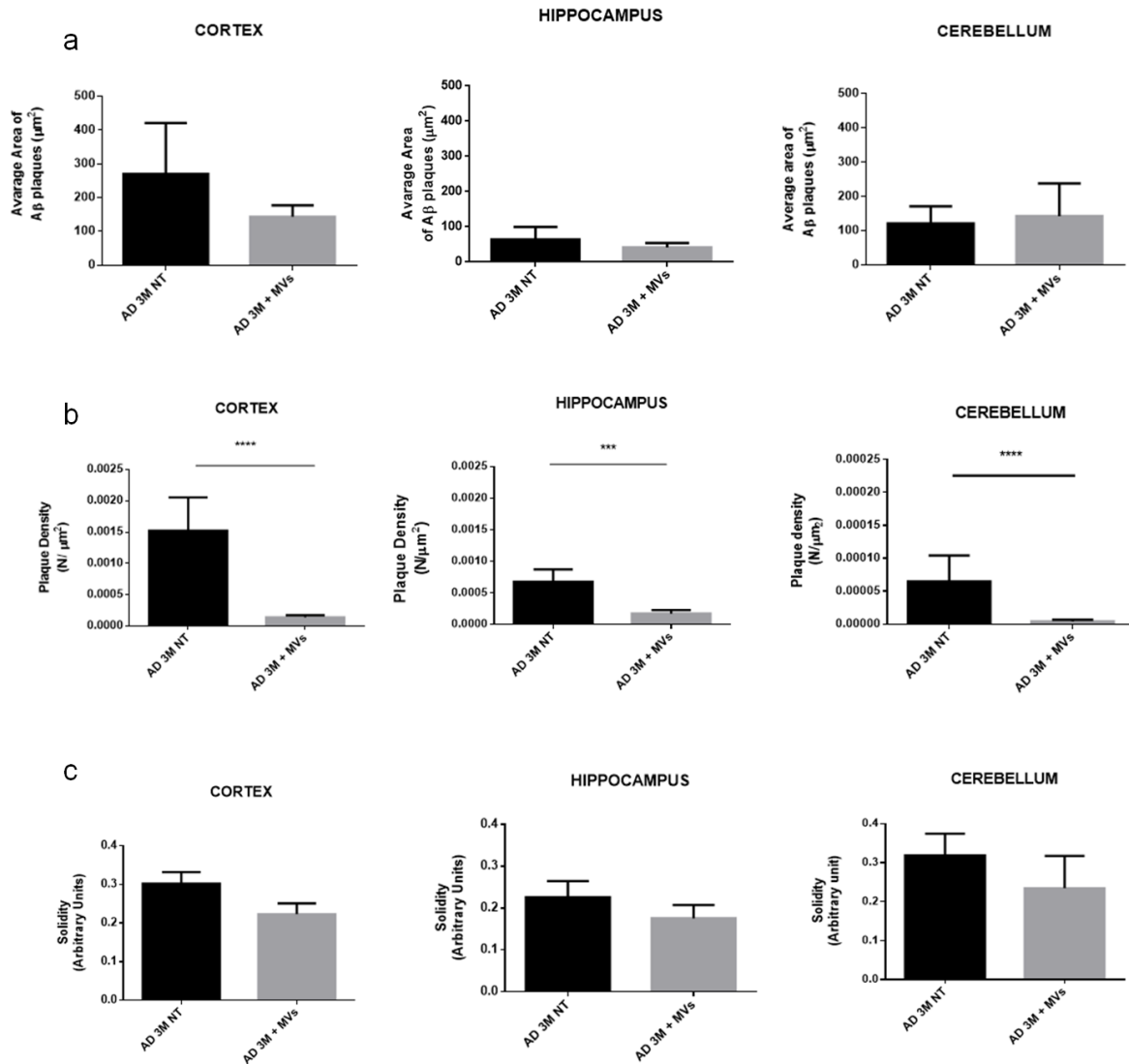


**Figure19. Effect of MV injection in 4 month old APP/PS1 mice.** The graphs show the tendency of MVs to decrease, compared with their age-matched controls, the solidity (a) and the average area (c) of 4 month old mice in cortex, hippocampus and cerebellum. b) Plaque density of APP/PS1 treated mice was statistically decreased in all the areas analyzed. (N=2. 6 mice for control and 8 for treatment).

On the basis of these results, we can hypothesize that MVs may operate not only by promoting the disaggregation of  $\text{A}\beta_{42}$  pre-existing deposits, but also preventing or slowing the formation of new plaques.

These data are in line with observations by Katsuda and colleagues (2013) on MVs released from adipose tissue (AD)-derived MSCs. Indeed, they showed that exosomes derived from AD-MSC carried Nepriylisin (neutral endopeptidase: NEP), a type II membrane associated metalloendopeptidase, that is involved in the proteolysis of  $\text{A}\beta$ . When added to N2a line cells, AD-MSC exosomes reduced both extracellular and intracellular  $\text{A}\beta_{42}$  deposits (Katsuda et al, 2013).

Future experiments will be directed to investigate the status of cell components in brain after BM-MSC derived MV treatment, in order to assess if there is a change of cell morphology and phenotype (as showed previously in in vitro experiments) and in order to verify possible changes in the enzymatic activity, as suggested by Katsuda and Yang (Katsuda, 2013; Yang et al., 2013).

In particular, Katsuda and co-workers focused on NEP carried by exosomes. Yang H and co-workers found that intravenous infusion of human umbilical cord MSCs (HUMSCs) increased glutathione (GSH) activity as well as superoxide dismutase activity, while decreasing malondialdehyde activity and protein carbonyl level, and they suggested that HUMSC infusion alleviated oxidative stress in APP/PS1 mice. In addition, HUMSCs reduced  $\beta$ -secretase 1 and the 99-amino acid C-terminal fragment of APP (CTFb), both considered main players in AD progress, reducing Ab deposition in mice. In light of these evidences we will focused on the possible modulation of the above enzymes upon MV treatment in APP/PS1 mice.

### c. Detection of soluble $A\beta_{42}$ in brain and in blood

In order to find out whether the reduction of the plaques might correlate with a reduction of the levels of soluble  $A\beta_{42}$ , we evaluated the amount of human amyloidogenic peptide in brains of treated and not mice with MVs, , evaluated after homogenization of total brains.

On the basis of the results about emerging plaques in MV-treated younger mice, we hypothesized the occurrence of a possible increased  $A\beta_{42}$  clearance. This would correspond to a decrease of fibrillar  $A\beta$  in the plaques of AD aged mice and/or a concomitant increase of the  $A\beta$  species in soluble homogenate fraction, in younger mice, as a consequence of the MV treatment.

With the purpose to investigate this issue, levels of human soluble  $A\beta_{42}$  from APP/PS1 mice treated with vehicle or with MVs were quantified by ELISA (figure 20). Tissues were homogenated with Tris- buffer containing 1% triton, and the soluble  $A\beta$  species contained in obtained supernatant, were detected by 6E10 antibody that recognised the  $A\beta$  N- terminal portion.

Noteworthy, MV treatment appeared to increase the levels of human soluble  $A\beta_{42}$  in brain, compared with their age-matched controls both in 4 and 6 month old mice (figure 20, A and B).

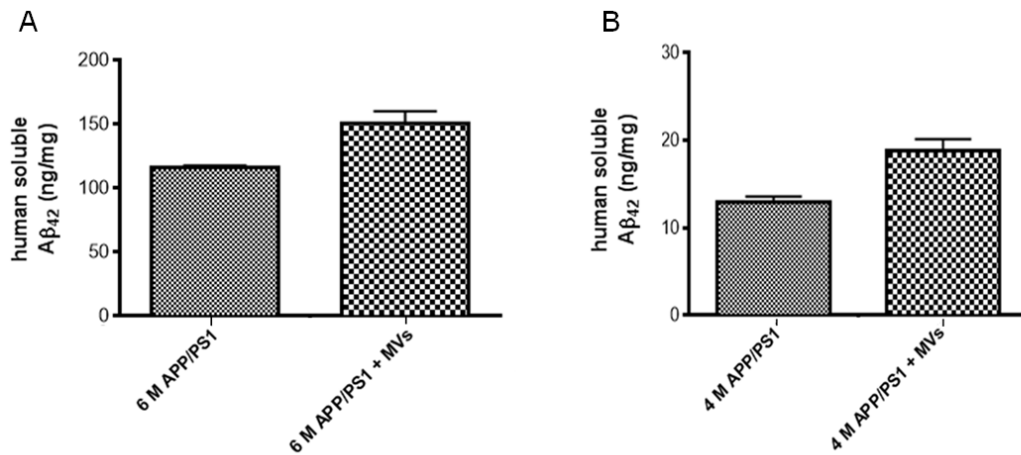


**Figure 20. Quantification of human soluble Aβ<sub>42</sub> in APP/PS1 in brain mice, treated with MVs or vehicle.** A) Levels of human Aβ<sub>42</sub> in 6 month old APP/PS1 MV treated mice compared with age-matched controls appeared to increase, although not significantly. B) In 4 month old mice the same trend of reduction was observed. (N=1, 4 mice for group).

Since in both groups we observed an increase in soluble Aβ<sub>42</sub> levels in mice treated with MVs compared to age-related control mice, it is reasonable to hypothesize that MV treatment might induce the activation of the microglial alternative phenotype, that could enhance Aβ<sub>42</sub> phagocytosis and degradation, as it occurs following MSC treatment (Lee et al., 2012; Zhang et al., 2012<sup>1</sup>; Shin et al., 2014). To confirm this hypothesis we will extract with different detergents soluble and insoluble forms and quantify them in order to assess the possible occurrence of changes in Aβ plaque composition before and after treatments (Mc Donald et al. 2013). We will also assess the possibility that MVs may influence the Aβ clearance and the proteostasis by performing experiments in brain slices. Finally, the levels of soluble Aβ in the plasma of MV-treated or untreated mice will be quantified at different time windows, in order to detect possible effects on Aβ clearance.

#### d. MV treatment reduces TNFα levels without affecting IL10 in APP/PS1 mice

Since our in vitro experiments showed that MVs affect microglial cytokine release, we assessed whether such effect could be recorded also in vivo.

To this aim we measured, by ELISA the levels of TNFα and IL10 in the blood. The same experiments will be repeated in the brain.

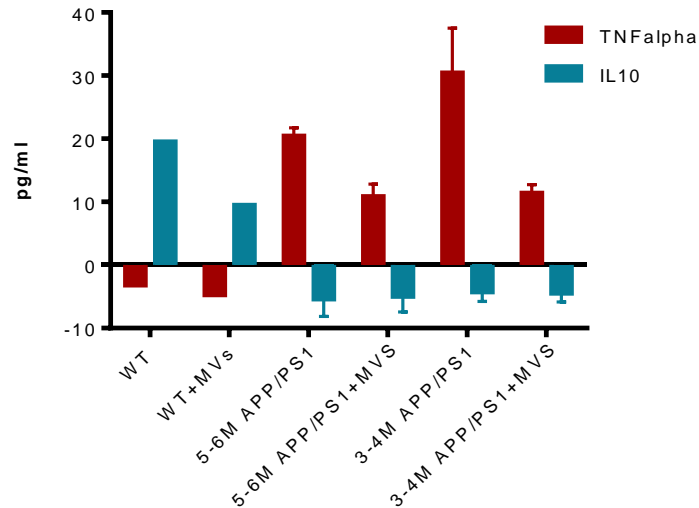


**Figure 21. MV treatment induced a decrease of TNF $\alpha$  secretion in APP/PS1 treated mice.** The graph shows the levels of the pro-inflammatory cytokine (TNF $\alpha$ ) and the anti-inflammatory cytokine (IL10), in WT and APP/PS1 mice, both treated and not treated with MVs. In WT mice any production of TNF $\alpha$  both in treated (red bars) and control mice was detected in blood. Conversely, levels of IL10 appeared to be attenuated in mice treated with MVs. In 4 month old APP/PS1 mice MV treatment induced the reduction of TNF $\alpha$  levels. In 6 month old mice APP/PS1 was observed the same trend. On the other hand, levels of IL10 in APP/PS1 mice (blue bars) both treated with vehicle or MVs were not detected. (N=1. 2 WT and 4 APP/PS1 mice).

Figure 21, shows that TNF $\alpha$  levels were not detectable neither in the blood of MV treated nor in control WT mice, as expected. APP/PS1 6 month old vehicle-treated mice, showed a strong increase in TNF $\alpha$  levels compared with their age-matched APP/PS1 mice. In this experimental group, MV treatment induced a trend of reduction.

The main differences were observed in 4 month old mice, where a strong decrease of TNF $\alpha$  levels was observed in treated mice, compared with age-matched control. On the other hand, IL10 release could be detected only in WT mice, which was reduced by the treatment with MVs. In APP/PS1 mice instead, the levels of the antiinflammatory cytokine were not detectable at any age, even following treatment with MVs.

We can suppose that treatment window did not allow us to detect IL10 presence into blood. It will be necessary to indagate the levels of these cytokines in the whole brain, in order to assess if there was a change of inflammatory status of cerebral environment.

On the basis of our results, that showed the decrease of the amyloid area size and the decrease of A $\beta$ <sub>42</sub> into plaques after treatment with MVs in 6 month old mice, and a minor density of formed

plaques in younger mice, we can hypothesize that MVs may operate by promoting the disaggregation of A $\beta$ <sub>42</sub> pre-existing deposits and favoring the prevention of the formation of new plaques. These data would be in agreement with the observations by Katsuda and colleagues (2013) on MVs released from adipose tissue-derived MSCs.

Also the quantification of the amount of the human peptide in mouse brains were partially in line with the hypothesis that in MV treated mice could occurred a disaggregation of plaques, favoring the production of soluble A $\beta$  which could be then cleared via the circulation. ELISA of soluble A $\beta$  in the plasma of treated mice at different time windows after the treatment will contribute to confirm this possibility.

It reasonable to hypothesize that MV treatment may induce the activation of the microglial alternative phenotype, that enhances A $\beta$ <sub>42</sub> phagocytosis and clearance, as it occurs following MSC treatment (Lee HJ et al., 2012; Zhang W. et al., 2012<sup>1</sup>; Shin et al., 2014). This point will be deeply investigate through the evaluation of phenotype status of microglia status in primis, but also in others cell components since also these are involved in AD progression (astrocytes and neurons) and estimating the presence of neurodegenerative and neuroprotective markers in whole brain.

We finally estimated the levels of two cytokines in blood: TNF $\alpha$  and IL10. Quantitative analyses of preliminary results revealed that MV treatment led to a strong reduction in the inflammatory cytokine levels compared with vehicle-treated aged matched control mice, suggesting that MVs can act also in modulating the inflammatory process, in line with that achieved by MSC transplantation (see above, Lee et al., 2008; Lee HJ et al., 2012). levels in the blood. ELISA are mandatory in order to assess the levels of the same cytokines in the mice brain.

The role and the effects of IL10, are actually very/much debated. In fact in brain IL10 is the anti-inflammatory cytokines for excellence, together with IL4, released by activated microglia and so far it has been presented as an important factor that supports the decrease of pro- inflammatory cytokines allowing to establish repairing and neuroprotective mechanism (Safar MM et al., 2014; Park et al., 2015).

Two independent studies showed that the presence (by overexpressing IL10, Chakrabarty et al., 2015) or the absence (by knockingdown IL 10 mouse model, Guillot-Sestier et al., 2015) of IL10 modifies AD progress in vivo. In fact, the over-expression of adeno-associated virus (AAV2/1)-mediated IL10, in brains of APP transgenic mouse models, showed that IL10 expression induces

increased A $\beta$  accumulation and memory impairment in APP mice; on the other hand, IL10 deficiency model mouse, obtained by crossing the APP/PS1 mouse with a mouse deficient in IL10 (APP/PS1(+)IL10(-/-)) showed a preservation of synaptic integrity and mitigation of cognitive disturbance in APP/PS1 mice. Since in AD patient brains IL10 signalling pathway is abnormally elevated, the authors suggested that blocking IL10 anti-inflammatory response may be therapeutically relevant for AD (Chakrabarty et al., 2015; Guillot-Sestier et al., 2015).

However our preliminary *in vivo* results show that IL10 is not expressed at detectable levels in AD transgenic mice and MVs do not increase the anti-inflammatory cytokine. Therefore, our data indicate that, in contrast to what observed *in vitro*, *in vivo* MVs do not alter IL10 expression. In this sense our results could be in line with the two studies mentioned above. However, the discrepancy of the results of *in vitro* and *in vivo* MV effects must be investigated in future experiments to better understand the mechanisms of action of MVs. Nonetheless, the reduction of TNF $\alpha$ , especially in 4 month old mice, prompts towards an anti-inflammatory effect of MVs also *in vivo*, possibly via an IL10-independent mechanism.

Finally, MVs reduced A $\beta$  plaques in APP/PSE1 mice. Considering that in the literature cognitive deficits have been extensively demonstrated to be closely associated with A $\beta$  load (Lee et al., 2010; Zhang et al., 2012<sup>2</sup>; Zhang et al., 2012<sup>3</sup>), our results suggest that MVs may be able to improve cognitive impairment. To support this hypothesis, we will perform behavioral tests on MV injected animals.

## CONCLUSIONS

My PhD project aimed at investigating the possible therapeutic actions of microvesicles (MVs) released by Mesenchymal Stem Cells (MSCs) derived from mouse Bone Marrow in experimental models of Alzheimer's Disease (AD). The study provided both *in vitro* and *in vivo* evidences, designed to assess the MV immunomodulatory effects and their ability to affect  $\beta$ -Amyloid deposition, in order to examine the molecular mechanisms at the basis of their possible beneficial effects.

In the literature MSC the ability to modulate cytokines secretion, by microglial cells, has extensively been demonstrated (Giunti et al., 2012; Rahmat et al., 2013).

Hence we isolated MV from BM-MSCs and investigated their ability to affect the brain immune cells *in vitro*, to verify that MSC-derived MVs might alter microglial release of molecules associated with an anti-inflammatory action. Preliminary data allowed us to observe that MVs not only influence microglia IL10, TNF $\alpha$  and IL6 secretion, but also they induce a phenotypical change, probably boosting microglia activation from M1 towards M2 phenotype (Tsay et al., 2013). Since several studies showed that MSCs can induce a phenotypical microglial switch in transplanted animals, *in vivo* future studies will be performed in order to examine the real contribution of MVs in playing a protective role in AD. On the other hand, the use of transgenic mice highlighted the ability of MVs to participate (directly or indirectly via microglial activation is still to be determined) in the clearance of the plaques depending on the age of treated mice. Indeed MVs promoted the disgregation of the pre-existing plaques and prevented the formation of new ones.

Finally, altogether our results support the possibility that MVs can be, at least partially, the mediators of the positive actions for MSC treatment in AD. In fact, it has been reported that MSC administration exert positive effects on plaque deposition, especially in cortex and hippocampus, by enhancing A $\beta$  clearance capacity of microglial cells (Yang et al., 2013). In spite of these considerations, surely many questions still remain open. Thereby, in order to clarify MV mechanisms of actions, the molecules underlying MV effects need to be ascertained. In this sense, great importance could be ascribed to the content of MVs that many studies present as regulatory in the pathological conditions and participating to tissue repair (Bruno, 2013<sup>2</sup>; Lopatina et al. 2014). It has been reported that MVs contain different molecules that includes lipids, proteins and also genetic materials (miRNA, mRNA). Among these, lipids and proteins present on MV

membrane, trophic factors and miRNAs inside the lumen that could be horizontally transferred to the target cells, could be responsible of the above described actions. The discovery of these molecules will be a challenge to be addressed in future experiments.



## REFERENCES

- Adlard P.A., Tran B.A., Finkelstein D.I., Desmond P.M., Johnston L.A., Bush A.I., Egan G.F. (2014). A review of  $\beta$ -amyloid neuroimaging in Alzheimer's disease. *Frontiers in neuroscience*, 8. n°327. 1-23.
- Akers J.C., Gonda D., Kim R., Carter B.S., Chen C.C. (2013). Biogenesis of extracellular vesicles (EV): exosomes, microvesicles, retrovirus-like vesicles, and apoptotic bodies. *J Neurooncol.*, 113. 1-11.
- Akyurekli C., Le Y., Richardson R.B., Fergusson D., Tay J., Allan D.S. (2015). A systematic review of preclinical studies on the therapeutic potential of mesenchymal stromal cell-derived microvesicles. *Stem Cell Rev*; 11. n°1. 150-160.
- Altmann A., Tian L., Henderson V.W., Greicius M.D. (2014). Sex Modifies the APOE-Related Risk of Developing Alzheimer's Disease. *Annals of Neurology*. 1-33.
- Arslan F., Lai R.C., Smeets M.B., Akeroyd L., Choo A., Agur E.N.E., Timmers L., Van Rijen H.V., Doevendans P.A., Pasterkamp G., Lim S.K., De Kleijn D.P. (2013). Mesenchymal stem cell-derived exosomes increase ATP levels, decrease oxidative stress and activate PI3K/Akt pathway to enhance myocardial viability and prevent adverse remodeling after myocardial ischemia/reperfusion injury. *Stem Cell Research*, 10. 301-312.
- Balducci C., Mancini S., Minniti S., La Vitola P., Zotti M., Sancini G., Mauri M., Cagnotto A., Colombo L., Fiordaliso F., Grigoli E., Salmona M., Snellman A., Haaparanta-Solin M., Forloni G., Masserini M., Re F. (2014). Multifunctional Liposomes Reduce Brain  $\beta$ -Amyloid Burden and Ameliorate Memory Impairment in Alzheimer's Disease Mouse Models. *J Neurosci*, 34. n°42. 14022-14031.
- Bao F., Wicklund L., Lacor P.N., Klein W.L., Nordberg A., Marutle A. (2012). Different  $\beta$ -amyloid oligomer assemblies in Alzheimer brains correlate with age of disease onset and impaired cholinergic activity. *Neurobiol Aging*, 33.
- Barry F.P., Boynton R.E., Haynesworth S., Murphy J.M., Zaia J. (1999). The monoclonal antibody SH-2, raised against human mesenchymal stem cells, recognizes an epitope on endoglin (CD105). *Biochem Biophys Res Commun.*, 265. n°1. 134-139.
- Bernardo M.E., Fibbe W.E. (2012). Safety and efficacy of mesenchymal stromal cell therapy in autoimmune disorders. *Ann. N.Y. Acad. Sci.*, 1266. 107-117.
- Bernardo M.E., Fibbe W.E. (2013). Mesenchymal Stromal Cells: Sensors and Switchers of Inflammation. *Cell Stem Cell*, 13. 392-402.
- Bhojak T.J., DeKosky S.T., Ganguli M., Kamboh M.I. (2000). Genetic polymorphisms in the cathepsin D and interleukin-6 genes and the risk of Alzheimer's disease. *Neuroscience Letters*, 288. 21-24.
- Bi B., Schmitt R., Israilova M., Nishio H., Cantley L.G. (2007). Stromal cells protect against acute tubular injury via an endocrine effect. *J Am Soc Nephrol.*, 18. 2486-2496.
- Biancone L., Bruno S., Deregibus M.C., Tetta C., Camussi G. (2012) Therapeutic potential of mesenchymal stem cell-derived microvesicles. *Nephrol Dial Transplant*, 27. 3037-3042.
- Blennow K., De Leon M.J., Zetterberg H. (2006). Alzheimer's disease. *Lancet*, 368. 387-403.
- Block M.L., Hong J.S. (2005). Microglia and inflammation-mediated neurodegeneration: Multiple triggers with a common mechanism. *Progress in Neurobiology*, 76. 77-98.
- Bossolasco P., Cova L., Calzarossa C., Rimoldi S.G., Borsotti C., Lambertenghi Delilieri G., Silani V., Soligo D., Polli E. (2005). Neuro-gliial differentiation of human bone marrow stem cells in vitro. *Experimental Neurology*, 193. 312-325.
- Boxall S.A., Jones E. (2012). Markers for Characterization of Bone Marrow Multipotential Stromal Cells. *Stem Cells International*, 2012. 1-12.
- Braak H., Braak E. (1994). Morphological criteria for the recognition of Alzheimer's disease and the distribution pattern of cortical changes related to this disorder. *Neurobiol Aging*, 15. 355-356.
- Bruno S., Grange C., Deregibus M.C., Calogero R.A., Saviozzi S., Collino F., Morando L., Busca A., Falda M., Bussolati B., Tetta C., Camussi G. (2009) Mesenchymal stem cell-derived microvesicles protect against acute tubular injury. *J Am Soc Nephrol.*, 20 n°5. 1053-1067.
- Bruno S., Grange C., Collino F., Deregibus M.C., Cantaluppi V., Biancone L., Tetta C., Camussi G. (2012). Microvesicles Derived from Mesenchymal Stem Cells Enhance Survival in a Lethal Model of Acute Kidney Injury. *PLoS One*, 7. n°3. 1-11.
- Bruno S., Collino F., Deregibus M.C., Grange C., Tetta C., Camussi G. (2013<sup>2</sup>). Microvesicles Derived from Human Bone Marrow Mesenchymal Stem Cells Inhibit Tumor Growth. *Stem Cell Dev.*, 22. n° 5. 758-771.
- Bruno S. and Camussi G. (2013<sup>1</sup>) Role of mesenchymal stem cell-derived microvesicles in tissue repair. *Pediatr Nephrol* 28:2249-2254
- Bruno S., Deregibus MC, Camussi G.(2015) The secretome of mesenchymal stromal cells: Role of extracellular vesicles in immunomodulation. *Immunology Letters*.
- Iván Carrera, Ignacio Etcheverría, Yi Li, Lucía Fernández-Novoa, Valter Lombardi, Carmen Vigo, Hector H. Palacios, Valery V. Benberin, Ramón Cacabelos, and Gjumrakch Aliev, (2013) Immunocytochemical Characterization of Alzheimer Disease Hallmarks in APP/PS1

- Transgenic Mice Treated with a New Anti-Amyloid- $\beta$  Vaccine. Hindawi Publishing Corporation BioMed Research International
25. Camussi G., Deregibus M.C., Bruno S., Cantaluppi V., Biancone L. (2010). Exosomes/microvesicles as a mechanism of cell-to-cell communication. *Kidney International*, 78. 838-848.
  26. Caplan A.I. (1991). Mesenchymal stem cells. *Journal of Orthopaedic Research*, 9. n°5. 641-650
  27. Caplan Arnold I. and Diego Correa, (2011), *The MSC: An Injury Drugstore*, Cell Stem Cell
  28. Chakrabarty P., Li A., Ceballos-Diaz C., Eddy J.A., Funk C.C., Moore B., DiNunno N., Rosario A.M., Cruz P.E, Verbeeck C., Sacino A., Nix S, Janus C., Price N.D., Das P., Golde T.E. (2015). IL-10 Alters Immunoproteostasis in APP Mice, Increasing Plaque Burden and Worsening Cognitive Behavior. *Neuron*, 85. n°3. 519-33.
  29. Chargaff E., West R. (1946). The biological significance of the thromboplastic protein of blood. *J Biol Chem.*, 166. n°1. 189-197.
  30. Chaput N., Théry C. (2011). Exosomes: immune properties and potential clinical implementations. *Semin Immunopathol.*, 33. 419-440.
  31. Chau D.M., Crump C.J., Villa J.C., Scheinberg D.A., Li Y.M. (2012). Familial Alzheimer Disease Presenilin-1 Mutations Alter the Active Site Conformation of  $\gamma$ -secretase. *J Biol Chem.*, 287. n°21. 17288-17296.
  32. Jonathan D Cherry, John A Olschowka and M Kerry O'Banion (2014) Neuroinflammation and M2 microglia: the good, the bad, and the inflamed. *Journal of Neuroinflammation* 2014, 11:98
  33. Chhor V., Le Charpentier T, Lebon S., Oré M.V., Celador IL, Josserand J., Degos V., Jacotot E., Hagberg H., Sävman K., Mallard C., Gressens P., Fleiss B. (2013). Characterization of phenotype markers and neuronotoxic potential of polarised primary microglia in vitro. *Brain Behav Immun.*, 32. 70-85.
  34. Cocucci E., Racchetti G., Podini P., Meldolesi J. (2007). Enlargeosome Traffic: Exocytosis Triggered by Various Signals Is Followed by Endocytosis, Membrane Shedding or Both. *Traffic*; 8. 742-757.
  35. Cocucci E., Racchetti G, Meldolesi J. (2009). Shedding microvesicles: artefacts no more. *Trends in Cell Biology*, 19. n°2. 43-51.
  36. Collino F., Deregibus M.C., Bruno S, Sterpone L., Aghemo G., Viltono L., Tetta C., Camussi G. (2010). Microvesicles Derived from Adult Human Bone Marrow and Tissue Specific Mesenchymal Stem Cells Shuttle Selected Pattern of miRNAs. *PLoS One*, 5. n°7.
  37. Colter D.C., Sekiya I., Prockop D.J. (2001). Identification of a subpopulation of rapidly self-renewing and multipotential adult stem cells in colonies of human marrow stromal cells. *Proc Natl Acad Sci U S A.*, 98. n°14. 7841-7845.
  38. Conforti A., Scarsella M., Starc N., Ezio Giorda E., Biagini S. Proia A., Carsetti R., Locatelli, Bernardo M.E. (2014). Microvesicles Derived from Mesenchymal Stromal Cells Are Not as Effective as Their Cellular Counterpart in the Ability to Modulate Immune Responses In Vitro. *Stem Cell Dev.*, 00. n°00. 1-9.
  39. Crews L., Rockenstein E., Masliah E. (2010). APP transgenic modeling of Alzheimer's disease: mechanisms of neurodegeneration and aberrant neurogenesis. *Brain Struct Funct.*, 214. 111-126.
  40. Cuadros M.A., Martin C., Coltey P., Almendros A., Navascues J. (1993). First appearance, distribution, and origin of macrophages in the early development of the avian central nervous system. *J Comp Neurol.*, 330. 113-129.
  41. Dai S., Wei D., Wu Z., Zhou X., Wei X., Huang H., Li G. (2008). Phase I clinical trial of autologous ascites-derived exosomes combined with GM-CSF for colorectal cancer. *Mol Ther.*, 16. 782-790.
  42. Da Silva Meirelles L., Nardi N.B. (2003). Murine marrow-derived mesenchymal stem cell: isolation, in vitro expansion, and characterization. *British Journal of Haematology*, 123. 702-711.
  43. De Bari C., Dell'Accio F., Tylzanowski P., Luyten F.P. (2001). Multipotent mesenchymal stem cells from adult human synovial membrane. *Arthritis Rheum.*, 44. n°8. 1928-1942.
  44. Dicker A., Le Blanc K., Astrom G., van Harmelen V., Götherström C., Blomqvist L., Arner P., Rydén M. (2005). Functional studies of mesenchymal stem cells derived from adult human adipose tissue. *Exp Cell Res.*, 308. 283-290.
  45. Direkze N.C., Forbes S.J., Brittan M., Hunt T., Jeffery R., Preston S.L., Poulosom R., Hodivala-Dilke K., Alison M.R., Wright N.A. (2003). Multiple organ engraftment by bone-marrow-derived myofibroblasts and fibroblasts in bone-marrow-transplanted mice. *Stem Cells*, 21. n°5. 514-520.
  46. Dickson D.W. (1997). The pathogenesis of senile plaques. *J Neuropathol Exp Neurol.*, 56. 321-339.
  47. Djouad F., Plence P., Bony C., Tropel P., Apparailly F., Sany J., Noël D., Jorgensen C. (2003). Immunosuppressive effect of mesenchymal stem cells favors tumor growth in allogeneic animals. *Blood*, 102. n°10. 3837-3844.
  48. Dodel R., Hampel H., Depboylu C., Lin S., Gao F., Schock S., Jäckel S., Wei X., Buerger K., Höft C., Hemmer B., Möller H.J., Farlow M., Oertel W.H., Sommer N., Du Y. (2002). Human antibodies against amyloid beta peptide: a potential treatment for Alzheimer's disease. *Ann Neurol.*, 52. n°2. 253-256.

49. Dominici M., Le Blanc K., Mueller I., Slaper-Cortenbach I., Marini F.C., Krause D.S., Deans R.J., Keating A., Prockop D.J. Horwitz D.J. (2006). Minimal criteria for defining multipotent mesenchymal stromal cells. The International Society for Cellular Therapy position statement. *Cytotherapy*, 8, n°4, 315-317.
50. Duff K., Eckman C., Zehr C., Yu X., Prada C.H., Perez-Tur J., Hutton M., Buee L., Harigaya Y., Yager D., Morgan D., Gordon M.N., Holcomb L., Refolo L., Zenk B., Hardy J., Younkin S. (1996). Increased amyloid-b42(43) in brains of mice expressing mutant presenilin 1. *Nature*, 383, 710-713.
51. Eckle T., Füllbier L., Wehrmann M. Khoury J., Mittelbronn M., Ibla J., Rosenberger P., Eltzschig H.K. (2007). Identification of ectonucleotidases CD39 and CD73 in innate protection during acute lung injury. *J Immunol*, 178, n°12, 8127-8137.
52. Eirin A., Riestler S.M., Zhu X.Y., Tang H., Evans J. M., O'Brien D., Van Wijnen A. J., Lerman L.O. (2014). MicroRNA and mRNA cargo of extracellular vesicles from porcine adipose tissue-derived mesenchymal stem cells. *Gene*. 1-10.
53. El Khoury J and Andrew D. Luster (2008) Mechanisms of microglia accumulation in Alzheimer's disease: therapeutic implications. *Trends in Pharmacological Sciences* Vol.29 No.12
54. Escudier B., Dorval T., Chaput N., Andre F., Caby M.P., Novault S., Flament C., Leboulaire C., Borg C., Amigorena S., Boccaccio C., Bonnerot C., Dhellin O., Movassagh M., Piperno S., Robert C., Serra V., Valente N., Le Pecq J.B., Spatz A., Lantz O., Tursz T., Angevin E., Zitvogel L. (2005). Vaccination of metastatic melanoma patients with autologous dendritic cell (DC) derived-exosomes: results of the first phase I clinical trial. *J Transl Med.*, 3, n°1. 1-10.
55. Fang F., Lue L.F., Yan S., Xu H., Luddy J.S., Chen D., Walker D.G., Stern D.M., Yan S., Schmidt A.M., Chen J.X., Yan S.S. (2010). RAGE-dependent signaling in microglia contributes to neuroinflammation, A $\beta$  accumulation, and impaired learning/memory in a mouse model of Alzheimer's disease. *The FASEB Journal*, 24, 1043-1055.
56. Ferreira S.T., Klein W.L. (2011) The A $\beta$  oligomer hypothesis for synapse failure and memory loss in Alzheimer's disease. *Neurobiol Learn Mem.*, 96, 529-543.
57. Ferri C.P., Prince M., Brayne C., Brodaty H., Fratiglioni L., Ganguli M., Hall K., Hasegawa K., Hendrie H., Huang Y., Jorm A., Mathers C., Menezes P.R., Rimmer E., Scazufca M. (2005). Global prevalence of dementia: Adelphi consensus study. *Lancet*, 366, 2112-2117.
58. Friedenstein A.J., Chailakhyan R.K, Latsinik N.V, Panasyuk A.F, Keiliss-Borok I.V. (1974). Stromal cells responsible for transferring the microenvironment of the hemopoietic tissues. Cloning in vitro and retransplantation in vivo. *Transplantation*, 4, 331-40.
59. Galea I, Bechmann I, Perry V.H. (2007). What is immune privilege (not)? *Trends Immunol.*, 28, n°1, 12-18.
60. Games D., Adams D., Alessandrini R., Barbous R., Berthelette P., Blackwell C., Carr T., Clemens J., Donaldson T, Gillespie F., Guido T., Hagopian S., Johnson-Wood K., Khan K., Lee M., Leibowitz P., Lieberburg I., Little S., Masliah E., McConlogue L., Montoya-Zavala M., Mucke L., Paganini L., Penniman E., Power M., Schenk D., Seubert P., Snyder B., Soriano F., Tan H., Vitale J., Wadsworth S., Wolozin B., Zhao J. (1995). Alzheimer-type neuropathology in transgenic mice overexpressing V717F  $\beta$ -amyloid precursor protein. *Nature*, 373, 523-527.
61. Garcia-Alloza M., Robbins E.M., Zhang-Nunes S. X., Purcell S.M., Betensky R.A., Raju S., Prada C., Greenberg S.M., Bacskai B.J., Frosch M.P. (2006). Characterization of amyloid deposition in the APP<sub>swE</sub>/PS1<sub>dE9</sub> mouse model of Alzheimer disease. *Neurobiol Dis.*, 24, 516-524.
62. Garzetti L., Menon R., Finardi A., Bergami A., Sica A., Martino G., Comi G., Verderio C., Farina C., Furlan R. (2014). Activated macrophages release microvesicles containing polarized M1 or M2 mRNAs. *Journal of Leukocyte Biology*, 95, 817-825.
63. Ginhoux F., Greter M., Leboeuf M., Nandi S., See P. Gokhan S., Mehler M.F., Conway S.J., Ng L.G., Stanley E.R., Samokhvalov I.M., Merad M. (2010). Fate mapping analysis reveals that adult microglia derive from primitive macrophages. *Science*, 330, 841-45.
64. Ginhoux F., Lim S., Hoeffel G., Low D., Huber T. (2013). Origin and differentiation of microglia. *Front Cell Neurosci.*, 7, n°45, 1-14.
65. Gebler A., Zabel O., Seliger B. (2012). The immunomodulatory capacity of mesenchymal stem cells. *Trends Mol Med.*, 18, n°2, 128-134.
66. Giuffrida M.L., Caraci F., Pignataro B., Cataldo S., De Bona P., Bruno V., Molinaro G., Pappalardo G., Angela Messina A., Palmigiano A., Garozzo D., Nicoletti F., Rizzarelli E., Copani A. (2009).  $\beta$ -Amyloid Monomers Are Neuroprotective. *J Neurosci.*, 29, n°34, 10582-10587.
67. Giunti D., Parodi B., Usai C., Vergani L., Casazza S., Bruzzone S., Mancardi G., Uccelli A. (2012). Mesenchymal stem cells shape microglia effector functions through the release of CX3CL1. *Stem Cells*, 30, n°9, 2044-2053.
68. Goate A., Chartier-Harlin M.C., Mullan M., Brown J., Crawford F., Fidani L., Guiffra L., Haynes A., Irving N., James L., Mant R., Newton P, Rooke K,

- Roques P., Talbot C., Pericak-Vance M., Roses A., Williamson R., Rossor M., Owen M., Hardy J. (1991). Segregation of a missense mutation in the amyloid precursor protein gene with familial Alzheimer's disease. *Nature*, 349. 704-706.
69. Goldmann T., Prinz M. (2013). Role of Microglia in CNS Autoimmunity. *Clin Dev Immunol*, 2013. 1-8.
  70. Gotz J., Schild A., Hoerndli F., Pennanen L. (2004). Amyloid-induced neurofibrillary tangle formation in Alzheimer's disease: insight from transgenic mouse and tissue-culture models. *Int J Devl Neuroscience*, 22. 453-465.
  71. Götz J., Götz N.N. (2009). Animal models for Alzheimer's disease and frontotemporal dementia: a perspective. *ASN Neuro*, 1. 251-264.
  72. Greter M., Merad M. (2013). Regulation of microglia development and homeostasis. *Glia*, 61. 121-127.
  73. Gu L., Guo Z. (2013). Alzheimer's A $\beta$ 42 and A $\beta$ 40 peptides form interlaced amyloid fibrils. *J Neurochem.*, 126. n°3. 305-311.
  74. Guillot-Sestier M.V., Doty K.R., Gate D., Rodriguez J. Jr., Leung B.P., Rezai-Zadeh K., Town T. (2015). Il10 deficiency rebalances innate immunity to mitigate Alzheimer-like pathology. *Neuron*, 85. n°3. 534-48.
  75. György B., Szabó T.G., Pásztoi M., Pál Z., Misják P., Aradi B., László V., Pállinger E., Pap E., Kittel A., Nagy G., Falus A., Buzás E.I. (2011). Membrane vesicles, current state-of-the-art: emerging role of extracellular vesicles. *Cell Mol Life Sci.*, 68. 2667-2688.
  76. Haass C., Hung A.Y., Selkoe D.J. (1991). Processing of  $\beta$ -amyloid precursor protein in microglia and astrocytes favors a localization in internal vesicles over constitutive secretion. *J Neurosci.*, 11. 3783-3793.
  77. Haeryfar S.M.M., Hoskin D.W. (2004). Thy-1: more than a mouse pan-T cell marker. *J Immunol*, 173. n° 6. 3581-3588.
  78. Harada H., Tamaoka A., Ishii K., Shoji S., Kametaka S., Kametani F., Saito Y., Murayama S. (2006). Beta-site APP cleaving enzyme 1 (BACE1) is increased in remaining neurons in Alzheimer's disease brains. *Neurosci Res.*, 54. 24-29.
  79. Harry G.J., Kraft A.D. (2012). Microglia in the developing brain: A potential target with lifetime effects. *NeuroToxicology*, 33. 191-206.
  80. Harry G.J. (2013). Microglia during development and aging. *Pharmacol Ther.*, 139. 313-326.
  81. He J, Yan Wang, Xingyan Lu, Bei Zhu, Xiaohua Pei, Jianqing Wu And Weihong Zhao (2015) Microvesicles derived from bone marrow stem cells protect the kidney both in vivo and in vitro by microRNA-dependent repairing. *Nephrology* **20** 591-600
  82. Hickman E.S., Allison E.K., El Khoury J. (2008). Microglial dysfunction and defective  $\beta$ -amyloid clearance pathways in aging Alzheimer's disease mice. *J Neurosci.*, 28. n°33. 8354-8360.
  83. Higgins G.A., Jacobsen H. (2003). Transgenic mouse models of Alzheimer's disease: phenotype and application. *Behav Pharmacol.*, 14. n°5-6. 419-438.
  84. Howlett DR<sup>1</sup>, Bowler K, Soden PE, Riddell D, Davis JB, Richardson JC, Burbidge SA, Gonzalez MI, Irving EA, Lawman A, Miglio G, Dawson EL, Howlett ER, Hussain I. (2008) Abeta deposition and related pathology in an APP x PS1 transgenic mouse model of Alzheimer's disease. *Histol Histopathol.* Jan;23(1):67-76.
  85. Hsiao K., Borchelt D.R., Olson K., Johannsdottir R., Kitt C., Yunis W., Rothacher S., Ledermann B., Bürki K., Frey P., Paganetti P.A., Waridel C., Calhoun M.E., Jucker M., Probst A., Staufenbiel M., Sommer B. (1995). Age related CNS disorder and early death in transgenic FVB/N mice overexpressing Alzheimer amyloid precursor proteins. *Neuron*, 15. 1203-1218.
  86. Hunter, M.P., Ismail N., Zhang X., Aguda B.D., Lee E.J., Yu L., Xiao T., Schafer J., Lee M.L., Schmittgen T.D., Nana-Sinkam S.P., Jarjoura D., Marsh C.B. (2008) Detection of microRNA expression in human peripheral blood microvesicles. *PLoS One*, 3. 1-11.
  87. Illenberger S., Zheng-Fischhofer Q., Preuss U., Stamer K., Baumann K., Trinczek B., Biernat J., Godemann R., Mandelkow E.M., Mandelkow E. (1998). The endogenous and cell cycle-dependent phosphorylation of tau protein in living cells: implications for Alzheimer's disease. *Mol Biol Cell.*, 9. 1495-1512.
  88. Im H., Shao H., Park Y.I., Peterson V.M., Castro C. M., Weissleder R., Lee H. (2014). Label-free detection and molecular profiling of exosomes with a nano-plasmonic sensor. *Nature Biotechnology*, 32. 490-495.
  89. Jarrett J.T., Berger E.P., Lansbury P.T. jr. (1993). The carboxy terminus of the beta amyloid protein is critical for the seeding of amyloid formation: implications for the pathogenesis of Alzheimer's disease. *Biochemistry*, 32. 4693-4697.
  90. Jiang Y., Jahagirdar B.N., Reinhardt R.L., Schwartz R.E, Keene C.D., Ortiz-Gonzalez X.R, Reyes M., Lenvik T., Lund T., Blackstad M., Du J., Aldrich S., Lisberg A., Low W.C., Largaespada D.A., Verfaillie C.M. (2002). Pluripotency of mesenchymal stem cells derived from adult marrow. *Nature*, 418. 41-49.
  91. Karussis D., Kassis I., Kurkalli B.G.S., Slavin S. (2008). Immunomodulation and neuroprotection with mesenchymal bone marrow stem cells

- (MSCs): A proposed treatment for multiple sclerosis and other neuroimmunological/neurodegenerative diseases. *J Neurol Sci.*, 265. 131-135.
92. Katsuda T., Tsuchiya R., Kosaka N., Yoshioka Y., Takagaki K., Oki K., Takeshita F., Sakai S., Kuroda M., Ochiya T. (2013). Human adipose tissue-derived mesenchymal stem cells secrete functional neprilysin-bound exosomes. *Sci Rep.*, 3. n°1197. 1-11.
  93. Kenneth W. Witwer, Edit I. Buzás, Lynne T. Bemis, Adriana Bora, Cecilia Lässer, Jan Lötval, Esther N. Nolte-t Hoen, Melissa G. Piper, Sarada Sivaraman, Johan Skog, Clotilde Théry, Marca H. Wauben, and Fred Hochberg (2013) Standardization of sample collection, isolation and analysis methods in extracellular vesicle research. *J Extracell Vesicles.* 2: 10.3402/jev.v2i0.20360
  94. Kenji Sasahara, Kenichi Morigaki and Kyoko Shinya, (2013) Effects of membrane interaction and aggregation of amyloid b-peptide on lipid mobility and membrane domain structure. *Phys.Chem. Chem. Phys.*, 2013,15, 8929
  95. Khakoo A.Y., Pati S., Anderson S.A., Reid W., Elshal M.F., Rovira I.I., Nguyen A.T., Malide D., Combs C.A., Hall G., Zhang J., Raffeld M., Rogers T.B., Stetler-Stevenson W., Frank J.A., Reitz M., Finkel T. (2006). Human mesenchymal stem cells exert potent antitumorogenic effects in a model of Kaposi's sarcoma. *J Exp Med.*, 203. 1235-1247.
  96. Kierdorf K., Erny D., Goldmann T., Sander V., Schulz C., Perdiguero E.G., Wieghofer P., Heinrich A., Riemke P., Hölscher C., Müller D.N., Luckow B., Broucker T., Debowski K., Fritz G., Opdenakker G., Diefenbach A., Biber K., Heikenwalder M., Geissmann F., Rosenbauer F., Prinz M. (2013). Microglia emerge from erythromyeloid precursors via Pu.1- and Irf8-dependent pathways. *Nat Neurosci.*, 16. 273-30.
  97. Kim H.S., Choi D.Y., Yun S.J., Choi S.M., Kang J.W., Jung J. W., Hwang D., Kim K.P., Kim D.W. (2012). Proteomic Analysis of Microvesicles Derived from Human Mesenchymal Stem Cells. *J Proteome Res.*, 11. 839-849.
  98. Kettenmann H., Banati R., Walz W. (1993). Electrophysiological behavior of microglia. *Glia*, 7. 93-101.
  99. . Kobayashi D.T., Chen K.S. (2005). Behavioral phenotypes of amyloid-based genetically modified mouse models of Alzheimer's disease. *Genes, Brain and Behavior*, 4. 173-196.
  100. Krampera M., Pizzolo G., Aprili G., Franchini M. (2006). Mesenchymal stem cells for bone, cartilage, tendon and skeletal muscle repair. *Bone*, 39. 678-683.
  101. Kreutzberg G.W. (1996). Microglia: a sensor for pathological events in the CNS. *Trends Neurosci.*, 19. n°8. 312-318.
  102. LaFerla F.M., Green K.N., Oddo S. (2007) Intracellular amyloid-beta in Alzheimer's disease. *Nat Rev Neurosci.*, 8. 499-509.
  103. Lai R.C., Yeo R.W.Y., Tan K.H., Lim S.K. (2013). Exosomes for drug delivery - a novel application for the mesenchymal stem cell. *Biotechnology Advances*, 31. 543-551.
  104. Lambert M.P., Barlow A.K., Chromy B.A., Edwards C., Freed R., Liosatos M., Morgan T.E., Rozovsky I., Trommer B., Viola K.L., Wals P., Zhang C., Finch C.E., Krafft G.A., Klein W.L. (1998). Diffusible, nonfibrillar ligands derived from Abeta1-42 are potent central nervous system neurotoxins. *Proc Natl Acad Sci U S A.*, 95. 6448-6453.
  105. Lavoie J.R., Rosu-Myles M. (2013). Uncovering the secreted of mesenchymal stem cells. *Biochimie*, 95. 2212-2221.
  106. Lee J.W., Lee Y.K., Yuk D.Y., Choi D.Y., Ban S.B., Oh K.W., Hong J.T. (2008). Neuro-inflammation induced by lipopolysaccharide causes cognitive impairment through enhancement of beta-amyloid generation. *J Neuroinflammation*, 5. n°37. 1-14.
  107. Lee J.K., Jin H.K., Bae J.S. (2009). Bone marrow-derived mesenchymal stem cells reduce brain amyloid- $\beta$  deposition and accelerate the activation of microglia in an acutely induced Alzheimer's disease mouse model. *Neuroscience Letters*, 450. 136-141.
  108. Lee J.K., Jin H.K., Endo S., Schuchman E.H., Carter J.E., Bae J.S. (2010). Intracerebral Transplantation of Bone Marrow-Derived Mesenchymal Stem Cells Reduces Amyloid-Beta Deposition and Rescues Memory Deficits in Alzheimer's Disease Mice by Modulation of Immune Responses. *Stem Cells*, 28. 329-343.
  109. . Lee H.J., Lee J.K., Lee H., Carter J.E., Chang J.W., Oh W., Yang Y.S., Suh J.G., Lee B.H., Jin H.K., Bae J.S. (2012). Human umbilical cord blood-derived mesenchymal stem cells improve neuropathology and cognitive impairment in an Alzheimer's disease mouse model through modulation of neuroinflammation. *Neurobiol Aging*, 33. 588-602.
  110. Lee J.K., Schuchman E.H., Jin H.K., Bae J.S. (2012). Soluble CCL5 Derived from Bone Marrow-Derived Mesenchymal Stem Cells and Activated by Amyloid  $\beta$  Ameliorates Alzheimer's Disease in Mice by Recruiting Bone Marrow-Induced Microglia Immune Responses. *Stem Cells*, 30. 1544-1555.
  111. Lee J.K., Park S.R., Jung B.K., Jeon Y.K., Lee Y.S., Kim M.K., Kim Y.G., Jang J.Y., Kim C.W. (2013). Exosomes Derived from Mesenchymal Stem Cells Suppress Angiogenesis by Down-Regulating VEGF

- Expression in Breast Cancer Cells. *PLoS One*, 8, n°12. 1-11.
112. Lennon D.P., Caplan A.I. (2006). Isolation of rat marrow-derived mesenchymal stem cells. *Exp Hematol.*, 34. 1606-1607.
  113. Lewis J., McGowan E., Rockwood J., Melrose H., Nacharaju P., Van Slegtenhorst M., Gwinn-Hardy K., Paul Murphy M., Baker M., Yu X., Duff K., Hardy J., Corral A., Lin W.L., Yen S.H., Dickson D.W., Davies P., Hutton M. (2000). Neurofibrillary tangles, amyotrophy and progressive motor disturbance in mice expressing mutant (P301L) tau protein. *Nat Genet.*, 25. 402-405.
  114. Lewis J., Dickson D.W., Lin W.L., Chisholm L., Corral A., Jones G., Yen S.H., Sahara N., Skipper L., Yager D., Eckman C., Hardy J., Hutton M., McGowan E. (2001). Enhanced neurofibrillary degeneration in transgenic mice expressing mutant tau and APP. *Science*, 293.1487-1491.
  115. Lian H, Zheng H (2015) Signaling pathways regulating neuron-glia interaction and their implications in Alzheimer's disease. *J Neurochem*. Nov 6.
  116. Liu C.C., Kanekiyo T., Xu H., Bu G. (2013). Apolipoprotein E and Alzheimer disease: risk, mechanisms, and therapy. *Nat Rev Neurol.*, 9. n°2. 106-118.
  117. Lodi D., Iannitti T., Palmieri B. (2011). Stem cells in clinical practice: applications and warnings. *Journal of Experimental & Clinical Cancer Research*, 30. n°9. 1-20.
  118. Lopatina T., Stefania Bruno, Ciro Tetta, Natalia Kalinina, Massimo Porta and Giovanni Camussi (2014) Platelet-derived growth factor regulates the secretion of extracellular vesicles by adipose mesenchymal stem cells and enhances their angiogenic potential. *Cell Communication and Signaling*
  119. Lotfy A., Salama M., Zahran F., Jones E., Badawy A., Sobh M. (2014). Characterization of mesenchymal stem cells derived from rat bone marrow and adipose tissue: a comparative study. *Int J Stem Cells*, 7. n°2. 135-42.
  120. Ludwig A.K., Giebel B. (2012). Exosomes: Small vesicles participating in intercellular communication. *Int J Biochem Cell Biol.*, 44. 11-15.
  121. Lynch M.A. (2009). The Multifaceted Profile of Activated Microglia. *Mol Neurobiol*, 40. 139-156.
  122. Ma T., Gong K., Ao Q., Yan Y., Song B., Huang H., Zhang X., Gong Y. (2013). Intracerebral Transplantation of Adipose-Derived Mesenchymal Stem Cells Alternatively Activates Microglia and Ameliorates Neuropathological Deficits in Alzheimer's Disease Mice. *Cell Transplant.*, 22. n°1. S113-S126.
  123. Mantovani A., Biswas S.K., Galdiero M.R., Sica A., Locati M. (2013). Macrophage plasticity and polarization in tissue repair and remodelling. *J Pathol.*, 229. 176-185.
  124. Marin-Teva J.L., Dusart I., Colin C., Gervais A., Van Rooijen N., Mallat M. (2004). Microglia promote the death of developing Purkinje cells. *Neuron*, 41. 535-547.
  125. Marx J. (1992). News and Comment: Major setback for Alzheimer's models. *Science*, 255. 1200-1202.
  126. Mattsson N., Zetterberg H., Hansson O., Andreasen N., Parnetti L., Jonsson M., Herukka S. K., Van Der Flier W. M., Blankenstein M. A., Ewers M., Rich K., Kaiser E., Verbeek M., Tsolaki M., Mulugeta E., Rosén E., Aarsland D., Visser P. J., Schröder J., Marcusson J., De Leon M., Hampel H., Scheltens P., Pirttilä T., Wallin A., Jönhagen M. E., Minthon L., Winblad B., Blennow K. (2009). CSF Biomarkers and Incipient Alzheimer Disease in Patients With Mild Cognitive Impairment. *JAMA*, 302. n°4. 385-393.
  127. McClay D.R., Gooding L.R., Fransen M.E. (1977). A requirement for trypsin-sensitive cell-surface components for cell-cell interactions of embryonic neural retina cells. *J Cell Biol.*;75. n°1. 56-66.
  128. Mc Donald Jessica M., Nigel J. Cairns, Lisa Taylor-Reinwald2, David Holtzman, and Dominic M. Walsh,(2013) The levels of water-soluble and triton-soluble A $\beta$  are increased in Alzheimer's disease brain . 23; 1450: 138–147
  129. McGhee D.J.M., Ritchie C.W., Thompson P.A., Wright D.E., Zajicek J.P., Counsell C.E. (2014). A Systematic Review of Biomarkers for Disease Progression in Alzheimer's Disease. *PLoS One*, 9. n°2. 1-9.
  130. Meraz-Ríos M.A., Toral-Rios D., Bocanegra D.F., Hernández J.V., Campos-Peña V. (2013). Inflammatory process in Alzheimer's Disease. *Front Integr Neurosci.*, 7. n°59. 1-15.
  131. Michaud JP and Serge Rivest, 2015, Anti-inflammatory signaling in microglia exacerbates Alzheimer's disease-related pathology. *Neuron*, Feb 4.
  132. Michelucci A., Tony Heurtaux, Luc Grandbarbe, Eleonora Morga, Paul Heuschling (2009) Characterization of the microglial phenotype under specific pro-inflammatory and anti-inflammatory conditions: Effects of oligomeric and fibrillar amyloid- $\beta$ . *Journal of Neuroimmunology* 210- 3–12
  133. Minkeviciene R., Rheims S., Dobszay M.B., Zilberter M., Hartikainen J., Fülöp L., Penke B., Zilberter Y., Harkany T., Pitkänen A., Tanila H. (2009). Amyloid beta-induced neuronal hyperexcitability triggers progressive epilepsy. *J Neurosci.*, 29. n°11. 3453-3462.

134. Miura M., Gronthos S., Zhao M., Lu B., Fisher L.W., Robey P.G., Shi S. (2003). SHED: Stem cells from human exfoliated deciduous teeth. *Pnas*, 100. n°10. 5807-5812.
135. Mokarizadeh A., Delirezh N., Morshedi A., Mosayebi G., Farshid A.A., Mardani K. (2012). Microvesicles derived from mesenchymal stem cells: Potent organelles for induction of tolerogenic signaling. *Immunol Lett.*, 147. 47-54.
136. Montecalvo A., Larregina A.T., Shufesky W.J., Stolz D.B., Sullivan M.L.G., Karlsson J.M., Baty C.J., Gibson G.A., Erdos G., Wang Z., Milosevic J., Tkacheva O.A., Divito S.J., Jordan R., Lyons-Weiler J., Watkins S.C., Morelli A.E. (2012). Mechanism of transfer of functional microRNAs between mouse dendritic cells via exosomes. *Blood*, 119. n°3. 756-766.
137. Moreth J., Mavoungou C., Schindowski K. (2013). Passive anti-amyloid immunotherapy in Alzheimer's disease: What are the most promising targets? *Immun Ageing*, 10. n°1. 10-18.
138. Morigi M., Imberti B., Zoja C., Corna D., Tomasoni S., Abbate M., Rottoli D., Angioletti S., Benigni A., Perico N., Alison M., Remuzzi G. (2004). Mesenchymal stem cells are renoprotective, helping to repair the kidney and improve function in acute renal failure. *J Am Soc Nephrol.*, 15. 1794-1804.
139. Mosher K.I., Wyss-Coray T. (2014). Microglial dysfunction in brain aging and Alzheimer's disease. *Biochemical Pharmacology*, 88. 594-604.
140. Mucke L., Masliah E., Yu G.Q., Mallory M., Rockenstein E.M., Tatsuno G., Hu K., Kholodenko D., Johnson-Wood K., McConlogue L. (2000). High-level neuronal expression of abeta 1-42 in wild-type human amyloid protein precursor transgenic mice: Synaptotoxicity without plaque formation. *J Neurosci.*, 20. 4050-4058.
141. Muraglia A., Cancedda R., Quarto R. (2000). Clonal mesenchymal progenitors from human bone marrow differentiate in vitro according to a hierarchical model. *J Cell Sci.*, 113. 1161-1166.
142. Murphy M.P., LeVine H.3rd. (2010). Alzheimer's disease and the amyloid- beta peptide. *J Alzheimer's Dis.*, 19. 311-323.
143. Nayak D., Zinselmeyer B.H., Corps K., McGavern D.B. (2012). In vivo dynamics of innate immune sentinels in the CNS. *IntraVital*, 1. n°2. 95-106.
144. Nayak D., Roth T.L., McGavern D.B. (2014). Microglia Development and Function. *Annu Rev Immunol.*, 32. 367-402.
145. Nimmerjahn A., Kirchhoff F., Helmchen F. (2005). Resting microglial cells are highly dynamic surveillants of brain parenchyma in vivo. *Science*, 308. 1314-1318.
146. Noda M., Doi Y., Liang J., Kawanokuchi J., Sonobe Y., Takeuchi H., Mizuno T., Suzumura A. (2011). Fractalkine attenuates excitoneurotoxicity via microglial clearance of damaged neurons and antioxidant enzyme heme oxygenase-1 expression. *J Biol Chem.*, 286. 2308-2319.
147. Oddo S., Caccamo A., Shepherd J.D., Murphy M.P., Golde T.E., Kaye R., Metherate R., Mattson M.P., Akbari Y., LaFerla F.M. (2003)<sup>1</sup>. Triple-Transgenic Model of Alzheimer's Disease with Plaques and Tangles: Intracellular A $\beta$  and Synaptic Dysfunction. *Neuron*, 39. 409-421.
148. Oddo S., Caccamo A., Shepherd J.D., Murphy M.P., Golde T.E., Kaye R., Metherate R., Mattson M.P., Akbari Y., LaFerla F.M. (2003)<sup>2</sup>. Triple-transgenic model of Alzheimer's disease with plaques and tangles: intracellular Abeta and synaptic dysfunction. *Neuron*, 39. 409-421.
149. Orlic D., Kajstura J., Chimenti S., Jakoniuk I., Anderson S.M., Li B., Pickel J., McKay R., Nadal-Ginard B., Bodine D.M., Leri A., Anversa P. (2001). Bone marrow cells regenerate infarcted myocardium. *Nature*, 410. n°6829. 701-705.
150. Papassotiropoulos A., Hock C., Nitsch R.M. (2001). Genetics of interleukin 6: implications for Alzheimer's disease. *Neurobiol Aging*, 22. n°6. 863-871.
151. Park JS, Yi TG, Park JM, Han YM, Kim JH, Shin DH, Tak SJ, Lee K, Lee YS, Jeon MS, Hahm KB, Song SU, Park SH. (2015). Therapeutic effects of mouse bone marrow-derived clonal mesenchymal stem cells in a mouse model of inflammatory bowel disease. *J Clin Biochem Nutr*. Nov;57(3):192-203.
152. Parkinson J., Ploeger B., Appelkvist P., Bogstedt A., Bergstedt K.D., Eketjäll S., Visser S.A.G. (2013). Modeling of age-dependent amyloid accumulation and  $\gamma$ -secretase inhibition of soluble and insoluble A $\beta$  in a transgenic mouse model of amyloid deposition. *Pharma Res Per.*, 1. n°2. 1-15.
153. Patrick G.N., Zukerberg L., Nikolic M., De La Monte S., Dikkes P., Tsai L.H. (1999). Conversion of p35 to p25 deregulates Cdk5 activity and promotes neurodegeneration. *Nature*, 402. 615-622.
154. Pepe G., Calderazzi G., De Maglie M., Villa A.M., Vegeto E. (2014). Heterogeneous induction of microglia M2a phenotype by central administration of interleukin-4. *J Neuroinflammation*, 11. n°1.
155. Pérez M. Ribe E., Rubio A., Lim F., Moran M.A., Gómez Ramos P., Ferrer I., Isla M.T.G., Avila J. (2005). Characterization of a double (amyloid precursor precursor protein-tau) transgenic: Tau phosphorylation and aggregation. *Neuroscience*, 130. 339-347
156. Perez S.E., Lumayag S., Kovacs B., Mufson E.J., Xu S. (2009).  $\beta$ -Amyloid Deposition and Functional Impairment in the Retina of the APP<sup>swE</sup>/PS1 $\Delta$ E9

- Transgenic Mouse Model of Alzheimer's Disease. *Invest Ophthalmol Vis Sci.*, 50. n°2. 793-800.
157. Perry R.T., Collins J.S., Wiener, H., Acton, R., Go R.C. (2001). The role of TNF and its receptors in Alzheimer's disease. *Neurobiol Aging*, 22. n°6. 873-883.
  158. Philipson O., Lord A., Gumucio A., O'Callaghan P., Lannfelt L., Nilsson L.N.G. (2010). Animal models of amyloid-beta-related pathologies in Alzheimer's disease. *FEBS J*, 277. 1389-1409.
  159. Phinney D.G., Sensebè L. (2013). Mesenchymal stromal cells: misconceptions and evolving concepts. *Cytotherapy*, 15. 140-145.
  160. Pittenger M.F., Mackay A.M., Beck S.C., Jaiswal R.K., Douglas R., Mosca J.D., Moorman M.A., Simonetti D.W., Craig S., Marshak D.R. (1999). Multilineage potential of adult human mesenchymal stem cells. *Science*, 284. 143-147.
  161. Pittenger M., Vanguri P., Simonetti D., Young R. (2002). Adult mesenchymal stem cells: potential for muscle and tendon regeneration and use in gene therapy. *J Musculoskelet Neuronal Interact.*, 2. n°4. 309-320.
  162. Pountos I, Giannoudis P.V. (2005). Biology of mesenchymal stem cells. *Injury*, 36. n°3. S8-S12.
  163. Pountos I., Corscadden D., Emery P., Giannoudis P.V. (2007). Mesenchymal stem cell tissue engineering: Techniques for isolation, expansion and application. *Injury*, 38. n°4. S23-S33.
  164. Prajeeth C.K., Löhr K., Floess S., Zimmermann J., Ulrich R., Gudi V., Beineke A., Baumgärtner W., Müller M., Huehn J., Stangel M. (2014). Effector molecules released by Th1 but not Th17 cells drive an M1 response in microglia. *Brain Behav Immun.*, 37. 248-259.
  165. Quesenberry P.J., Goldberg L.R., Aliotta J.M., Dooner M.S., Pereira M.G., Wen S.N., Camussi G. (2014). Cellular Phenotype and Extracellular Vesicles: Basic and Clinical Considerations. *Stem Cell Dev.*, 23. n°13. 1429-1436.
  166. Quon D., Wang Y., Catalano R., Scardina J.M., Murkami K., Cordell B. (1991). Formation of b-amyloid protein deposits in brains of transgenic mice. *Nature*, 352. 239-241.
  167. Rahmat Z., Jose S., Ramasamy R., Vidyadaran S. (2013). Reciprocal interactions of mouse bone marrow-derived mesenchymal stem cells and BV2 microglia after lipopolysaccharide stimulation. *Stem Cell Res Ther.*, 4. n°12. 1-11.
  168. Ramasamy R., Lam E.W., Soeiro I., Tisato V., Bonnet D., Dazzi F. (2007). Mesenchymal stem cells inhibit proliferation and apoptosis of tumor cells: impact on in vivo tumor growth. *Leukemia*, 21. n°2. 304-310.
  169. Ramasamy R., Tong C.K., Seow H.F., Vidyadaran S., Dazzi F. (2008). The immunosuppressive effects of human bone marrow-derived mesenchymal stem cells target T cell proliferation but not its effector function. *Cellular Immunology*, 251. 131-136.
  170. Raposo G., Stoorvogel W. (2013). Extracellular vesicles: Exosomes, microvesicles, and friends. *J Cell Biol.*, 200. n°4. 373-383.
  171. Ratajczak J., Miekus K., Kucia M., Zhang J., Reca R., Dvorak P. Ratajczak M.Z. (2006)<sup>1</sup>. Embryonic stem cell-derived microvesicles reprogram hematopoietic progenitors: evidence for horizontal transfer of mRNA and protein delivery. *Leukemia*, 20. 847-856.
  172. Ratajczak J., Wysoczynski M., Hayek F., Janowska-Wieczorek A., Ratajczak M.Z. (2006)<sup>2</sup>. Membrane-derived microvesicles: important and underappreciated mediators of cell-to-cell communication. *Leukemia*, 20. 1487-95.
  173. Relkin N. (2014). Clinical trials of intravenous immunoglobulin for Alzheimer's disease *J Clin Immunol.*, 34 n°1. 74-79.
  174. Richardson J.A., Burns D.K. (2002). Mouse Models of Alzheimer's Disease: A Quest for Plaques and Tangles. *ILAR Journal*, 43. n°2. 89-99.
  175. Rowan M.J., Klyubin I., Wang Q., Anwyl R. (2005). Synaptic plasticity disruption by amyloid  $\beta$  protein: modulation by potential Alzheimer's disease modifying therapies. *Biochem Soc Trans.*, 33. 563-567.
  176. Rubio-Perez JM and Morillas-Ruiz JM (2012) A Review: Inflammatory Process in Alzheimer's Disease, Role of Cytokines. *The Scientific World Journal*
  177. Safar MM, Arab HH, Rizk SM, El-Maraghy SA, 2014. Bone Marrow-Derived Endothelial Progenitor Cells Protect Against Scopolamine-Induced Alzheimer-Like Pathological Aberrations. *Mol Neurobiol*. Dec 21.
  178. Salem A.M., Ahmed H.H., Atta H.M., Ghazy M.A., Aglan H.A. (2014). Potential of bone marrow mesenchymal stem cells in management of Alzheimer's disease in female rats. *Cell Biol Int.*, 38. n°12. 1367-1383.
  179. Salloway S., Mintzer J., Weiner M.F., Cummings J.L. (2008). Disease-modifying therapies in Alzheimer's disease. *Alzheimer's & Dementia*, 4. 65-79.
  180. Salloway S., Sperling R., Fox N.C., Blennow K., Klunk W., Raskind M., Sabbagh M., Honig L.S., Porsteinsson A.P., Ferris S., Reichert M., Ketter N., Nejadnik B., Guenzler V., Miloslavsky M., Wang D., Lu Y., Lull J., Tudor I.C., Liu E., Grundman M., Yuen E., Black R., Brashear H.R.; Bapineuzumab301 and 302 Clinical Trial Investigators. (2014). Two phase 3 trials of bapineuzumab in mild-to-moderate



- Alzheimer's disease. *N Engl J Med.*, 370. n°4. 322-333.
181. Sanchez-Ramos J., Song S., Cardozo-Pelaez F., Hazzi C., Stedeford T., Willing A., Freeman T.B., Saporta S., Janssen W., Patel N., Cooper D.R., Sanberg P.R. (2000). Adult Bone Marrow Stromal Cells Differentiate into Neural Cells in Vitro. *Experimental Neurology*, 164, 247-256.
  182. Sardi F, L. Fassina, L. Venturini, M. Inguscio, F. Guerriero c, E. Rolfo, G. Ricevuti (2011) Alzheimer's disease, autoimmunity and inflammation. The good, the bad and the ugly. *Autoimmunity Reviews* 11- 149-153
  183. Savonenko A., Xu G.M., Melnikova T., Morton J. L., Gonzales V., Wong M.P.F., Price D. L., Tang F., Markowska A.L., Borchel D.R. (2005). Episodic-like memory deficits in the APP<sup>swe</sup>/PS1<sup>dE9</sup> mouse model of Alzheimer's disease: Relationships to  $\beta$ -amyloid deposition and neurotransmitter abnormalities. *Neurobiol Dis.*, 18. 602-617.
  184. Schurgers, E. Hilde Kelchtermans, Tania Mitera, Lies Geboes, and Patrick Matthys. 2010 Discrepancy between the in vitro and in vivo effects of murine mesenchymal stem cells on T-cell proliferation and collagen-induced arthritis. *Arthritis Res. Ther*
  185. Selkoe D.J. (2001). Alzheimer's Disease: Genes, Proteins, and Therapy. *Physiological Reviews*, 81. n°2. 741-766.
  186. Shin J.Y., Park H.J., Kim H.N., Oh S.H., Bae J.S., Ha H.J., Lee P.H. (2014). Mesenchymal stem cells enhance autophagy and increase  $\beta$ -amyloid clearance in Alzheimer disease models. *Autophagy*, 10. n°1. 32-44.
  187. Shulman J.M., Chen K., Keenan B.T., Chibnik L.B., Fleisher A., Thiyyagura P., Roontiva A., McCabe C., Patsopoulos N.A., Corneveaux J.J., Yu L., Huentelman M.J., Evans D.A., Schneider J.A., Reiman E.M., De Jager P.L., Bennett D.A. (2013). Genetic Susceptibility for Alzheimer Disease Neuritic Plaque Pathology. *JAMA Neurol.*, 70. n°9. 1150-1157.
  188. Singh M., Kaur M., Kukreja H., Chugh R., Silakari O., Singh D. (2013). Acetylcholinesterase inhibitors as Alzheimer therapy: From nerve toxins to neuroprotection. *Eur J Med Chem.*, 70. 165-188.
  189. Smith JA, T. Leonardi B. Huang N. Iraci B. Vega S. Pluchino (2014) Extracellular vesicles and their synthetic analogues in aging and age-associated brain diseases. *Biogerontology*
  190. Suresh Mathivanan, Hong Ji, Richard J. (2010) Exosomes: Extracellular organelles important in intercellular communication Simpson J of Proteom
  191. Sturchler-Pierrat C., Abramowski D., Duke M., Wiederhold K.H., Mistl C., Rothacher S., Ledermann B., Bürki K., Frey P., Paganetti P.A., Waridel C., Calhoun M.E., Jucker M., Probst A., Staufenbiel M., Sommer B. (1997). Two amyloid precursor protein transgenic mouse models with Alzheimer disease-like pathology. *Proc Natl Acad Sci USA*, 94. 13287-13292.
  192. Szczepanik A.M., Funes S., Petko, W., Ringheim G.E. (2001). IL-4, IL-10 and IL-13 modulate A $\beta$  (1-42)-induced cytokine and chemokine production in primary murine microglia and a human monocyte cell line. *J Neuroimmunol.*, 113. n°1. 49-62.
  193. Théry C., Boussac M., Veron P., Ricciardi-Castagnoli P., Raposo G., Garin J., Amigorena S. (2001). Proteomic analysis of dendritic cell-derived exosomes: a secreted subcellular compartment distinct from apoptotic vesicles. *J Immunol.*, 166. 7309-7318.
  194. Théry C., Clayton A., Amigorena S., Raposo G. (2006). Isolation and Characterization of Exosomes from Cell Culture Supernatants and Biological Fluids. *Curr Protoc Cell Biol.*, 3. n°22. 1-29.
  195. Tetta C., Bruno S., Fonsato V., Deregibus M.C., Camussi G. (2011). The role of microvesicles in tissue repair. *Organogenesis*, 7. n°2. 105-115.
  196. Tian T., Wang Y., Wang H., Zhu Z., Xiao Z. (2010). Visualizing of the cellular uptake and intracellular trafficking of exosomes by live-cell microscopy. *J Cell Biochem.*, 111. 488-96.
  197. Tofoleanu F. and Nicolae-Viorel Buchete (2012) Molecular Interactions of Alzheimer's A $\beta$  Protofilaments with Lipid Membranes. *J. Mol. Biol.* 421, 572-586
  198. Tsai M.S., Lee J.L., Chang Y.J. Hwang S.M. (2004). Isolation of human multipotent mesenchymal stem cells from second-trimester amniotic fluid using a novel two-stage culture protocol. *Human Reproduction*, 19. n°6. 1450-1456.
  199. Uccelli A., Pistoia V., Moretta L. (2007). Mesenchymal stem cells: a new strategy for immunosuppression? *Trends Immunol.*, 28. n°5. 219-226.
  200. Uccelli A., Moretta L., Pistoia V. (2008). Mesenchymal stem cells in health and disease. *Nature Reviews Immunology*, 8. 726-736.
  201. Ueno M., Fujita Y., Tanaka T., Nakamura Y., Kikuta J., Ishii M., Yamashita T. (2013). Layer V cortical neurons require microglial support for survival during postnatal development. *Nat Neurosci.*, 16. 543-551.
  202. Van Niel, G., Porto-Carreiro I., Simoes S., Raposo G. (2006). Exosomes: a common pathway for a specialized function. *J Biochem.*, 140. 13-21.
  203. Varnum M.M., Ikezu T. (2012). The Classification of Microglial Activation Phenotypes on Neurodegeneration and Regeneration in Alzheimer's Disease Brain. *Arch Immunol Ther Exp.*, 60. 251-266.

204. Vilhardt F. (2005). Microglia: phagocyte and glia cell. *Int J Biochem Cell Biol.*, 37. 17-21.
205. Wang J., Tanila H., Puolivälä J., Kadish I., Van Groen T. (2003). Gender differences in the amount and deposition of amyloid $\beta$  in APPswe and PS1 double transgenic mice. *Neurobiol Dis.*, 14. 318-327.
206. Wang Y., Zhang Z., Chi Y., Zhang Q., Xu F., Yang Z., Meng L., Yang S., Yan S., Mao A., Zhang J., Yang Y., Wang S., Cui J., Liang L., Ji Y., Han Z.B., Fang X., Han Z.C. (2013). Long-term cultured mesenchymal stem cells frequently develop genomic mutations but do not undergo malignant transformation. *Cell Death Dis.*, 4. 1-11.
207. Wang Y, Fu B, Sun X, Li , Huang, Zhao , Chen X (2015) Differentially expressed microRNAs in bone marrow mesenchymal stem cell-derived microvesicles in young and older rats and their effect on tumor growth factor- $\beta$ 1-mediated epithelial-mesenchymal transition in HK2 cells. *Stem Cell Res Ther.* Sep 28;6:185.
208. Walsh DM, Selkoe DJ.(2007) A beta oligomers - a decade of discovery. *J Neurochem.* 2007 Jun;101(5):1172-84.
209. Waterman R. S., Tomchuck S. L., Henkle S. L., Betancourt A. M. (2010). A New Mesenchymal Stem Cell (MSC) Paradigm: Polarization into a Pro-Inflammatory MSC1 or an Immunosuppressive MSC2 Phenotype. *PLoS One*, 5. n°4. 1-14.
210. Weidemann A., Konig G., Bunke D., Fischer P., Salbaum J.M., Masters C.L., Beyreuther K. (1989). Identification, biogenesis and localization of precursors of Alzheimer's disease A4 amyloid protein. *Cell*, 57. 115-126.
211. Wilkinson D. (2012). A review of the effects of memantine on clinical progression in Alzheimer's disease. *Int J Geriatr Psychiatry*, 27. 769-776.
212. Wirenfeldt M., Dissing-Olesen L., Babcock A.A., Nielsen M., Meldgaard M., Zimmer J., Azcoitia I., Leslie R.G., Dagnaes-Hansen F., Finsen B. (2007). Population control of resident and immigrant microglia by mitosis and apoptosis. *Am J Pathol.*, 171. 617-631.
213. Wobus A.M., Boheler K.R. (2005). Embryonic Stem Cells: Prospects for Developmental Biology and Cell Therapy. *Physiol Rev.*, 85. 635-678.
214. Wollert T., Hurley J.H. (2010). Molecular Mechanism of Multivesicular Body Biogenesis by ESCRT Complexes. *Nature*, 464. n°7290. 864-869.
215. Yan H., Wua M., Yuan Y., Wang Z. Z., Jiang H., Chen T. (2014). Priming of Toll-like receptor 4 pathway in mesenchymal stem cells increases expression of B cell activating factor. *Biochem Biophys Res Commun.*, 448. 212–217.
216. Yan Y., Ma T., Gong K., Ao Q., Zhang X., Gong Y. (2014) Adipose-derived mesenchymal stem Cell Transplant. promotes adult neurogenesis in the brains of Alzheimer's disease mice. *Neural Regen Res.*, 9. n°8. 798-805.
217. Yan J, Shenglai Liu, Xia Sun, Ke Liu, Huangquan Lin, Shaosong Kuang, Xiaojiang Tang (2014). Evidences for B6C3-Tg (APPswe/PSEN1dE9) Double-Transgenic Mice Between 3 and 10 Months as an Age-Related Alzheimer's Disease Model. *J Mol Neurosci* 53:370–376
218. Yang L., Li S., Hatch H., Ahrens K., Cornelius J.G., Petersen B.E., Peck A.B. (2002). In vitro trans-differentiation of adult hepatic stem cells into pancreatic endocrine hormone-producing cells. *Proc Natl Acad Sci U S A*, 99. n° 12. 8078-8083.
219. Yang H., Yue C., Yang H., Xie Z., Hu H., Wei L., Wang P., Zhao C., Bi J. (2013). Intravenous Administration of Human Umbilical Cord Mesenchymal Stem Cells Improves Cognitive Impairments and Reduces Amyloid-Beta Deposition in an A $\beta$ PP/PS1 Transgenic Mouse Model. *Neurochem Res.*, 38. 2474-2482.
220. Yu X., Harris S.L., Levine A.J. (2006). The regulation of exosome secretion: a novel function of the p53 protein. *Cancer Res.*; 66. 4795-4801.
221. Zanier E.R., Pischiutta F., Riganti L., Marchesi F., Turola E., Fumagalli S. Perego C., Parotto E., Vinci P., Pietro Veglianesi P., D'Amico G., Verderio C., De Simoni M. G. (2014). Bone Marrow Mesenchymal Stromal Cells Drive Protective M2 Microglia Polarization After Brain Trauma. *Neurotherapeutics*, 11. n°3. 679-695.
222. Zappia E., Casazza S., Pedemonte E., Benvenuto F., Bonanni I., Gerdoni E., Giunti D., Ceravolo A., Cazzanti F., Frassoni F., Mancardi G., Uccelli A. (2005). Mesenchymal stem cells ameliorate experimental autoimmune encephalomyelitis inducing T-cell anergy. *Blood*, 106. 1755-61.
223. Zhang J., Li Y., Chen J., Cui Y., Lu M., Elias S.B., Mitchell J.B., Hammill L., Vanguri P., Chopp M. (2005). Human bone marrow stromal cell treatment improves neurological functional recovery in EAE mice. *Exp Neurol.*, 195. 16-26.
224. Zhang Y.W., Thompson R., Zhang H., Xu H. (2011)<sup>1</sup>. APP processing in Alzheimer's disease. *Molecular Brain*, 4. n°3. 1-13.
225. Zhang Y W., Jian Hao J., Liu R., Zhang Z., Lei G., Su C., Miao J., Li Z. (2011)<sup>2</sup>. Soluble A $\beta$  levels correlate with cognitive deficits in the 12-month-old APPswe/PS1dE9 mouse model of Alzheimer's disease. *Behav Brain Res.*, 222. 342-350.
226. Zhang W., Bai M., Xi Y., Hao J., Liu L., Mao N., Su C., Miao J., Li Z. (2012)<sup>1</sup>. Early memory deficits precede plaque deposition in APPswe/PS1dE9 mice: Involvement of oxidative stress and cholinergic dysfunction. *Free Radic Biol Med.*, 52. 1443-1452.

227. Zhang W., Bai M., Xi Y., Hao J., Zhang Z., Su C., Lei G., Miao J., Li Z. (2012)<sup>2</sup>. Multiple inflammatory pathways are involved in the development and progression of cognitive deficits in APPswe/PS1dE9 mice. *Neurobiol Aging*, 33. 2661-2677.
228. Zhang W., Zhang W., Li Z., Hao J., Zhang Z., Liu L., Mao N., Miao J., Zhang L. (2012)<sup>3</sup>. S14G-Humanin improves cognitive deficits and reduces amyloid pathology in the middle-aged APPswe/PS1dE9 mice. *Pharmacol Biochem Behav.*, 100. 361-369.
229. Zhao W., Phinney D.G., Bonnet D., Dominici M., Krampera M. (2014). Mesenchymal Stem Cell Biodistribution, Migration, and Homing In Vivo. *Stem Cells International*, 2014. 1-2.
230. Zhiyong Zhong & Lin Yang & Xiansheng Wu & Wei Huang &
231. Zolezzi J.M., Candia S.B., Santos M.J., Inestrosa N.C. (2014). Alzheimer's disease: relevant molecular and physiopathological events affecting amyloid- $\beta$  brain balance and the putative role of PPARs. *Front Aging Neurosci.*, 6. n°176. 1-12.